

Role of the E-3 ligase CHIP in the negative regulation of the transcription factor TAp63

by

Stephen Robert Armstrong

A thesis submitted in partial fulfillment of the requirements for the degree of

Doctor of Philosophy

Medical Sciences - Laboratory Medicine and Pathology
University of Alberta

© Stephen Robert Armstrong, 2016

Abstract

The p53 family of tumor suppressors is an important group of transcription factors preventing the development of cancer by targeting cell-cycle arrest and apoptosis mediator proteins for transcription. The most studied, p53, is frequently inactivated in carcinomas by mutation or genetic silencing, while the other two members TAp63 (transactivation domain-containing p63) and TAp73 are rarely mutated, but rather are regulated at the protein level. The most common regulation method for TAp63 is post-translational modification, and one of the most prominent ways to negatively regulate expression and function of TAp63 is by ubiquitination followed by proteasome-mediated degradation. Ubiquitination of TAp63 is carried out by an E-3 ligase enzyme that is able to catalyze the attachment of a small peptide called ubiquitin to a target substrate. Poly-ubiquitin chains are required in order for the proteasome to recognize a substrate, and there are many E-3 ligases that can catalyze the attachment of poly-ubiquitin chains to the TAp63 protein. These include the primary regulator of TAp63, Itch/AIP4. In this study, we identify and characterize another primary regulator of TAp63, the E-3 ligase CHIP, which is a key mediator of ubiquitination during the heat shock response. We observed that CHIP is able to bind to TAp63, facilitating the attachment of poly-ubiquitin chains. The over-expression of CHIP in carcinoma cells results in a reduction in TAp63 protein expression, accompanied by oncogenic effects including an increase in cell survival, and a decrease in apoptosis and cell cycle arrest. Knockdown of endogenous CHIP results in an increase in TAp63 expression accompanied by tumor suppressive effects including a decrease in cell survival and migration, and an increase in apoptosis and cell cycle arrest. CHIP expression is negatively correlated with TAp63 expression in various carcinoma cell lines, and invasive prostate carcinoma patient tissue samples. This research supports an oncogenic role for

CHIP in the negative regulation of TAp63 expression and function, and provides a possible therapeutic target for carcinoma treatment in the future.

Preface

This thesis is an original work by Stephen Armstrong. The research project, of which this is a part, received research ethics approval from the Health Research Ethics Board – Biomedical Panel (University of Alberta) for the use of prostate tissue samples.

Project Name: Detection of p53 family members and related regulatory factors in prostate cancer

Study ID: Pro00024519

Date: August 5, 2014

I dedicate this thesis to Robert and Jamie Armstrong, without whom my scholarly endeavors and scientific passions would not have been possible.

Acknowledgements

I'd like to thank my supervisor, Dr. Roger Leng, for his support and guidance during my program, helping me to design my project, helping me problem solve, encouraging me, and providing me with the tools and materials necessary to go about my research. I'd also like to thank Dr. Roger Leng's lab personnel, particularly Dr. Benfan Wang who helped me overcome technical difficulties with assays, and who was very helpful in making it possible for me to complete my experiments, along with Dr. Hong Wu, who developed the CHIP shRNA constructs used in my experiments. I would like to thank my committee members Dr. Michael Weinfeld, Dr. Robert Ingham, and Dr. Andrew Shaw who helped me develop my research directions, discussed my project with me, and offered me versatile views and diverse insights on how to continue my project. I would like to thank the Laboratory Medicine and Pathology department staff who gave me administrative and professional development support throughout my time as a student, including Dr. Monika Keelan, who not only was my chair during my candidacy exam but also provided me with teaching opportunities to develop my teaching skills, and Chris Ward, my teaching mentor, who provided helpful feedback during my teaching experience. I'd also like to thank Cheryl Titus, who was so helpful in answering any administrative questions, and kept important administrative details for myself and other students straight. I'd also like to thank my family for their love and support, particularly my parents Robert and Jamie Armstrong, who not only supported me emotionally, but also financially, and went out of their way providing me support even more valuable and prestigious in my eyes than a scholarship, to make it possible for me to live away from my hometown and complete my degree.

Table of Contents

Abstract	ii
Preface	iv
Dedication	v
Acknowledgements	vi
Table of Contents	vii
List of Tables	x
List of Figures	xi
List of Abbreviations	xiii
Chapter 1 – Introduction	1
1.01 – The Problem of Cancer	2
1.02 – The p53 Family of Tumor Suppressors	7
1.03 – Structure and Properties of p63	12
1.04 – Expression of p63	17
1.05 – Function of p63	19
1.06 – Regulation of p63	24
1.07 – The Ubiquitin Proteasome System (UPS)	28
1.08 – Regulation of p63 – E-3 Ligases	32
1.09 – The E-3 ligase CHIP	37
1.10 – Summary, Hypothesis, and Objectives	41

Chapter 2 – Materials and Methods	43
2.01 – PCR	44
2.02 – Cloning	46
2.03 – Other Constructs	49
2.04 – Maximum Preparation DNA	49
2.05 – Cell Culture conditions and Cell Lines	50
2.06 – Transient Transfection Assay	51
2.07 – Stable Transfection Assay	52
2.08 – Whole-Cell Protein Extract	52
2.09 – SDS Page/ Transfer	53
2.10 – Immunoblot Assay (IB)	54
2.11 – Co-Immunoprecipitation Assay	57
2.12 – His-Ubiquitin Pull-Down Assay	57
2.13 – MG132 Treatment	58
2.14 – Colony Forming Assay.....	59
2.15 – Luciferase Reporter Assay and β -Galactosidase Assay	60
2.16 – Cell Scattering Assay	61
2.17 – Flow Cytometry for Apoptosis Analysis	62
2.18 – Flow Cytometry for Cell Cycle Analysis	64
2.19 – Tissue Handling and Preparation	65
2.20 – Statistical Analysis	66

Chapter 3 – Results	67
3.01 – CHIP is a TAp63 α -Interacting Partner	68
3.02 – CHIP Negatively Regulates TAp63 α Levels.....	76
3.03 – CHIP Negatively Regulates TAp63 α Function.....	83
3.04 – CHIP and p63 Levels are Negatively Correlated in Carcinoma Cell Lines and Patient Tissue Samples.....	109
 Chapter 4 – Discussion and Conclusions	 113
4.01 – Discussion	114
4.02 – Conclusions	125
 Chapter 5 – Future Directions	 126
5.01 – Further Characterizing CHIP’s Negative Regulation of TAp63 Levels.....	127
5.02 – Further Investigating CHIP’s Negative Regulation of TAp63 Function.....	128
 Bibliography	 130

List of Tables

Table 1 – TAp63 α Constructs	45
Table 2 – CHIP shRNA Constructs.....	48
Table 3 –Antibodies	56

List of Figures

Figure 1 – Development of Carcinomas	5
Figure 2 – Cell Cycle Arrest as Induced by p21	9
Figure 3 – Apoptosis as Induced by the p53 Tumor Suppressor Family	11
Figure 4 – p53, p63, and p73 Wild-Type Proteins	13
Figure 5 – p63 Isoforms	15
Figure 6 – The 26S Mammalian Proteasome	29
Figure 7 – Process of Ubiquitination	31
Figure 8 – Types of E-3 Ligases	33
Figure 9 – The E-3 Ligase CHIP – Protein Structure	38
Figure 10 – Exogenous CHIP Binds to Exogenous TAp63 α	69
Figure 11 – Endogenous CHIP Binds to Endogenous p63.....	70
Figure 12 – The SAM Domain is Required for CHIP Binding to TAp63 α	72
Figure 13 – TAp63 α is Ubiquitinated in the Presence of CHIP.....	75
Figure 14 – Ectopic TAp63 α Expression is Negatively Impacted in the Presence of CHIP...	77
Figure 15 – Increasing CHIP Expression Reduces Endogenous p63 Expression.....	78
Figure 16 – Ablation of Endogenous CHIP Restores Endogenous p63 Expression.....	79
Figure 17 – Inhibition of the Proteasome Stabilizes Endogenous p63 Expression.....	81
Figure 18 – Increasing Expression of Ectopic CHIP is Reduces the Expression of Both Alpha Isoforms of p63 (TAp63 α and Δ Np63 α).....	82
Figure 19 – Ectopic CHIP is Associated With Increased Cell Survival.....	84

Figure 20 – Ablation of Endogenous CHIP is Associated with Decreased Cell Survival.....	88
Figure 21 – Both TAp63 α -Induced and p53-Induced Apoptosis is Inhibited in the Presence of Ectopic CHIP	92
Figure 22 – UV-Induced Apoptosis is Reduced as Ectopic CHIP Expression Increases	95
Figure 23 – Both TAp63 α -Induced and p53-Induced Transcription of p21 is Inhibited in the Presence of Ectopic CHIP	97
Figure 24 – p53 and TAp63 α -induced G1 Arrest is Reduced in the Presence of Ectopic CHIP.....	102
Figure 25 – Ablation of Endogenous CHIP is Associated with Increased Percentage of Cells in G1.....	104
Figure 26 – Ablation of CHIP Reduces Cell Scattering.....	107
Figure 27 – Endogenous p63 and CHIP Expression in Selected Squamous Cell Carcinoma Cell Lines	110
Figure 28 – Endogenous p63 and CHIP Expression in Nine Invasive Prostate Carcinoma Tissue Samples	112

List of Abbreviations

L - liters

M – molarity (moles/liter)

mL – milliliters

μ L – microliters

S – subunit

x g – number multiplied by the earth's gravitational force of 9.8 m/sec^2 (g)

$^{\circ}\text{C}$ – degrees Celsius

ΔN – p63 protein lacking the N-terminus

A – adenine

AA – amino acid

AEC – Ankyloblepharon-ectodermal dysplasia-clefting

AIF – Apoptosis inducing factor

AIP4 – Atrophin 1 interacting protein 4)

Ala – alanine

α -MEM – Alpha modification - minimum essential medium

Arg – arginine

Asn – asparagine

Asp – aspartic acid

ASPP1 – Apoptosis stimulating of p53 protein 1

ASPP2 – Apoptosis stimulating of p53 protein 2

ATM – Ataxia telangiectasia mutated

ATR – Ataxia telangiectasia and Rad-3 related

Bax – Bcl-2-associated x protein

C – cytosine

C108 – amino acid 108 to C-terminus TAp63 construct

C393 – amino acid 393 to C-terminus TAp63 construct

C541 – amino acid 541 to C-terminus TAp63 construct

CA – Canada

CC – Coiled-coil domain

CD95 – Cluster of differentiation 95

CDK – Cyclin-dependent kinase

CML – Chronic myeloid leukemia

Cys – cysteine

DBD – DNA-binding domain

dH₂O – purified water

DH5 α – *Escherichia coli* bacteria D. Hanahan 5 strain

DMSO – Dimethyl sulfoxide

DNA – Deoxyribonucleic acid

dNTP – Deoxynucleotide triphosphate

dpi – dots per inch

E-1 – Ubiquitin activating enzyme

E-2 – Ubiquitin transfer enzyme

E2F1 – E2F transcription factor 1

E-3 – Ubiquitin ligase enzyme

E-4 – Ubiquitin chain elongation enzyme

EDTA – Ethylene-diamine-tetraacetic acid

EEC - electroductyly-ectodermal dysplasia-clefting

EGFR – epidermal growth factor receptor

EU - European Union

FBS – Fetal bovine serum

G – guanosine

Gln – glutamine

Glu – glutamic acid

Gly – glycine

HECT – Homologous to E6-AP carboxyl terminus domain

HEPES – 4-(2-hydroxyethyl)-1-piperazineethanesulfonic acid

HER-2 – Human epidermal growth receptor 2

hr./hrs. – hour/hours

HSF1 – Heat shock factor 1

Hsp70 – Heat shock protein 70

Hsp90 – Heat shock protein 90

GTP – Guanosine triphosphate

IgG – Immunoglobulin G

Ile – isoleucine

INF-1 – Interferon regulator factor

ING1 – Inhibitor of growth protein 1

Itch – Itchy mice protein (**see AIP4*)

kDa – kilo Dalton

LB – lysogeny broth

Leu – leucine

Lys – lysine

Mdm2 – murine double minute 2

MEF – mouse embryo fibroblast cells

Met – methionine

min – minutes

miRNA – micro-interfering ribonucleic acid

mRNA – messenger ribonucleic acid

N362 – N-terminus to AA362 TAp63 construct

N540 – N-terminus to AA540 TAp63 construct

Nedd4 – Neural precursor cell expressed developmentally down-regulated protein 4

Noxa – (Latin for “damage”)

NP40 – nonyl-phenoxypolyethoxylethanol

OD – oligomerization domain

PBS – phosphate buffered saline

PCR - polymerase chain reaction

PERP – p53 apoptosis Effector Related to PMP-22

PFU – *Pyrococcus furiosus* polymerase

Phe – phenylalanine

PRD – proline rich domain

Pro – proline

PUMA – p53 up-regulated modulator of apoptosis

RACK1 – Receptor for Activated C Kinase 1

RB – Retinoblastoma protein

RING – Really Interesting New Gene

RNA – Ribonucleic Acid

SAM – Sterile Alpha Motif domain

sec – seconds

Ser – serine

SHFM – Split Hand and Foot Malformation

shRNA – small-hairpin Ribonucleic Acid

siRNA – small-interfering Ribonucleic Acid

SV40 – Simian Virus 40

TA2 – second Transactivation Domain in p63

TAD – Transactivation Domain

TAp63 – p63 protein containing the TAD

TGF- β – Tumor Growth Factor beta

Thr - threonine

TLR3 – Toll-like Receptor 3

TBS – Tris-buffered Saline

TBST – Tris-buffered Saline with 1% Tween added

TE buffer – Tris-EDTA buffer

TI – Transactivation Inhibition domain

TNFR – Tumor Necrosis Factor Receptor

TP53 – Tumor Protein 53 gene

TP63 – Tumor Protein 63 gene

TP73 – Tumor Protein 73 gene

TPR – Tetratricopeptide Repeat domain

TRAIL-R – Tumor necrosis factor-related apoptosis-inducing ligand receptor

Tris – Tris(hydroxymethyl)aminomethane

Trp – tryptophan

Tyr – tyrosine

UK – United Kingdom

UPS – Ubiquitin Proteasome System

USA – United States of America

UV – Ultraviolet Radiation

Val – valine

VEGF – Vascular Endothelial Growth Factor

WWP1 – WW-domain containing E-3 ubiquitin protein ligase 1

Chapter 1 - Introduction

1.01 – The Problem of Cancer

Cancer is defined as malignant neoplasia (new growth) [1, 2], characterized by cell populations that have accumulated sufficient mutations in their genomic machinery able to grant them the following abilities: to proliferate (divide) without limitation forming tumorous masses (tumorigenesis), to invade surrounding tissues (invasiveness), and to migrate to distant sites and seed metastases (metastasis) [2]. Neoplasia can be contrasted from hyperplasia, a state in which normal cells undergo proliferation, but retain normal genetic characteristics [3], such as endometriosis, the hyperplastic proliferation of uterine epithelium [4], or benign prostate hyperplasia – hyperplastic proliferation of prostate epithelium and stromal tissues [5]. In contrast to hyperplasia, neoplasia involves proliferation without external stimulus, and possesses aberrant genetic characteristics [6]. Cancer is the second leading cause of death in North America, with 1.7 million new incidences, and almost 600, 000 mortalities in the United States in 2015 [7], and roughly 200, 000 new incidences, and an estimated 78, 000 mortalities in Canada in 2015 [8] . It is expected to overtake heart disease as the primary cause of death in North America in the next few years [7].

Cancer develops through a process called neoplastic transformation [9], where mutations in proto-oncogenes (genes that encode normal proteins that promote proliferative pathways [10]) mutate the proto-oncogene into an oncogene – resulting in deregulation of the encoded protein, and its proliferative pathways, thereby rendering the protein an oncoprotein [10, 11]. One example involves mutations in the HRas GTPase, which result in the proliferation-related protein unable to be inactivated, and leads to unregulated cellular proliferation [12, 13]. Other proteins called tumor suppressors negatively regulate these proliferative pathways, and these proteins must also be inactivated [14]. Mutations in tumor suppressor genes that result in loss of function

are sufficient to drive cancer progression, although both alleles of the gene must be inactivated for the tumor suppressor to be rendered inactive (two hit hypothesis, or Knudson-type tumor suppressor) [15]. The classic example of a tumor suppressor is the protein RB, which negatively regulates the cell cycle [16]. When both alleles of the *RB* gene are inactivated through mutation, a blastoma-type eye cancer (retinoblastoma) tends to develop in childhood at greater rates (30 to 300 times more frequently) [16, 17]. Once enough mutations accumulate for a cell population to be considered neoplastic, tumorigenesis (formation of tumors) occurs. This can lead to benign tumors which cannot spread to surrounding tissues, or neoplastic transformation can continue to progress from either a pre-existing benign tumor, or concurrently from cancer *in situ* (pre-cancer) to malignant neoplasia (however, not all benign tumors become malignant, and not all malignant tumors go through a benign stage) [18, 19]. Malignancy is accomplished by accumulating additional mutations that promote the following cellular characteristics: increased blood vascularization (angiogenesis) [20], tissue invasion, migration to distant sites, and metastatic proliferation (formation of secondary tumors) [2, 21].

Cancers can be categorized from the tissue-type that they arise from, and these include carcinomas (crab growths) – those arising from epithelial and endothelial tissues of the ectoderm and endoderm, sarcomas (flesh growths) – those arising from non-hematopoietic connective tissues of the mesoderm, leukemias/lymphomas – those that arise from blood or lymph tissues of the mesoderm, and germinoma/blastomas – those arising from germ or precursor cells [2, 22]. Of those classes, carcinomas comprise the vast majority of cancer cases (85%) in humans [23]. These include the most commonly occurring cancers of the skin, head and neck, lung, breast, prostate, ovarian, pancreatic, colon, cervical, kidney, and liver tissues [2, 23].

The standard model for carcinoma development involves a population of neoplastic cells that transition from epithelium to a mesenchymal morphology, resulting from loss of cell-to-cell and cell-to-membrane adhesion. Epithelial to mesenchymal transition allows for these cells to penetrate the basement membrane separating the epithelium from the stromal layer [2]. Penetration into the stromal layer and spreading to the lymph and blood systems is the hallmark of malignancy [24] (Figure 1). These neoplasms can then metastasize to remote locations and generate secondary tumors [2, 21]. At early stages, before spreading occurs, surgery is a very effective treatment and patient prognosis is good [25-27], but at later stages, once invasion and metastasis are underway, tumors are difficult to treat and patients have a poor prognosis [28, 29].

Treatment of cancer has traditionally involved surgery, radiation therapy, and broad-range chemotherapy [25]. Chemotherapy agents are diverse in effect, and among them are DNA (deoxyribonucleic acid) damaging agents (e.g. cisplatin), which create DNA damage in the form of purine cross-links that ultimately leads to apoptosis [30], and microtubule-assembly agents (e.g. paclitaxel), which interfere with microtubule disassembly and forces proliferating cells into cell-cycle arrest, a state of non-proliferation [31, 32]. Chemotherapy is often the preferred choice if the cancer is in a metastatic stage [33]. Broad-range chemotherapy agents are not cancer-specific and have severe toxic effects on all quickly-proliferating cells [34]. Because of this, traditional chemotherapeutics are associated with reduced quality of life [34], with side effects including neuropathy (neuronal pain) [35], and neutropenia (reduction in white blood cell count) [36]. Furthermore, remission of cancer after treatment with these broad range cytotoxic drugs is often temporary, with cancer reemergence common [37], and often acquiring drug resistance to chemotherapy agents [38, 39], the recurring cancer being either resistant (reduced time to remission) or refractory (no treatment response) to the drug [40]. To make matters

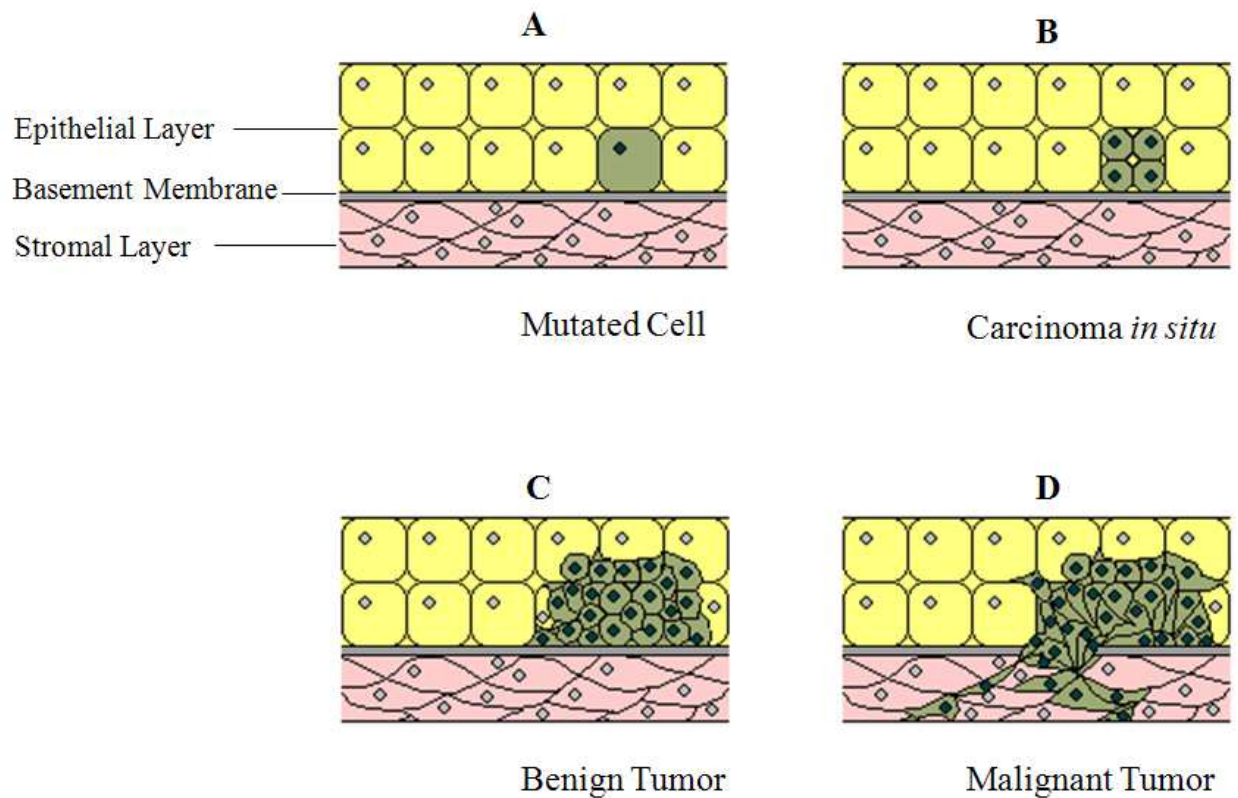


Figure 1 – Development of Carcinomas.

A carcinoma originates from one mutated cell. A group of mutated cells growing in place is called *Carcinoma in situ* (B). If this mass continues to grow but cannot penetrate the basement layer, then the tumor is benign (C). However, if additional mutations occur that allow for epithelial to mesenchymal cell transition and invasion into the stromal layers, then the tumor is malignant and is defined as a carcinoma (D). This figure was based on information obtained in Weinberg et al. 2007 [2], and Marino-Enriquez et a. 2014 [18].

worse, multi-drug resistance is commonly observed, where the recurring cancer is resistant not only to the drugs it was previously treated with, but to many other broad range chemotherapeutics [41]. In order to increase cytotoxic efficacy against cancer cells, and reduce side effects of treatment, new types of treatments called “targeted therapy” have been developed that target specific cancer phenotypes [42, 43]. These targeted therapies often involve inactivating oncogenes or re-activating tumor suppressor function [43]. One of the most striking examples of targeted therapy involves HER-2 (human epidermal growth factor receptor 2) positive breast cancer, which used to have a poor prognosis [44]. Unlike normal cells, this type of cancer cell heavily relies on the HER-2 receptor for its neoplastic proliferative function [45]. However, with the development of trastuzumab (known commercially as Herceptin), a monoclonal antibody that blocks the HER-2 growth receptor [46], the prognosis for this type of cancer improved remarkably with 33% less recurrence of cancer, and 20% increased survival [47]. Another example of the success of targeted therapy is imatinib (known commercially as Gleevec); a small molecule that can inhibit the oncoprotein Bcr-abl, a chimeric tyrosine kinase found to be the primary cause of CML (Chronic myeloid leukemia) [48]. CML used to have poor survival rates prior to 2001, with a five year survival of 31%, but with imatinib treatment approved, five-year survival rates doubled to 60% (as measured between 2004 and 2010) [49].

The benefits of targeted therapy are invaluable in cancer treatment, but one problem is that targeted therapies must be developed for specific cancers, exploiting specific cellular pathways. Since cancer phenotypes are unique, developing specific therapies for each one not only takes a great deal of research, but many cancers have no obvious weaknesses to be exploited such as a unique chimeric protein (in the case of CML), or reliance on a specific growth receptor for proliferation (in the case of HER-2 positive breast cancer) [50]. In fact,

despite all of the research defining the roles of tumor suppressors in cancer development, the specific mechanisms in which cancer cells are able to keep tumor suppressors inactivated are not fully understood, and sometimes targeted therapies fail in clinical settings [51].

Further understanding of how tumor suppressors are regulated in cancer is crucial to developing targeted therapies, and one of the most commonly inactivated tumor suppressors in cancers are those belonging to the p53 family [52-55].

1.02 - The p53-Family of Tumor Suppressors

The p53 family is an important group of transcription factors related to development and growth suppression in response to genotoxic stress [55]. Members of this family include the famous p53 tumor suppressor discovered in 1979, along with two other members, p73 and p63 discovered later in 1997 [56-62], with p63 being cloned in 1998 [58, 60].

In the 1970s, a major hypothesis of cancer development was that viruses were responsible for cellular transformation. The SV40 (Simian Virus 40) was one such virus being investigated. In the SV40 model, three proteins were associated with normal to cancerous cell transformation, one of these weighing 55 kDa (kilo-Daltons). However, when identifying the protein, researchers discovered that it was not part of the SV40 proteome, but rather, it was a protein from the host cell [63]. The protein was later named p53, designated so in 1983 by Lionel Crawford [63]. It was originally considered to be an oncogenic candidate, as it was frequently overexpressed in some cancer cells, but in later studies p53's role was revised, and it was discovered to be an important tumor suppressor protein, with both alleles frequently inactivated in other cancer cells [63, 64]. The original observation of p53 being expressed in association with cancer development was explained by its oncogenic gain of function when mutated in

cancer cells [65]. The original p53 being observed was likely a mutated form of p53 [66]. In fact, p53 is mutated in over 50% of all human cancers, and furthermore is inactivated in up to 80% of all cancers [52, 53], including almost all cancer types [54], making it the single most common mutated target in cancer, and the most striking example of tumor suppressor inhibition.

The primary role of the p53 protein in normal cells is as a sensor of genotoxic stress [67, 68]. Occurrence of DNA-damage leads to activation of DNA-damage response signaling pathways mediated by the ATM (ataxia telangiectasia mutated) and ATR (ataxia telangiectasia and Rad-3 related) proteins, which are serine/threonine kinases that sense different forms of DNA damage [69, 70]. ATM recognizes double strand breaks and chromatin disruption, while ATR recognizes single strand breaks [70]. ATM signaling can activate p53 [71] by phosphorylating p53 [72]. Once p53 is activated, it is able to bind to p53 response elements (p53RE) on DNA to target genes for transcription [54]. The most notable of these genes are those that transcribe proteins promoting cell cycle arrest (such as p21), and those promoting apoptosis (such as bax) [54].

The cell cycle involves four major phases, the Gap 1 phase (G1), the DNA-replication phase (S), the Gap 2 phase (G2), and the cell proliferation/mitosis phase (M) [73] (Figure 2). There is also a G0 phase that differentiated cells (such as neurons) are in, characterized by quiescence (reversible long-term non-proliferative state) [73, 74]. Quiescence is not to be confused with senescence, a non-reversible non-proliferative state [75]. Cyclin/CDK (cyclin dependent kinase) complexes control cell cycling through these phases [73]. If the DNA damage can be repaired in time, cell-cycle arrest is mediated by p53-induced expression of p21, which inactivates the cyclin E/CDK2 checkpoint complex and results in G1 arrest [73, 76]

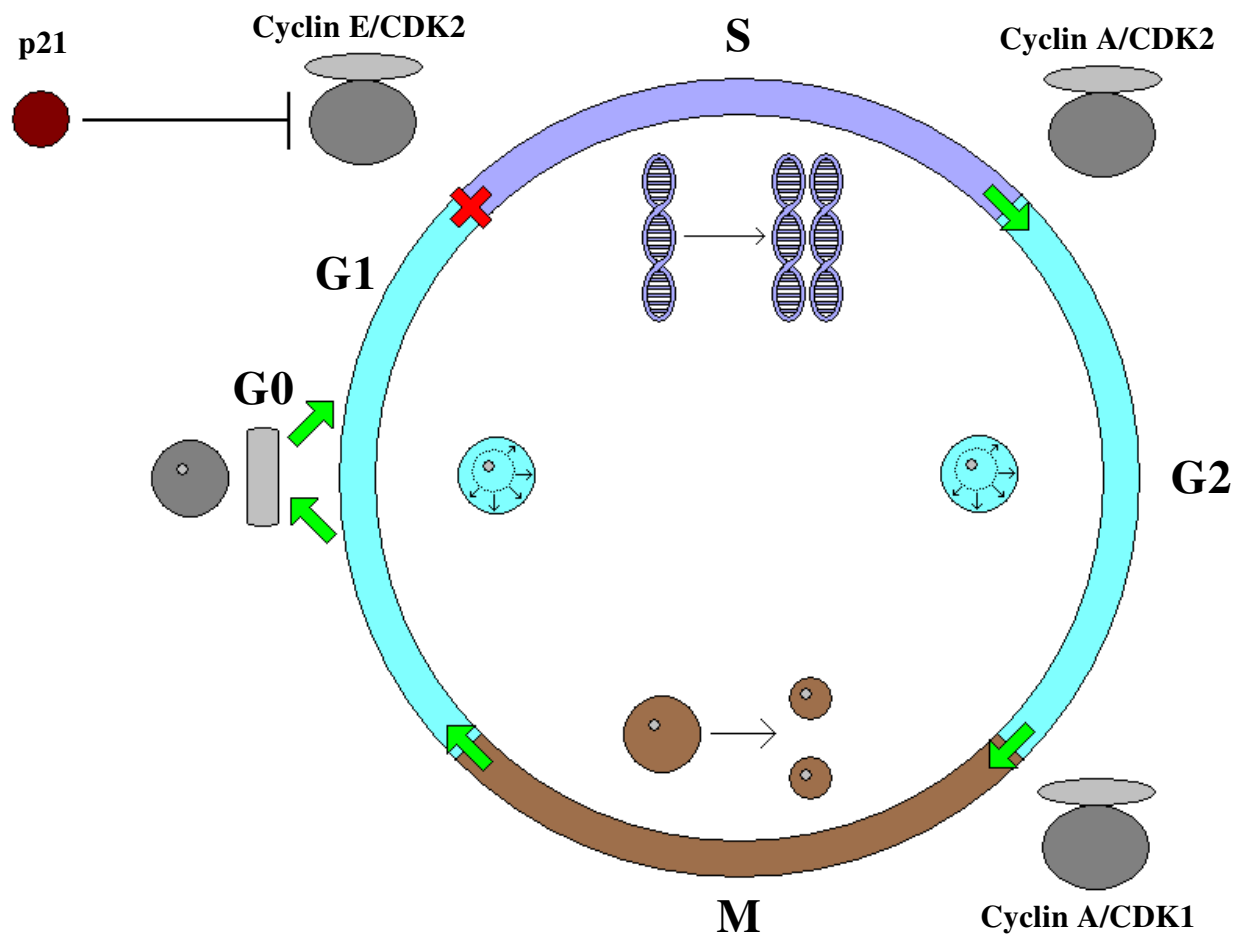


Figure 2 – Cell Cycle Arrest as Induced by p21.

The cell cycle progresses from G1 when the cell undergoes the first growth period, to S when the cell undergoes DNA replication, to G2 when the cell undergoes the second growth period, to the M phase when the cell undergoes mitosis/proliferation. G0 represents quiescent (non-proliferative) cells. Cell cycle arrest can occur during the G1 phase when p21 inhibits CDK2, preventing the cell from progressing into the S phase. Under cell cycle arrest, the cell cannot progress beyond G1, and therefore cannot undergo proliferation. This figure was based on information obtained in Vermeulen et al. 2003 [73].

(Figure 2). The cell comes out of cell-cycle arrest once the DNA damage is repaired, and p53 expression is reduced by a negative feedback loop with its primary regulator, Mdm2 (described in Section 1.08), which p53 itself induces transcription of [77]. If DNA damage cannot be repaired, then p53 instead promotes the activation of apoptosis by trans-activating apoptotic activator proteins [78, 79]. It is thought that apoptosis induced by p53 is either expression dependent, where higher amounts or more frequent activation of p53 induces apoptosis instead of cell cycle arrest [78]; or inducing apoptosis is post-translational modification dependent, as phosphorylation on a particular serine residue, Ser 46 of p53 promotes apoptotic pathways [79].

Apoptosis is an energy-dependent form of programmed cell death, hallmarks of which include non-inflammatory cell death characterized by cellular shrinkage, pyknosis (condensation of chromatin), karyorrhexis (fragmentation of DNA), blebbing (protrusion) of the plasma membrane, and cellular budding that forms apoptotic bodies (compartmentalized cellular remnants) [80]. Apoptotic pathways can be divided into two major classes: those that activate apoptosis intrinsically, usually relying on the release of mitochondrial cytochrome c by pro-apoptotic p53 transcription targets such as bax; and those that can activate apoptosis extrinsically through death receptors also induced by p53 such as TNFR (tumor necrosis factor receptor) [80, 81]. Both pathways lead to downstream activation of caspase proteins which initiate apoptosis [80] (Figure 3). Because of these functions, p53 is considered to be a master regulator of proliferation and cell survival, and one of the key tumor suppressors preventing cancer development – some researches even calling it the “guardian of the genome” [82, 83]. However, p53 is not the only tumor suppressor able to induce transcription of cell cycle arrest and apoptotic targets – also included in the p53 family are two other proteins, p63 (also known as

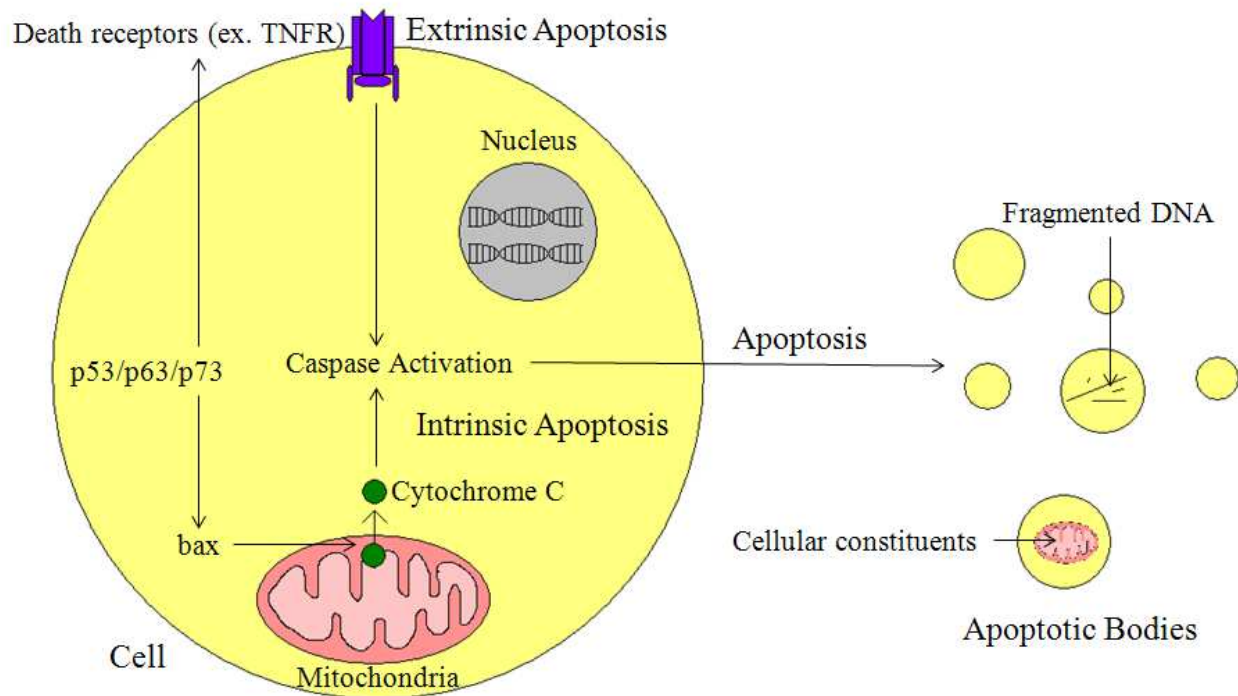


Figure 3 – Apoptosis as Induced by the p53 Tumor Suppressor Family.

The p53 family can induce the transcription of factors that induce extrinsic apoptosis (ex. TNFR death receptor), and those that induce intrinsic apoptosis (ex. bax), which promotes cytochrome c release. Both extrinsic and intrinsic routes initiate apoptosis by activating caspases which lead to programmed cell death involving DNA fragmentation and the formation of apoptotic bodies. This figure was based on information obtained in Elmore et al. 2007 [80], and Ouyang et al. 2012 [81].

KET [61], CUSP [84], AIS [84, 85], p40, p51, and p73L [85, 86]), and p73, which are two p53-like homologues [57, 60] (Figure 4). Both p63 and p73 have roles in development in addition to cell cycle and apoptotic control, with p63 involved in early epithelial development [60], and p73 involved in neurological development [68]. All three proteins are structurally similar and share considerable identity between their domains. The p63 protein is the most evolutionarily conserved of the three family members, being the ancestor to both p73 and p53 [60]. The p73 protein is in turn more primitive than p53 [57]. In contrast to p53, both p63 and p73 are rarely mutated in cancer [87], and therefore are not considered canonical tumor suppressors by the Knudson definition (Knudson type tumor suppressors undergo targeted loss of expression or function during tumorigenesis [88]), however, both demonstrate similar function to p53.

Since p53 is often mutated in cancers, reactivation of p53 using targeted therapy is often not feasible [89], but since p63 and p73 rarely are mutated (so they exist in cancer as their wild-type forms but are likely dysregulated by other means), they may be good targets for reactivation in cancer by targeted therapy. Therefore, it is important to understand how these proteins are inactivated in cancer. This research focuses on the regulation of p63, and subsequent sections will describe p63 in detail – its structure, function, and regulation.

1.03 - Structure and Properties of p63

The gene that encodes p63, *TP63*, is located on the human chromosome 3, in the region q27-29 [60]. It is conserved evolutionarily from mollusks to humans [88]. Unlike *TP53* (but similar to *TP73*), *TP63* has two promoters. The first promoter (P1) is located upstream of the *TP63* coding sequence [88] and encodes the full length p63 protein designated TAp63 [60]. A second, alternative promoter (P2) is located between the second and third exon in intron 3

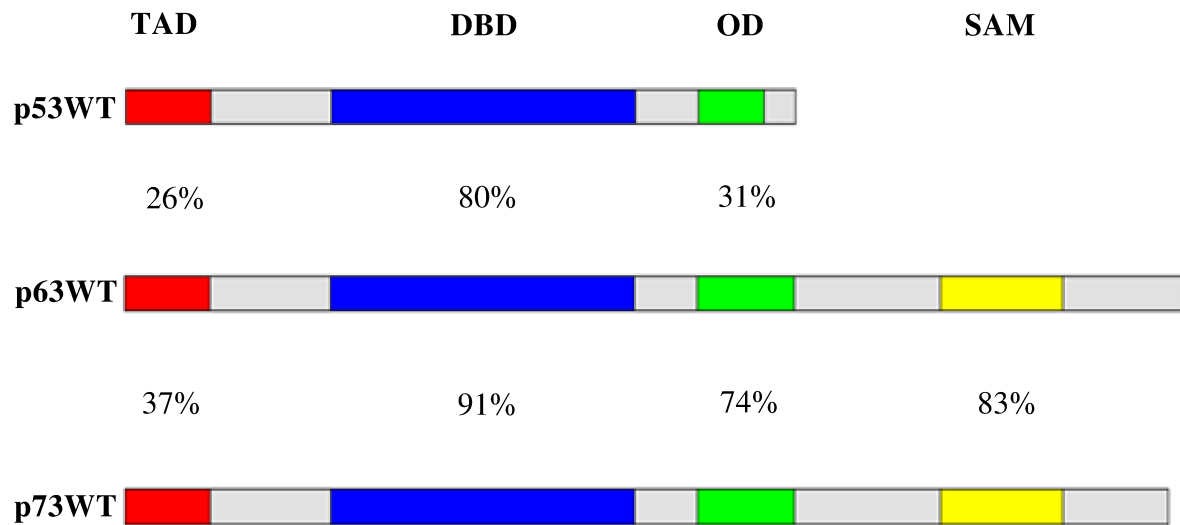


Figure 4 – p53, p63, and p73 Wild-Type Proteins.

Percent identity between the major domains including the transactivation domain (TAD), DNA binding domain (DBD), oligomerization domain (OD), and the sterile alpha motif domain (SAM) of p53, p63, and p73 wild-type proteins. This figure was created with information taken from Levrero et al. 2000 [90], Melino et al. 2003 [55], and Yang et al. 2002 [86].

[60, 88]. This promoter encodes an N-terminal truncated variant of p63, designated Δ Np63 [54, 60]. Further complicating matters is the occurrence of additional variants generated by alternative splicing of exons 10 through 14 at the C-terminus [88], and this property is shared with both p53 and p73. Splice variants of p63 include p63 α , p63 β and p63 γ [54, 60, 88, 91]. These two processes taken together are able generate at least six p63 isoforms [60, 91]: the full-length isoform TAp63 α (85 kDa), the splice variant TAp63 β (68 kDa), the splice variant TAp63 γ (58 kDa); and the N-terminally truncated isoform Δ Np63 α (65 kDa), the splice variant Δ Np63 β (55 kDa); and the splice variant Δ Np63 γ (47 kDa) [60, 91, 92]. The average half-lives of these isoforms range from 1 hr to 8 hr with Δ N variants having the longest, and TA variants having the shortest [91] (Figure 5).

The p63 protein shares three domains in common with p53, along with other unique domains. The transactivation domain (TAD), which is present in all isoforms designated “TAp63” [60], is located at the N-terminus of the protein and spans from AA 1 to AA 64 [93]. This domain is responsible for the transactivation of target genes, and is absent in all Δ N isoforms. A proline-rich domain (PRD) occurs after the TA domain, spanning from AA 67 to AA 127, and it is responsible for protein recognition by some p63 regulators and contributes to p63’s transactivation ability [94]. The DNA-binding domain (DBD – also known as the nuclear binding domain or NBD), is present in all p63 isoforms, spans from AA 142 to AA 323 [93, 95], and is responsible for recognizing and binding to response elements on DNA [60]. This domain is the most likely to be mutated in p53 [96], although similar mutations in p63 are rarely observed in cancer [58]. The oligomerization domain (OD) located on exon 10 [88] and spanning from AA 353 to AA 397 [93], is also present in all p63 isoforms, p53, and p73, and is responsible for oligomerization of p63 into active homotetramers. The p63 oligomerization

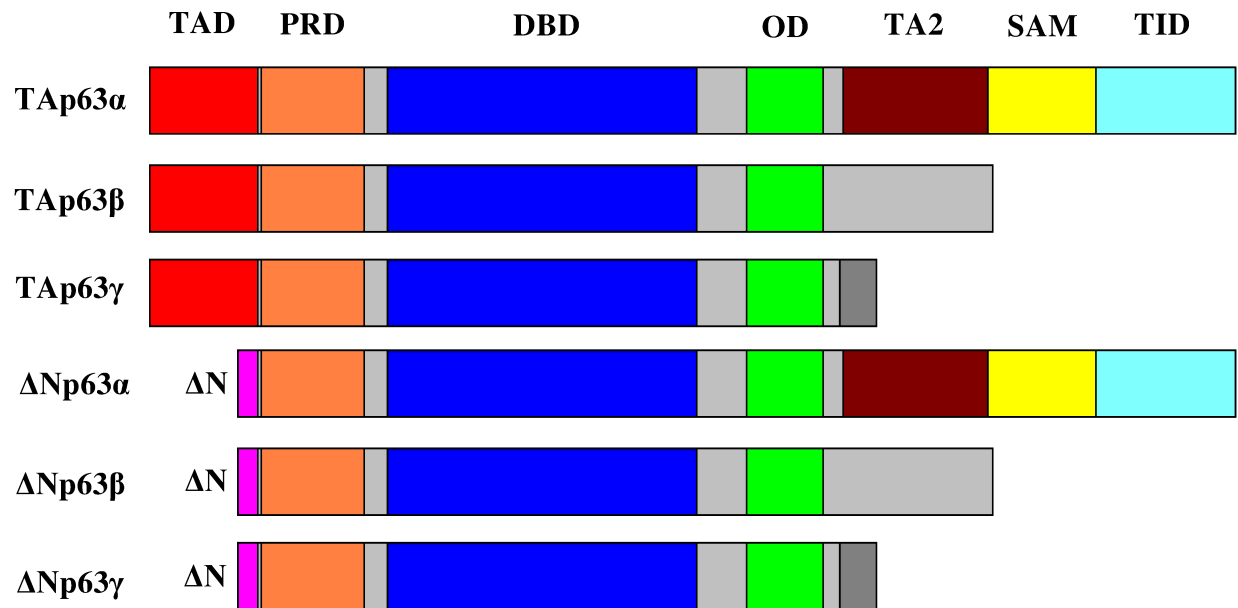


Figure 5 – p63 Isoforms.

A comparison between six isoforms of the p63 protein, showing the transactivation domain (TAD), proline rich domain (PRD), DNA-binding domain (DBD), the oligomerization domain (OD), the second transactivation domain (TA2), the sterile Alpha motif domain (SAM), and the transactivation inhibitory domain (TID). This figure was based on information obtained in Melino et al. 2011 [93], and Yang et al. 2000 [92].

domain can also form heterotetramers with other p63 isoforms, and also p73, but not p53 [60]. The Sterile alpha motif (SAM) domain, spanning from AA 502 to AA 566 [93] is only contained in the alpha spliced isoforms, TAp63 α and Δ Np63 α . SAM domains are responsible for protein-protein interactions [97, 98] in proteins involved in development. It is also present in p73 α isoforms while absent in p53, and is much shorter and terminates after its oligomerization domain [97, 99]. The SAM domain may inhibit the transactivation ability of TAp63 α and Δ Np63 α , as these variants are not as transcriptionally active as the beta or gamma variants, which have the SAM domain spliced out, and may be involved in mediating homo and heterodimerization of alpha variants into inactive dimers [97]. The TA2 (second transactivation domain), spanning from AA 410 to AA 512 [100], is responsible for the transactivation ability of the Δ N variants. Δ Np63 isoforms were thought to be transcriptionally inactive, since they lack the N-terminal TA domain. However, this second transactivation domain allows these truncated isoforms to transactivate genes likely involved in development [100, 101] as mutations in this particular domain are associated with developmental defects [100]. Finally, the TI (Transactivation inhibition) domain, located on the C-terminus of TAp63 α isoform and spanning from AA 568 to AA 641 [93, 102] is able to bind directly to the TA [88], and inhibit transactivation, a case of auto-regulation [102] by forming inactive dimeric TAp63 α [103]. There are other properties unique to specific p63 isoforms: In the gamma isoforms of both full length and Δ Np63 there are unique sequences in exon 15 alternatively spliced in that are not present in the other four isoforms, however, the function of these sequences is unknown [104].

The p63 protein shares identity with the other two members of its family p53 and p73. The p63 TA shares 26% identity with the p53 TA and 37% with the p73 TA; the p63 NBD shares roughly 80% identity with the p53 NBD and 91% with the p73 NBD; and the p63 OD

shares roughly 31% identity with the p53 OD and 74% with the p73 OD [55, 86]. Because of the presence of identical peptide sequences, p63 and p73 can target many of the same genes for transcription as p53 (see Section 1.05).

1.04 - Expression of p63

Under normal conditions, p63 expression is limited to epithelial tissues, predominantly in tissues of the embryonic ectoderm, and in basal cells of adult epithelium including that of the breast, lung, prostate, and skin [105, 106]. This is in contrast to p53, which is expressed ubiquitously in all tissues. Both TAp63 and Δ Np63 isoforms are co-expressed, and the Δ N isoforms having the highest expression [106]. Of the C-terminal alternatively spliced variants, the alpha isoforms (TAp63 α and Δ Np63 α) are the most highly expressed in tissues, with half-lives of approximately 1 hr [91, 105]. While Δ Np63 α is expressed quite highly in the embryonic ectoderm and basal cells, as these cells undergo differentiation, Δ Np63 α expression is reduced dramatically [107]. This pattern is observed in primary mouse keratinocytes where Δ Np63 α is the primary isoform [60]. Using these cells as a model of squamous epithelium, it was observed that the presence of both Δ Np63 α and Δ Np63 γ is associated with low levels of TAp63 γ . However, TAp63 γ levels increase in differentiating keratinocytes, and are associated with highly reduced Δ Np63 expression [104]. Two markers of differentiation, keratin 10 and filaggrin, are both inhibited by the overexpression of Δ Np63 α , while overexpression of TAp63 α is able to induce uptake of keratin 10 [98]. Some epithelial tissues express TAp63 variants while lacking Δ Np63 variants, such as those of the brain, heart, kidney, testis, and thymus [60]. TAp63 is also highly expressed in oocytes, usually as an inactive dimer [108], and is also considered to be the master regulator of oocyte cell death, involved in a pathway that results in the transcriptional

activation of bax followed by apoptosis [109]. Genotoxic stress can result in the downregulation of Δ Np63 in normal tissues at both the mRNA and protein levels [110, 111], possibly allowing a stress response pathway to occur through up-regulation of p53, TAp63, or TAp73.

Under neoplastic conditions, expression of p63 is highly variable: The *TP63* gene is amplified in squamous cell carcinomas of the head and neck [85, 112], and in lung cancers, a survey found it to be amplified in 88% of squamous cell carcinomas, 42% of large cell carcinomas, and 11% of adenocarcinomas [113]. The p63 protein is frequently under-expressed in invasive urothelial bladder carcinomas [114], although this study did not contrast different p63 isoforms. Δ Np63, but not TAp63, is overexpressed in advanced esophageal cancer [115], and also overexpressed in squamous cell carcinomas of the lung [113, 116]. When TAp63 and Δ Np63 expression levels were measured in primary bladder carcinomas, TAp63 variants were under-expressed in 53% of samples, while Δ Np63 was over-expressed in 64% of samples [117]. A separate study observed TAp63 to be under-expressed in 67% of osteosarcoma samples [118]. Loss of TAp63 expression is observed in transitional bladder carcinoma tumors where 93% of low grade early stage tumors expressed p63, 68% of high grade intermediate stage tumors expressed TAp63, and only 16% of invasive tumors expressed TAp63 [119]. This study specifically associates loss of TAp63 with invasiveness, an important difference between the two variants, suggesting the two have opposing functions. None of these studies reported any mutations of *TP63*. Amplification of the chromosome 3q region is one of the most common types of genetic amplification in solid tumors [113], which could imply an oncogenic role of p63, particularly the Δ Np63 variants. Interestingly, one study associated Δ Np63 with prolonged survival in non-small cell lung carcinomas [113], while a different study was unable to confirm any association between Δ Np63 and survival [116]. Reduced expression of TAp63 variants was

observed in buccal carcinomas, and contrasted with a higher expression of TAp63 in normal buccal mucosa tissue [120], associating TAp63 under-expression with tumorigenesis. Downregulation of TAp63 is also associated with tumorigenesis in laryngeal squamous cell carcinomas [121]. However, this association is not always present in other cancer types, and its role is controversial. One study made the striking observation that TAp63 variants were expressed in the majority of malignant lymphomas while Δ Np63 is absent [106], calling into question whether these variants have context dependent roles in cancer. The ratio of TAp63 to Δ Np63 expression may also be important [106], as this ratio is imbalanced in many cancers, often with TAp63 being under-expressed compared to Δ Np63 [88, 122]. Understanding the function of these p63 isoforms is necessary to clearly define their roles in cancer.

1.05 - Function of p63

The p63 protein is primarily involved in development, being responsible for epithelial cell maintenance, and development of epidermal tissues of the skin and tongue, hair follicles, tissues of the lacrimal and sweat glands, breast, prostate, and teeth [88, 123]. It is absolutely crucial for epithelial development, strikingly observed in embryonically lethal $p63^{-/-}$ mouse models [124]. While $p53^{-/-}$ mice develop normally and accumulate tumors over time, and $p73^{-/-}$ mice develop with minor developmental defects, $p63^{-/-}$ mice are not viable and do not develop fully-formed limbs or skin [88, 124]. Δ Np63 isoforms are involved in the regulation of embryonic stem cell populations, maintaining basal cells in a proliferative state, while TAp63 isoforms are involved in the initiation of epidermal stratification of simple epithelium, also inhibiting terminal differentiation [104]. Δ Np63 isoforms inhibit TAp63 and allow cells to respond to maturation signals [104].

Developmental diseases like EEC (ectrodactyly-ectodermal dysplasia-clefting [88]), AEC (ankyloblepharon-ectodermal dysplasia-clefting [88]), and SHFM (Split hand and foot malformation [125]) are a result of mutations in the p63 gene, either in the DBD domain or the SAM domain [88]. These include a frame-shift mutation at amino acid 525 in the SAM for EEC, and the following point mutations in the SAM domain for AEG: Lys 518 → Phe, Gly 534 → Val, Thr 537 → Pro [97, 100, 126]. AEG is characterized by alopecia, brittle nails, cleft lip, cleft palate, failure to develop teeth, and scalp infections [97]. SHFM is also caused by mutations in p63, specifically Lys 194 → Glu (exon 5), and Arg 280 → Cys (exon 7) in the DNA-binding domain of p63 [125]. The p63 protein is also involved in senescence [127, 128], glucose and lipid metabolism [129, 130], cell-cycle arrest and apoptosis, having a role in the DNA damage response to UV light [123].

Although expression data is sometimes conflicting (see Section 1.04), and some have concluded controversially that TAp63 is not a tumor suppressor [88], there is strong evidence that TAp63 functions as a tumor suppressor while Δ Np63 has oncogenic function by antagonizing the role of TAp63 [131, 132]. MEFs (mouse embryo fibroblasts) that have either p63 or p73 knocked-out are partially resistant to apoptosis induced by cisplatin, doxorubicin, or gamma irradiation. When either p63 or p73 was knocked out in coordination with p53, MEFs were more resistant to apoptosis than either p63^{-/-}, or p73^{-/-} knock out cells were alone, suggesting that p53 may have to cooperate with either p63 or p73 to induce apoptosis [131]. Transfection of TAp63 α into p63^{-/-} MEFs caused a significant increase in doxorubicin-induced apoptosis, which was not observed when Δ Np63 was transfected [131], indicating that p53 can cooperate with TAp63 α but not its dominant negative isoform. Lack of TAp63 is also linked with increased metastasis [93, 127-129, 133, 134]. TAp63 knockout mice (which still have

functional $\Delta Np63$ and are not lethal like whole p63 knockout mice) develop tumors that are metastatic when knocked out in concert with p53 [132]. This is contrasted to p53 knock-out mice that develop tumors that are non-metastatic. TAp63 γ is able to induce apoptosis when transfected into BHK (Baby hamster kidney cells), while $\Delta Np63\alpha$ variants cannot [60]. TAp63 apoptotic activity is reported to happen independently of p53 status [135], which is an interesting observation as it supports the role of TAp63 as a tumor suppressor not relying on p53, while p53 may require p63 or p73 for its apoptotic function. DNA-damage induced by irradiation and UV light results in up-regulation of TAp63 γ [136], and resistance to p53-mediated apoptosis in colorectal cells is reversed when treated with TAp63 γ [137], further supporting TAp63's tumor suppressor function. In contrast, $\Delta Np63$ negatively regulates p53, TAp63, and TAp73 function [60, 107, 138]. It can block p53 transcription targets by acting as a p53 negative regulator in addition to a TAp63 negative regulator mediated by its dominant negative function - being incorporated into heterotetramers with p53 - and through this process rendering the tetramer inactive [107]. $\Delta Np63\alpha$ is able to repress both TAp63 γ and p53 transcriptional activity when co-expressed with either TAp63 γ or p53 in SAOS-2 cells [60]. It is also involved in suppressing TAp73 dependent apoptosis, being implicated in survival of squamous cell carcinomas [138].

TAp63 recognizes specific DNA response elements including p53 response elements (p53RE) characterized by the sequence RRRC(A/T)(A/T)GYYYRRRC(A/T)(A/T)GYYY where R is any purine, and Y is any pyrimidine [139]. However, TAp63 specifically prefers to bind to p63 response elements (p63RE) that are similar in sequence to p53RE with important differences at the fifth and sixteenth positions. TAp63 can bind to these sequences with higher affinity, with at least two-fold greater expression of targets when bound to the p63RE compared to the p53RE. In fact, 86% of all p63 targets did not use the canonical p53RE and showed differences. The

specific p63RE sequence is 5'-RRRC(A/G)(A/T)GYYYRRRC(A/T)(C/T)GYYY-3' [139, 140]. Bold sections highlight important differences on the p63RE compared to the p53RE. One protein that showed higher transcription induced by TAp63 γ compared to p53 was the tumor suppressor ING1 (described later in this section) [139].

TAp63 has many transcriptional targets: Pro-apoptotic targets include bax [141], *Noxa* (PMAIP1 - Phorbol-12-myristate-13-acetate-induced protein 1 [142]) and PERP (p53 apoptosis effector related to PMP-22 [143]) [131], all intrinsic activators of apoptosis relying on caspase 9 that is activated by mitochondrial signals [144]. Bax induces mitochondrial mediated apoptosis by mediating the release of cytochrome c from the mitochondria, which activates the apoptosome and leads to activation of caspase-9, and is also a target of p53 and p73, although in p63^{-/-} p73^{-/-} double-knock-out MEFs, despite the presence of p53, bax was not induced in the presence of cellular stress [131], indicating that p53 alone cannot induce bax without p63 or p73, while p63 and p73 can induce bax independent of p53 status [88, 131]. This independent activation was shared for both *Noxa* and PERP as well [131]. Extrinsic targets of apoptosis (apoptotic pathways relying on caspase-8 initiated by death receptors [144] transactivated by p63 include CD95/Fas [141], TNF-R (tumor necrosis factor receptor) [141], and TRAIL-R (Tumor necrosis factor related apoptosis inducing ligand receptor) [141, 144], all able to be transactivated by TAp63 α [141].

TAp63 can mediate cell cycle arrest by inducing the transcription of p21 [100]. The p21 protein can be transactivated by all TAp63 isoforms [100], and is a shared target for both p53 [145] and TAp73 [146]. Surprisingly, Δ Np63 β and Δ Np63 γ can also activate p21 [100]. During malignant conversion from normal cells to malignant SCC (squamous cell carcinoma), the

binding capacities of TAp63, p53, and TAp73 to p21 are all reduced in malignant cells with only Δ Np63 retaining binding ability [147].

TAp63 is also able to transactivate targets involved in the suppression of invasion and metastasis, including dicer [134], and maspin [148]. Dicer is a type III RNase able process precursor miRNAs exported to the cytoplasm, providing the first interaction necessary to convert them into finished miRNAs [149]. This includes miRNA-10b, which is responsible for the anti-invasive and anti-metastatic effect seen in TAp63 regulation (TAp63 also directly targets this miRNA for transcription) [134]. This observation provides a mechanistic explanation of p63's anti-metastatic role as observed with TAp63^{-/-} mice. One of mutant p53's oncogenic gain-of-function effects is the ability to inhibit TAp63's activation of dicer, thereby promoting metastasis [150]. Maspin (mammary serpin [151]) is a serine protease inhibitor [152] that is a transcriptional target of TAp63 γ [148]. Maspin is involved with inhibiting tumorigenesis and metastasis in nude mice without affecting proliferation, and therefore acts as a secondary tumor suppressor by down-regulating malignant properties [151].

ING1 (inhibitor of growth protein 1) is tumor suppressor transactivated by TAp63, while not being transcribed at the same levels by p53, showing that p63 preferentially transactivates some genes over p53. It is involved in apoptosis [153], and senescence [154], and is associated with improved survival rates in squamous cell carcinoma [153] and breast carcinomas [155].

In addition to targeting tumor suppressive proteins for transcription, p63 also has oncogenic targets, including Mdm2 (Murine double-minute 2) [100], Hsp70 (Heat shock protein 70) [100], and VEGF (Vascular endothelial growth factor) [156]. Mdm2 (see Section 1.8 for description of this protein) is transactivated by Δ Np63 β , Δ Np63 γ , and surprisingly both TAp63 β , and TAp63 γ [100]. Hsp70 (see Section 1.9 for description of protein) is transactivated by

Δ Np63 α , but repressed by all TAp63 isoforms and ANp63 β [100]. VEGF is an important mediator of angiogenesis, often up-regulated in invasive cancer [157]. VEGF is repressed by TAp63 γ , and transactivated by Δ Np63 α [156]. Although there is controversy regarding p63's role as an oncogene or tumor suppressor, it is commonly accepted that TAp63 variants have tumor suppressor roles, while Δ Np63 variants have oncogenic roles [132, 134], and thus is important to understand the processes that regulate these proteins in order for targeted therapies involving these proteins to be feasibly developed.

1.06 - Regulation of p63

The p53 family including p63 is regulated by a multitude of different proteins and pathways. Positive regulation (activation) of p63 is mediated by the following proteins: The receptor TLR3 (Toll-like receptor 3 [144]) is able to up-regulate TAp63 α isoform expression specifically, and induces apoptosis through both extrinsic apoptotic TRAIL signaling, and intrinsic apoptotic *Noxa*-induced signaling [144]. This apoptotic activation was not seen in cells that over-express Δ Np63 α [144]. The tyrosine kinase c-Abl (Abelson murine leukemia viral oncogene homolog 1) is able to activate p63 expression using the post-translational modification of phosphorylation [158]. Both Δ Np63 and TAp63 are able to be activated in this manner by c-Abl [158, 159]. The tyrosine sites necessary for this activation are Tyr 55, Tyr 137, and Tyr 308 on Δ Np63, and Tyr 149, Tyr 171, and Tyr 289 in TAp63 [159]. TAp73 is activated by c-Abl through phosphorylation, and also contains three tyrosine sites which are analogous to those seen on the p63 protein [158, 159].

The proteins ASPP1, and ASPP2 (Ankyrin-rich, Src homology 3 domain, proline-rich proteins 1 and 2 [88]) stimulate p63, p53, and p73 mediated expression of bax, and PUMA

without inducing p21 expression [160], suggesting that p63 can be activated in such a way that induces transcription of only a subset of its targets. This illustrates the potentially vast flexibility of different p63 activation patterns and cellular effects.

The kinase IKK β (inhibitor of nuclear factor kappa-B kinase subunit beta) can also stabilize TAp63 γ protein levels by phosphorylation of the TA domain (specific amino acid is unknown). It is proposed that this phosphorylation prevents ubiquitination of TAp63 γ thereby stabilizing it. Other isoforms of TAp63 are not mentioned in this study [161].

Cables1 (CDK5 and Abl enzyme substrate 1) can associate with the TAD and SAM domains of TAp63 α , stabilizing this isoform's protein levels by preventing it from being ubiquitinated and undergoing subsequent proteasome degradation [162].

Both Pin1 and PML (pro-myelocytic leukemia protein) interact with TAp63 α and Δ Np63 α isoforms stabilizing their protein levels [163, 164].

Negative regulation of the p53 family is mediated by many different processes including mutations (common for *TP53*, but very rare for *TP63* [58, 84, 117]); loss of heterozygosity, which is defined as a chromosomal event that causes the deletion of the entire gene and chromosome region [165] (possible for *TP73* [86], but *TP63* does not undergo loss of heterozygosity and is frequently amplified in cancer [58, 85]; and epigenetic silencing (where *TP63* is often inactivated in this way in chronic lymphocytic leukemia [166], but not often in other cancers). In fact, the p63 protein is primarily regulated at the protein level rather than the gene and transcript levels: TAp63 α is specifically regulated by its own TI domain [102] (see section 1.05), and all TA isoforms of p63, p73, along with the p53 protein are negatively regulated by Δ Np63, which is able to inhibit their transactivation function [60] (see section 1.05). It is thought that Δ Np63 can do this in at least two ways: Direct competition of binding sites due

to high sequence identity between the nuclear binding sites of these proteins [60], and by a dominant negative effect, where $\Delta Np63$ is incorporated into heterotetramers with TAp63, TAp73, or p53, which are rendered transcriptionally incompetent. Under pre-cancerous and cancerous conditions, mutant p53 may also undergo an oncogenic gain-of-function where it mimics $\Delta Np63$, and is able to suppress p63 and p73 transactivation abilities by forming inactive heterotetramers with p63 or p73 variants [167, 168], even though p53 is normally unable to interact and form heterotetramers with p63 or p73 [167]. This is potentially crucial in understanding how inactivation of p53 can be sufficient to cripple tumor suppressor activity in developing malignancies, by not only through loss of its p53 tumor suppressor function by mutation, but also by interfering with TAp63-mediated anti-tumor pathways, promoting invasion, and metastasis. This is mediated specifically by forming heterotetramers with TAp63 and inactivating its transcriptional function [167, 168]. Since mutant p53 can specifically inactivate TAp63, this supports the hypothesis that the TA isoforms of p63 do indeed function as tumor suppressors, as they are targeted by specific cancer mechanisms. The classic definition of a tumor suppressor (Knudson two-hit hypothesis), does not sufficiently cover all of the important tumor suppressor proteins that do not undergo mutations in cancer. In fact, what constitutes a tumor suppressor has been re-classified into two groups – Type I and Type II tumor suppressors [169]. Type I fall under the Knudson hypothesis and are lost due to mutation or deletion (such as p53 and RB), while Type II tumor suppressors are not mutated or deleted at the gene level (such as ING1, and maspin) but have reduced protein levels in invasive cancers compared to normal tissues [169, 170]. TAp63 appears to function as a Type II tumor suppressor, and this would explain why it's not commonly mutated in cancer.

Besides its own family members, other proteins are able to negatively regulate p63: Dlx3 (Distal-less homeobox 3) induces Δ Np63 degradation dependent on post-translational phosphorylation of Δ Np63 [171], while RACK1 (Receptor for protein kinase C) [172], targets Δ Np63 for proteasome degradation [173]. The Ubc9 SUMO-conjugating enzyme can negatively regulate Δ Np63 α by the ubiquitin-like sumoylation of Lys 582 [174], while ATM [175], CDK2 (Cyclin-dependent kinase 2) [175], p60s6K [175], HIPK2 (homeodomain-interacting kinase 2) [176], GSK3 (glycogen synthase kinase 3) [177], p38 mitogen activated protein kinase [178], and Raf1 (Raf proto-oncogene serine/threonine kinase 1) [171] are all kinases that can negatively regulate Δ Np63 α through phosphorylation. The TAp63 isoforms are also negatively regulated by phosphorylation but by a different kinase than those regulating Δ Np63 isoforms. The kinase PIK1 (polo-like kinase 1) can negatively regulate TAp63 isoforms by phosphorylation of Ser 52 in the TA domain [179].

Phosphorylation and sumoylation are important mechanisms of post-translational regulation for the p63 protein, and the other members of the p53 family as well, but another very important and frequent method of negative regulation for the p63 protein involves the post-translational modification of ubiquitination, mediated by several members of the E-3 ligase family. The process of ubiquitination is described in the next section, but regulation by ubiquitination may result in many different inhibitory processes including protein-protein interference, sub-cellular localization, lysosome-mediated protein degradation, and proteasome-mediated protein degradation [180, 181]. Of these, proteasome-mediated degradation is a major process that ubiquitination results in to negatively regulate the p53 family [182, 183]. The next two sections will describe the ubiquitin-proteasome system, and the E-3 ligases responsible for regulating p63.

1.07 – The Ubiquitin-Proteasome System (UPS)

The proteome of the cell is maintained in part by the ubiquitin-proteasome system, a tightly regulated and complex cellular system that governs degradation of proteins [180, 181]. The proteasome is the primary protein-degradation factor; a multi-subunit protein complex located in both the cytoplasm and nucleus that can recognize tagged proteins for degradation [181, 184]. The 26S proteasome is composed of the 20S catalytic core and the 19S regulatory cap: The core is composed of two alpha and two beta rings each containing seven subunits, which form the catalytic pore that possesses three proteolytic abilities including trypsin-like, chymotrypsin-like, and caspase-like proteolysis, while the cap recognizes substrates ubiquitinated in a specific manner and selectively allows these into the catalytic core [181, 184] (Figure 6).

Ubiquitin itself is a small 8.5 kDa polypeptide that functions primarily as a regulatory molecule [185, 186]. It can be ligated onto specific lysine residues on target proteins [181, 184], and can also attach to itself at any of its own lysine residues including the Lys 6, Lys 11, Lys 27, Lys 29, Lys 33, Lys 48, and Lys 63 [186]. If a single ubiquitin molecule is attached to a substrate, this is referred to as mono-ubiquitination, and if many ubiquitin molecules are attached to different lysine residues on a substrate, then it is referred to as multi-ubiquitination [184, 186]. Mono- and multi-ubiquitination can result in protein activation, functional interference, endocytosis, membrane trafficking, and sub-cellular transport [186-188], but not proteasome degradation. Instead, when one long chain of ubiquitin molecules are attached to a lysine

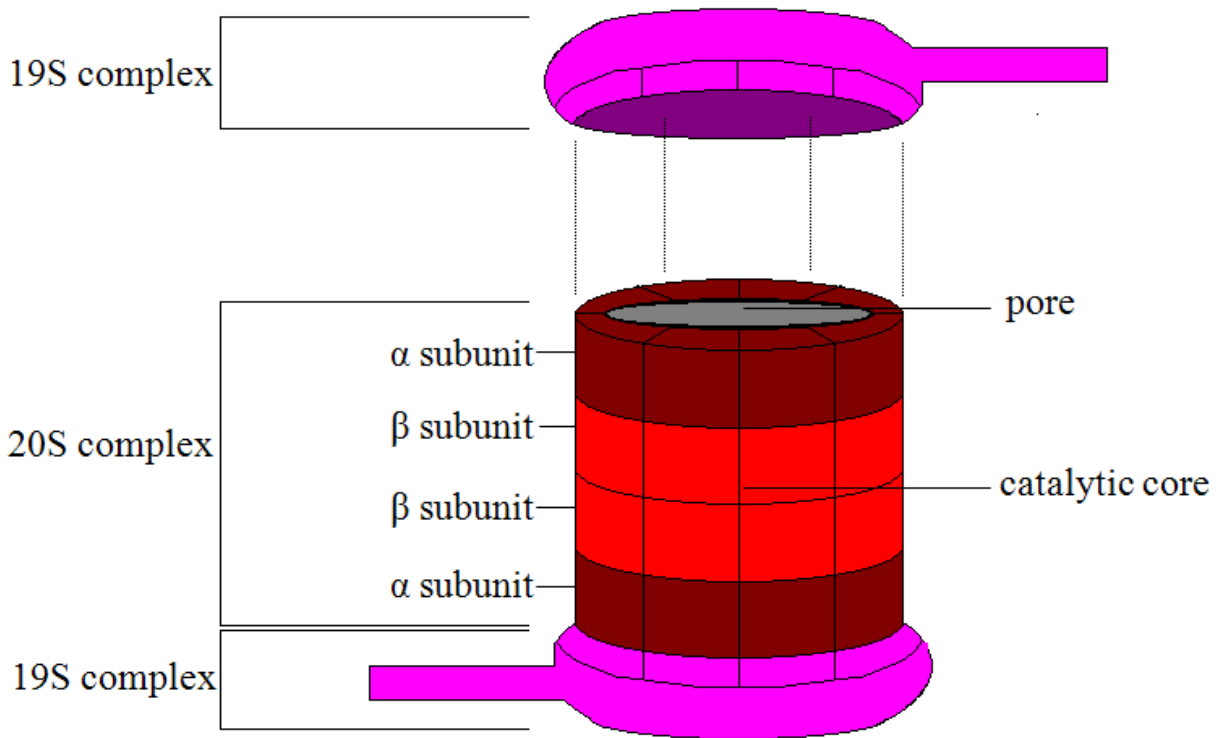


Figure 6 – The 26S Mammalian Proteasome.

Major sections of the 26S mammalian proteasome, including the two 19S regulatory complexes responsible for ubiquitin-recognition (“lid” section sticking out) and ATP hydrolysis (pink segmented “base” section), and the 20S core complex made up of two alpha subunits (each containing seven polypeptides – $\alpha 1$, $\alpha 2$, $\alpha 3$, $\alpha 4$, $\alpha 5$, $\alpha 6$, and $\alpha 7$) forming the entry sites into the core, and two beta subunits (each containing seven polypeptides $\beta 1$, $\beta 2$, $\beta 3$, $\beta 4$, $\beta 5$, $\beta 6$, and $\beta 7$) forming the core itself and also containing the proteasome’s enzymatic abilities. This figure was based on information obtained in Adams, 2004 [189], and Jung et al. 2009 [181].

residue on the target substrate, which is referred to as poly-ubiquitination [184, 186], only then can the 19S regulatory subunit recognize the protein substrate and target it for degradation [181]. Furthermore, the type of poly-ubiquitination that is recognized by the 19S proteasome unit is specific: poly-ubiquitin chains linked at Lys 48 (called a “closed” conformation) are selectively targeted by the proteasome [190], while those linked by Lys 63 are not recognized by the proteasome, and are instead involved in other pathways such as lysosome mediated degradation [191].

Ubiquitin is attached to a target substrate through a multi-step process involving three different classes of enzymes (Figure 7): An E-1 activating enzyme binds the C-terminal glycine residue of an ubiquitin molecule onto a cysteine residue on the E-1 enzyme forming a thioester bond. This reaction is ATP dependent. The E-1 enzyme then transfers the ubiquitin onto an E-2 transfer enzyme, which accepts the C-terminal glycine of the ubiquitin molecule onto a cysteine residue on the E-2 enzyme [181]. An E-3 ligase enzyme is then needed to catalyze the transfer of ubiquitin from the E-2 transfer enzyme to the target substrate [181]. Each type of E-3 ligase targets a specific set of substrates, and E-3 ligases are quite numerous, numbering in the hundreds [181, 192]. In the case of poly-ubiquitination, an additional step involving an E-4 chain elongation enzyme is necessary to form poly-ubiquitin chains [193]. Sometimes, the E-3 enzyme has an E-4 ability, and other times another protein is involved with ubiquitin chain elongation [194]. There are different categories of E-3 ligases, separated by how they catalyze the ligation of ubiquitin to the substrate. Those containing the HECT (homologous to E6-AP carboxyl terminus) [195] domain form a catalytic intermediate with ubiquitin, receiving ubiquitin directly from the E-2 transfer enzyme onto a cysteine residue and transferring the ubiquitin or ubiquitin chain ad-hoc onto a lysine residue on the target substrate [194, 196]. In contrast to

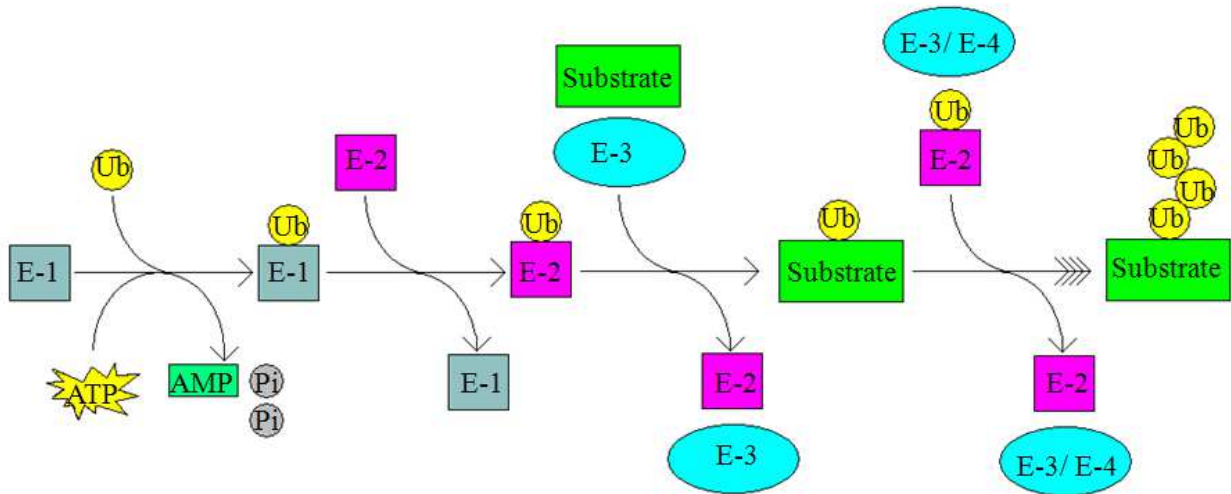


Figure 7 – Process of Ubiquitination.

The process of ubiquitination is carried out by at least three enzymes: An ubiquitin molecule is attached to a cysteine residue on an E-1 activation enzyme in an ATP-dependent process. Next, the ubiquitin is transferred onto the cysteine residue of an E-2 transfer enzyme. An E-3 ligase enzyme then coordinates ubiquitin transfer from the E-2 transfer enzyme onto a lysine residue of a target substrate. To attach poly-ubiquitin chains to one substrate requires an E-4 enzyme that can attach subsequent ubiquitin molecules onto each other's lysine residues. This ability may be possessed by the original E-3 ligase enzyme, or be acquired from another enzyme. This figure was based on information obtained in Hochstrasser 2006 [194], Hoppe et al. 2005 [193], Jung et al. 2009 [181], and Wong et al. 2003 [192].

HECT domains, the second major group of E-3 ligases contains the RING (really interesting new gene) domain [196]. RING domains form a double hairpin loop, coordinated by two zinc ions, which catalyze the transfer of ubiquitin by binding to the E-2 enzyme and the target substrate, thereby acting as a scaffold for direct E-2 to substrate ubiquitin transfer [194, 196] (Figure 8).

1.08 – Regulation of p63 – E-3 ligases

The E-3 ligase Mdm2 (Murine double minute 2 protein, also known as Hdm2 in humans [197]), is the most well-known E-3 ligase regulating the p53 family. The primary negative regulator of p53, Mdm2 is bound to and inactivating p53 in unstressed cells under normal conditions [198]. It is able to mono-ubiquitinate p53 by binding to its transactivation domain [199], resulting in subcellular transport and proteasome mediated degradation (after recruiting an E4-ligase for poly-ubiquitination, discussed later) [200]. Mdm2 has a RING domain located near the C-terminus [198, 200], responsible for its E-3 ligase activity, along with an N-terminal region necessary for interaction with p53 [199]. Mdm2 is able to interact with other members of the p53 family. It can bind to Δ Np63 in the nucleus with its N-terminal domain and mediate transport of Δ Np63 to the cytoplasm [177]. Mdm2 can also bind to and mono-ubiquitinate p63 [177, 201], however, it either has no effect on p63 protein levels [202], or actually stabilizes p63 protein levels [201]. Despite lack of degradation, Mdm2 is able to inhibit p73 function, and can weakly inhibit p63 function including p63-mediated p21 induction, and apoptotic activity [202]. In contrast to the last observation, a separate study did not find that Mdm2 was able to inhibit p63 transactivation function [203], casting doubt on whether Mdm2 is a major p63 regulator, although perhaps the effect was too weak to detect in the second study. If it does indeed regulate p63 function, this is likely due to it mediating the nuclear export of p63 [202], taking p63 into the

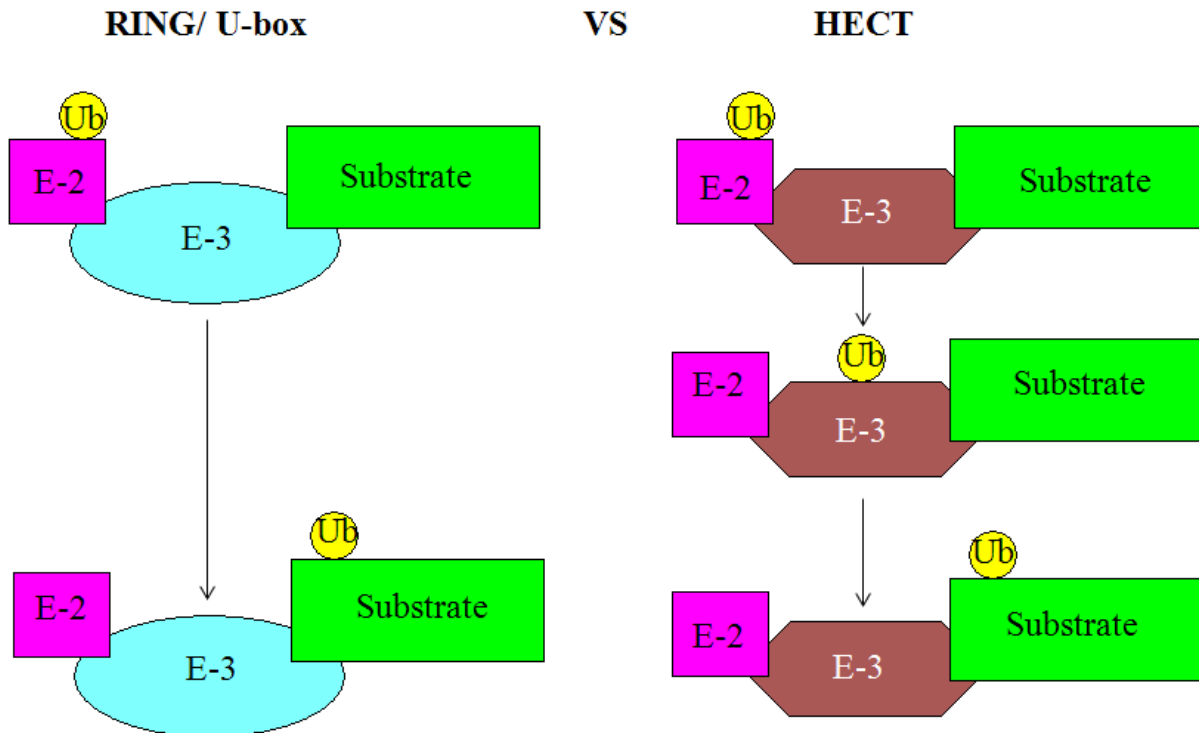


Figure 8 – Types of E-3 Ligases – Functional Comparison.

RING/ U-box-type E-3 ligases VS HECT-type E-3 ligases during ubiquitin (Ub) transfer from the E-2 transfer enzyme to the target substrate. RING and U-box E-3 ligases act as a scaffold between the E-2 and substrate proteins allowing for direct ubiquitin transfer from the E2 to the substrate. HECT-type E-3 ligases act as a catalytic intermediate, first accepting the ubiquitin molecule from the E-2 enzyme before transferring it onto the substrate. This figure was based on information obtained in Hochstrasser et al. 2006 [194], and Metzger et al. 2012 [196].

cytoplasm where it cannot target genes for transcription. A specific sequence in the TAD domains of p63, p73, and p53 is responsible for mediating Mdm2 binding: Phe-Phe-x-x- Φ -x-x-Lys (where x = any amino acid and Φ = either leucine or isoleucine) [89]. For Δ Np63, Mdm2 binds to a different site located in the SAM domain [177]. Interestingly, Mdm2 is trans-activated by p53 [204] and by TAp73 [88], illustrating a negative feedback loop where p53 is inducing the expression of its own negative regulator. Fbw7 is an E-3 ligase, that can target Δ Np63 for degradation in the cytoplasm, after it has been exported from the nucleus by Mdm2, demonstrating cooperation between those two E-3 ligases in degradation of the Δ Np63 isoform [177]. TAp63 is not mentioned as an Fbw7 target in this paper, and it may be the case that Fbw7 is not a major regulator of the TAp63 variants. Mdm2 is also assisted by another protein with E-4 ligase function to facilitate poly-ubiquitination of substrates.

The protein UBE4B (Ubiquitination factor E4 B [197]) is an E-4 ligase that promotes poly-ubiquitination of p53 in conjugation with Mdm2 using a U-box domain for its E-4 ligase function [197]. Since Mdm2 mono-ubiquitinates p53, this additional function is needed to result in p53 being tagged with a Lys 48 linked poly-ubiquitin chain for proteasome recognition. However, UBE4B is not known to regulate p63, possibly explaining why Mdm2 cannot target p63 for proteasome-mediated degradation.

A protein similar to Mdm2 called MdmX (also known as Mdm4) can also regulate members of the p53 family. Like Mdm2, MdmX also contains the p53-binding domain, along with the C-terminal RING domain. However, although some studies were unable to demonstrate that MdmX's RING domain functioned in the same capacity as Mdm2's RING domain, despite sharing almost 50% identity, one was able to show that like Mdm2, MdmX could indeed facilitate the ubiquitination of p53 [205]. Furthermore, MdmX is able to stabilize Mdm2 by

forming hetero-oligomers, increasing the capacity for Mdm2 to ubiquitinate target substrates [205]. However, MdmX is unable to target p53 for degradation despite being able to ubiquitinate the protein, although it does inhibit p53 transactivation ability [202]. Like p53, MdmX cannot target either p63 or p73 for degradation, and actually stabilizes p73 protein levels [202, 206]. Despite being unable to affect the protein levels of TAp63 α or TAp63 γ , one study did observe MdmX to interfere with the transactivation abilities of these proteins, by exporting the proteins into the cytoplasm from the nucleus [202]. MdmX often uses non Lys 48 linked chains for poly-ubiquitination of substrates [207], which could explain why it doesn't target any of members of the p53 family for proteasome-mediated degradation.

Another E-3 ligase shown to regulate p63 is Itch/AIP4 (Atrophin-1 interacting protein 4), an 113 kDa E-3 ligase belonging to the HECT family [195]. It is the primary negative regulator of p63 and p73, active as a monomer, and able to poly-ubiquitinate both proteins, thereby targeting them for proteasome degradation [195, 208, 209]. Itch/AIP4 contains four WW protein-protein interaction domains responsible for its binding with p63 by recognizing p63's Thr/Ser-Pro-Pro-Pro-x-Tyr (where x is any amino acid) sequence located just before the SAM domain on each protein (also called the PY motif) [195]. It also contains one proline rich motif, and one HECT domain at the C-terminus [195], responsible for its E-3 ligase function. Phosphorylation of threonine on the PY motif of p63 is crucial for interaction with Itch/AIP4's WW domain [210], thereby coupling post-translational phosphorylation regulation to E-3 ligase mediated ubiquitin-protein regulation of the p63 protein. Itch/AIP4 can also target p73 for proteasome mediated degradation [211], however, it is unable to target p53 [211].

The E-3 ligase Pirh2 (p53-induced protein with a RING-H2 domain [212]) is a RING-containing E-3 ligase able to interact with all three members of the p53 family. It is a

transcriptional target of p53 [212], and is part of a negative feedback loop where it can bind to and poly-ubiquitinate p53 in cooperation with the E-2 enzyme UbcH5b [213]. It can also bind to p73 and induces proteasome-mediated degradation [214, 215], and can also bind to and ubiquitinate both TAp63 and Δ Np63 to induce proteasome-mediated degradation [172, 216]. In addition, it can also bind to the p21 downstream target of the p53 family proteins, and target p21 directly for proteasome degradation [216].

The E-3 WWP1 (WW-containing E-3 ubiquitin protein ligase 1), targets both TAp63 and Δ Np63 for proteasome degradation [217]. Binding occurs between the PY motif on the p63 isoforms and the WW (tryptophan-tryptophan) domains on WWP1 [217]. The HECT domain is needed for this ubiquitination and degradation [217]. When WWP1 is knocked down by siRNA, endogenous levels of Δ Np63 decrease in immortalized breast cancer cell lines, but surprisingly this increases the protein levels of TAp63 and promotes apoptosis in HCT116 colon cancer cells, rendering the cells sensitive to genotoxic agents cisplatin and doxorubicin [217]. WWP1 may display oncogenic, or tumor suppressor roles depending on what cell line it is overexpressed in, thereby being an important example of a context-dependent protein.

The E-3 ligase Nedd4 (neural precursor cell expressed developmentally down-regulated protein 4 [218]) also regulates p63. Like Itch/AIP4 and WWP1, Nedd4 contains a HECT domain responsible for its ubiquitin function [174]. It is able to specifically target Δ Np63 α , but not Δ Np63 γ for proteasome mediated degradation, and like the other HECT-containing E-3 ligases that regulate p63 (Itch/AIP4 and WWP1) it recognizes the PY motif located on Δ Np63 α 's SAM domain, explaining why it can't target the SAM-lacking Δ Np63 γ [174]. Although TAp63 α also contains the SAM domain, there was no mention of Nedd4 being able to target that particular isoform for degradation [174].

Finally, the last E-3 ligase able to regulate p63 mentioned in this review and the focus of this research on p63 regulation is a protein called CHIP (described in the following section).

1.09 – The E-3 Ligase CHIP

CHIP (C-terminus of Hsp70 interacting protein [219]) is a 35 kDa, 303 AA long chaperone-associated E-3 ligase. Its gene is located on chromosome 6, and only one known isoform is produced [219, 220]. The CHIP protein can be divided into three domains (Figure 9): an N-terminal TPR (tetratricopeptide repeat) domain, a central CC (coiled-coil) domain, and a C-terminal U-box domain. The TPR domain is a 34 AA long (spanning from AA 26 to AA 131) sequence responsible for protein-protein interactions [219, 220]. The CC domain spans from AA 128 to AA 229 and is responsible for CHIP dimerization into its active form – an asymmetrical heterodimer where only one U-Box domain is active [219, 221]. The U-box domain spans from AA 232 to AA 298 and is composed of two hairpin loops responsible for its E-3 ligase function [219]. The U-Box domain is structurally identical to the RING domain on other E-3 ligases, with the exception that instead of zinc ions coordinating its hairpin structure, it is instead coordinated by hydrogen bonding [222]. In addition, it is functionally similar to RING domains as well, catalyzing the addition of ubiquitin to target substrates in much the same way RING domains are able to [222]. However, one important functional difference as observed in multiple proteins containing U-box domains like CHIP and UBE4B, is the U-box's ability to mediate poly-ubiquitin attachment, making it capable of E-4 ligase function [197]. CHIP is able to ubiquitinate target substrates in cooperation with the UbcH5 family of E-2 enzymes, and forms Lys 48 linked poly-ubiquitin chains that are recognized by the proteasome for degradation [219, 223]. CHIP is also able to form Lys 63 linked poly-ubiquitin chains by interacting with the E-2



Figure 9 – The E-3 Ligase CHIP – Protein Structure.

This figure shows the protein structure of CHIP (C-terminal of Hsp70-interacting protein) containing the N-terminal “tetra-tricopeptide repeat” (TPR) domain, the central coiled-coiled (CC) domain, and the C-terminal “U-box” domain responsible for CHIP’s E-3 ligase function. This figure was based on information obtained in Ballinger et al. 1999 [220], and Paul et al. 2014 [219].

enzyme Ubc13-Uev1A [224]. CHIP is a highly conserved protein [219], and is expressed quite highly in tissues with high protein turnover (ex, skeletal muscle) [220]. CHIP^{-/-} mice are unable to survive thermal stress, and 20% of them die in the embryonic stage [219, 225]. CHIP is a key protein linking the ubiquitin-proteasome system to the heat shock response pathway, the latter being activated in response to abnormal physiological stress conditions such heat, cold, and oxygen deprivation [226-228]. The heat shock response involves activation of HSF1 (Heat shock factor 1), a transcription factor that promotes the transcription of heat shock proteins, which are responsible for maintaining protein stability via chaperone functions, assisting in proper folding [229, 230]. CHIP provides the link between heat shock and protein degradation by interacting with HSF1 [225], and two chaperone proteins, Hsp70 and Hsp90, determining protein fate by targeting proteins for degradation, which is mediated by ubiquitination of target substrates bound to the CHIP-heat shock protein complex by CHIP's U-box domain [227], or in cooperation with other E-3 ligases [231]. CHIP can bind to heat-shock chaperone proteins using its TPR domain [232]. CHIP interacts with Hsp90 (Heat shock protein 90) and Hsp-90 bound substrates (that tend to be unfolded proteins [219]). Hsp90 is able to inactivate CHIP and also Mdm2 [233], promoting protein refolding over degradation, and thereby stabilizing mutant p53 in cancer. CHIP also interacts with Hsp70 (Heat shock protein 70), by binding to Hsp70's C-terminal lid domain, and promoting CHIP-induced protein ubiquitination and degradation of misfolded Hsp70-bound substrates [219, 226, 231].

CHIP is thought to have both tumor suppressor and oncogenic roles that may be context dependent [227]. CHIP was found to be under-expressed in various cancers such as breast, gastric, and prostate, but over-expressed in gallbladder, gliomas, and esophageal cancers [227]. CHIP's tumor suppressor roles include the targeted degradation of Smad3 in cooperation with

Hsp70, but not with Hsp90 [234]. Smad3 is involved with activation of TGF- β (tumor growth factor beta) signaling [234], and is considered a proto-oncogene. CHIP can target the proto-oncogene c-myc by binding to it via CHIP's TPR domain, ubiquitinating it, and targeting it for degradation, although its U-box domain was not necessary for ubiquitination [235] suggesting that CHIP may only participate in c-myc targeting and another E-3 ligase may be involved. CHIP can also target EGFR (Epidermal growth factor receptor) for proteasome mediated degradation and it is considered to be a tumor suppressor in various carcinomas such as pancreatic cancer [236].

Despite its tumor suppressive roles, CHIP may also have oncogenic roles. CHIP interacts and ubiquitinates IRF-1 (interferon regulator factor 1), a tumor suppressor involved in apoptosis by activating caspases [237], targeting IRF-1 for proteasome degradation in heat stressed cells [238]. CHIP can also ubiquitinate and target the tumor suppressor AIF (apoptosis inducing factor) for degradation, thereby promoting cell survival [239]. Most importantly CHIP can target wild-type p53 for proteasome degradation [240]. Furthermore, a yeast two-hybrid assay (unpublished data) revealed CHIP to be a possible p63 interacting partner. In summary, CHIP demonstrates both oncogenic and tumor suppressor activities, and may have context dependent roles in cancer.

Due to the combined observations that CHIP can degrade both wild-type and mutant p53, and being a p63-interacting candidate as a p63 interacting protein, this study proposes that CHIP is a regulating protein of p63.

1.10 – Summary, Hypothesis, and Research Objectives

Cancer ranks as the second leading cause of death in North America. The most common types of cancers, comprising 85% of all cases are those that develop from epithelial tissues and are called carcinomas. Targeted therapy represents the most promising type of treatment for advanced carcinomas, but many types of carcinoma lack targeted therapy options. By developing new targeted therapies for these diseases, treatment response, overall survival, and quality of life can be improved (Section 1.01). Tumor suppressors are valid targets for these therapies as they are able to repress cellular proliferation, inhibiting cancer development. The p53 family is an important group of tumor suppressors able to prevent cellular proliferation and cancer development by inducing cell cycle arrest, apoptosis, and inhibiting invasion and metastasis. Although the most studied member of the family, p53, is often mutated in cancer, TAp63 rarely is, and may represent an important target for re-establishing tumor suppressor function (Sections 1.02, 1.03, 1.04, and 1.05). Since TAp63 is largely regulated at the protein level, and several E-3 ligases repress its protein levels and transcriptional function (Sections 1.06, 1.07, and 1.08), the most important pathway for TAp63 regulation may be the ubiquitin-proteasome pathway. The E-3 ligase CHIP can interact with heat shock response proteins, including many that are often over-expressed in cancer such as CHIP's binding partner Hsp70. CHIP itself is considered by many to be a tumor suppressor protein, but it is able to target p53 for proteasome degradation, possibly demonstrating context-dependent oncogenic roles (Section 1.09). Since p53 and TAp63 share high sequence identity, and a yeast-two hybrid screen identified CHIP as a possible p63-interacting partner, it may be possible that CHIP is an important TAp63 negative regulator.

Due to the above observations, the hypothesis of this study is that the E-3 ligase CHIP is a major protein regulator of the transcription factor TAp63, targeting TAp63 for ubiquitin-mediated proteasome degradation, and negatively regulates TAp63 tumor suppressor function.

This research has four specific objectives:

- 1) To test whether CHIP is a p63-interacting protein and ubiquitinating agent
- 2) To determine whether CHIP negatively regulates p63 protein levels through the proteasome pathway
- 3) To investigate whether CHIP negatively regulates p63 function including cell-cycle arrest, apoptosis, and whether presence of CHIP is associated with oncogenic effects such as increased cell survival and migration
- 4) To determine whether levels of endogenous CHIP in carcinoma cell lines and patient tissue samples are negatively correlated with levels of endogenous p63

Chapter 2 – Materials and Methods

I'd like to acknowledge the post-doctoral fellow Dr. Benfan Wang for his technical support throughout the following experiments in this section.

2.01 PCR

Polymerase Chain Reactions (PCR) are carried out for the five TAp63 α constructs (see Table 1.1 for primer details). N362 spans from AA 1 through AA 362 and contains the TAD and the DBD domains. N540 spans from AA 1 through AA 540 and contains the TAD, DBD, and OD domains. C108 spans from AA 108 through AA 641 and contains the DBD, OD, and SAM domains. C393 spans from AA 393 through AA 641 and contains the OD and SAM domains. C541 spans from AA 541 through AA 641 and contains the SAM domain. Working primer at a concentration of 10 pM was used. First, dH₂O was added, followed by 10 mM PFU Buffer (Stratagene, USA), 10 mM dNTP (1 μ L), 2.5 mg/ μ L of Gelatin to reduce background, Primer 1 (10 pM/ μ L), Primer 2 (10 pM/ μ L), DNA at 50 ng/ λ (2 μ L), and the PFU polymerase (5 U/ μ L) (Stratagene, USA). Samples were vortexed to mix constituents, spun down quickly, and PCR was run in a GeneAmp PCR System 9700 thermal cycler (Applied Biosciences, USA) with the following conditions: One initial denaturation cycle at 95°C for 1.5 min, 30 cycles of denaturation at 95°C for 1 min, annealing at 50°C for 30 seconds, and extension at 72°C for 3 min, and 1 cycle of final extension at 72°C for 5 min, before resting at 4°C. To confirm DNA size from PCR, agarose gels were made using 1% agarose in TAE buffer (1.5 g in 150 mL) (1.2% was used for the smaller C541 fragment). Ethidium bromide (4 μ L) was added to visualize DNA from a stock solution of 10 mg/mL. Samples were loaded in 8 μ L of 6 x loading buffer (0.25% Bromophenol Blue, 0.25% Xylene Cyanol, 30% Glycerol in dH₂O – Sigma USA) (total = 50 μ L), beside a DNA Ladder (4 μ L), and ran at 130 volts for 1.5 hrs. DNA bands were visualized under a UV trans-illuminator (Entela, USA).

Table 1 – Tap63 α Constructs

N362

Primer 1 Sequence: *AT GGATCC* ATG AAT TTT GAA ACT TCA CGG TGT

Primer 2 Sequence: *AT CTCGAG* TCA CTG CTT TCT GAT GCT ATC TTC

N540

Primer 1 Sequence: *AT GGATCC* ATG AAT TTT GAA ACT TCA CGG TGT

Primer 2 Sequence: *AT CTCGAG* TCA TGG GGG TGT GCA GTG GGA GGT GGA

C108

Primer 1 Sequence: *AT GGATCC* CCT CCG TAT CCC ACA GAT TGC

Primer 2 Sequence: *AT CTCGAG* TCA CTC CCC CTC CTC TTT GAT GCG

C393

Primer 1 Sequence: *AT GGATCC* CGA AGA TCC CCA GAT GAT GAA CTG TTA

Primer 2 Sequence: *AT CTCGAG* TCA CTC CCC CTC CTC TTT GAT GCG

C541

Primer 1 Sequence: *AT GGATCC* TGG CCA CAG TAC ACG AAC GTG GGG CTC GTG

Primer 2 Sequence: *AT CTCGAG* TCA CTC CCC CTC CTC TTT GAT GCG

DNA sequence for each of the forward (Primer 1) and reverse (Primer 2) primers of the p63 constructs generated in this study. Italicized areas show *Bam*HI (for Primer 1 sequences) and *Xho*I (for Primer 2 sequences) restriction enzyme sites.

2.02 Cloning

TAp63 α constructs were cloned into the *Bam*HI-*Xho*I restriction site of the pCMV-Tag3B vector (Stratagene, USA), carrying a kanamycin resistance gene. Extraction of DNA was performed using the Qiagen II Agarose Gel Extraction Protocol (QiaexII handbook, Qiagen, USA). pCMV-Tag3B was digested by mixing 10 x Fast Digest buffer (20 μ L) with *Bam*HI (3 μ L), *Xho*I (3 μ L), dH₂O (124 μ L), and 3 μ L of pCMV-Tag3B. Samples were vortexed and spun down quickly, and cooled at 37°C for 1-2 hrs. Each sample (200 μ L) was mixed with 20 μ L sodium acetate and 600 μ L isopropanol, and stored for 30 min in -20°C, then spun at high speed (15,000 x g) for 20 min at 4°C (in a cold room). Purification of DNA was done as follows: DNA was washed with 75% ethanol and vortexed briefly, before being spun down for 2 min at 15,000 x g. Ethanol was then removed, and the samples quickly spun down. The residual ethanol was removed using small pipette tips, and samples were air dried for 10-15 min before being dissolved in 30 μ L of Tris buffer (pH = 8.0) (10 mM). Samples were stored at -20°C. Vector extraction was performed using the Qiagen II Agarose Gel Extraction Protocol (QiaexII handbook). For ligation, 8 μ L of dH₂O was added to microfuge tube (100 μ L tube) followed by 4 μ L of 5x buffer, 5 μ L of DNA construct, 1.5 μ L of vectors, and finally 1.5 μ L of T4 DNA ligase for a total of 20 μ L. Samples were vortexed, spun down quickly at 15,000 x g, and incubated at 20°C for 1 hr. DH5 α bacteria aliquots were taken from -80°C and put on ice. Samples were incubated on ice for 5 minutes alongside DH5 α bacteria. DH5 α bacteria aliquots (50 μ L) were added to 10 mL culture tubes. In each culture tube, for each sample, 3 μ L of sample was added to 50 μ L of DH5 α bacteria aliquot (one aliquot per sample), and these samples were kept on ice for 1 hr. Remaining ligation products were stored at -20°C. pCMV-Tag3B vector samples were grown on kanamycin plates. Samples were incubated in a 42°C water bath for 1 min, 10 sec, and then kept on ice for 3-5 min. Samples were taken off ice, and 1 mL of LB

medium (Sigma Aldrich, USA) was added to each culture tube, and tubes were placed in a MaxQ 4000 rocker (Barnstead, USA) and rocked for 1 hr, 30 min at 37°C. Samples were transferred from culture tubes into microfuge tubes and spun down at 15,000 x *g* for 1 min. All but 50 µL of supernatant was removed from each sample, and samples were aspirated using a pipette, and then in the presence of a flame, transferred onto the appropriate bacterial culture plate, and spread across the plate using a sterile glass pipette. Bacterial plates were incubated at 37°C for 18 hrs, before being stored at 4°C. Colonies were taken from each plate and added to 5 mL of LB medium (Sigma Aldrich, USA) with either Ampicillin (50 µg/mL) for ampicillin plate samples, or kanamycin (25 µg/mL) for kanamycin plate samples. From each plate, six samples (taken from six colonies) were made. Tubes containing each sample were rocked overnight (18 hrs) at 37°C. The next day, DNA mini-prep was conducted using GeneJet Plasmid Mini-prep Kit (Thermo Scientific, USA). Each sample was digested using the *Bam*HI and *Xho*I restriction enzymes, and run on a 1% agarose gel before being visualized under an Ultraviolet Transilluminator (UVP, USA). A positive sample for each construct and vector was selected for use in transfection-based experiments.

Table 2 – CHIP shRNA Constructs

CHIP shRNA1

Primer 1: *GATCCCCGGAGCAGGGAATCGTCTGTTCAAGAGACAGACGATTGC
CCTGCTCCTTTTTTC*

Primer 2: *TCGAGAAAAA GGAGCAGGGCAATCGTCTG TCTCTTGAA
CAGACGATTGCCCTGCTCCGGG*

CHIP shRNA2

Primer 1: *GATCCCCAGGCCCTGGCCGACTGCCGTTCAAGAGACGGCAGTCGG
CCAGGGCCTTTTTTC*

Primer 2: *TCGAGAAAAAAGGCCCTGGCCGACTGCCGTTCTTGAACGGCAGTC
GGCCAGGGCCTGGG*

CHIP shRNA3

Primer 1: *GATCCCCGAAGAAGCGCTGGAACAGCTTCAAGAGAGCTGTTCCAG
CGTTCTTCTTTTTTC*

Primer 2: *TCGAGAAAAAAGAAGAAGCGCTGGAACAGCTCTCTTGAAGCTGTTCC
AGCGCTTCTTCGGG*

CHIP shRNA4

Primer 1: *GATCCCCACCACGAGGGTGATGAGGATTCAAGAGATCCTCATCACC
CTCGTGGTTTTTTC*

Primer 2: *TCGAGAAAAAACACGAGGGTGATGAGGATCTCTTGAATCCTCATC
ACCCTCGTGGTGGG*

DNA sequence for each of the forward (Primer 1) and reverse (Primer 2) primers of the CHIP shRNA constructs generated in this study. Italicized areas show *BgIII* (for Primer 1 sequences) and *XhoI* (for Primer 2 sequences) restriction enzyme sites.

2.03 Other Constructs

T7-tagged wild-type TAp63 α (obtained from NIH, USA), Myc-tagged AIP4 (obtained from Dr. Tony Pawson, Toronto, CA), His-tagged ubiquitin (UB) (obtained from Dr. Wei Gu, USA), Δ Np63 α (obtained from Dr. Xinbin Chen), all cloned into the vector pcDNA3.1 (Stratagene, USA). Mdm2 was cloned into pCMV-BAM-Hdm2 by Dr. Roger Leng. FLAG-tagged AIP4 was cloned into pCMV7-3FLAG (obtained from Dr. Azeddine Atfi, France). FLAG-CHIP was cloned into pCMV-Tag3A (Stratagene, USA) containing a kanamycin resistant gene. CHIP shRNA constructs 1, 2, 3, and 4 were all cloned into the vector pSUPER.gfp.neo (Oligoengine, USA) using the *BglIII* and *XhoI* restriction sites (see Table 2.2 for CHIP shRNA constructs). CHIP shRNA construct cloning was conducted previously to this study by Dr. Hong Wu.

2.04 Maximum Preparation DNA

In order to prepare working amounts of mammalian DNA, maximum preparation of DNA using bacteria was performed. Ampicillin agar plates were prepared for culturing bacterial colonies containing constructs made with the pcDNA3 and pSUPER expression vectors, while kanamycin agar plates were prepared for culturing bacterial colonies containing constructs made with the pCMV expression vectors. Plate medium was made using LB Agar Lennox (Bioshop Canada Inc., CA) at a concentration of 35 mg/L, with either 50 μ g/mL ampicillin, or 25 μ g/mL kanamycin. For max prep DNA, 1 μ L of DNA was introduced to 15 μ L of DH5 α bacteria in 10 mL culture tubes on ice, and kept on ice for 1 hr. Bacteria were thermally shocked for DNA uptake by immersing tubes for 1 min, 15 sec in a water bath set to 42°C, and then put on ice for 5 min. 1 mL of LB medium was then added, and tubes were placed in a MaxQ 4000 rocker set to

37°C for 1 hr, 30 min. 50 µL of sample were added aseptically to either ampicillin or kanamycin resistant plates (depending on the construct used), and kept in a bacterial incubator at 37°C for 18 hrs. The next day, colonies were transferred into 300 mL of LB medium with either 300 µL of kanamycin, or 600 µL of ampicillin added and rocked at 37°C for 18 hrs. All DNA was prepared from these solutions using the GeneJet Maxiprep Kit (Thermo Scientific, EU) protocol. Extracted DNA was stored in TE buffer at pH 8.0 (1 mM Tris.CL, and 0.1 mM EDTA) (Sigma Aldrich, USA), and DNA concentration was measured using an UV spectrophotometer (adding 10 µL of DNA sample to 990 µL of dH₂O, and measuring against a 10 µL TE buffer/ 990 µL dH₂O blank using DNA nucleotide analysis on the D40 UV Spectrophotometer (Beckman Coulter, USA). DNA samples between absorbance ratios 1.8 and 2.0 were considered good quality for transfection assays.

2.05 Cell Culture conditions and Cell Lines:

All cell lines used in this study were purchased from the American Type Culture Collection (ATCC, USA). These include the H1229 lung carcinoma cell line; the SAOS-2 osteosarcoma cell line; the MCF10 α breast epithelial cell line; the skin fibroblast cell lines BJ and BJ/DD; the squamous cell carcinoma cell lines SCC9, SCC15, SCC25, FADU, and A431; and the invasive melanoma cell lines Sk-mel-2, Sk-mel-5, M2, Sk-mel-8, Loxi-mvi, Mewo, and Hs89S-T. All cell lines were cultured in α -MEM (Minimal Essential Medium alpha) (Gibco Life Technologies Corp, USA) with 8% FBS (Fetal Bovine Serum – Sigma Aldrich, USA) added. Cells were kept in a humidified Forma Steri-Cycle Incubator (Thermo Fischer, USA) at 37°C with 5% CO₂. Medium was changed every two days until cells reached 80-100% confluence, and then sub-cultured by removing medium, briefly washing the cells with PBS (Phosphate

Buffered Saline – 137 mM NaCl, 2.7 mM KCl, 10 mM Na₂HPO₄, and 2 mM KH₂PO₄ at pH 7.4) (Sigma Aldrich, USA), and then detaching cells from the plates by incubating in 1% Trypsin-EDTA (Sigma Aldrich, USA) for 3 min at 37°C. Detached cells were spun down into pellets, and medium removed, before being re-suspended in fresh medium and subdivided into new plates.

2.06 Transient Transfection Assay

In order to introduce ectopic protein into cells, transfection was used. Transfection was performed using the calcium phosphate method. Calcium phosphate precipitates form when CaCl₂ and HEPES buffer are mixed, and when DNA is present, it is absorbed into these precipitates and is taken up by cells to affect the expression of genes [241]. To perform this transfection assay, plasmid DNA was added to dH₂O. Amounts of DNA added did not exceed 25 µg. 63 µL of 2 M CaCl₂ was added to each transfection sample, and dH₂O was added to bring up the total sample volume to 500 µL. Aliquots of HEPES buffer (500 µL) were prepared with the following reagents: 280 mM NaCl, 1.5 mM Na₂HPO₄*2H₂O, 12 mM dextrose, and 50 mM HEPES (Sigma Aldrich, USA) at pH 7.05. 500 µL of HEPES buffer was mixed with each 500 µL sample drop wise in the presence of bubbling. Samples were incubated at 20°C for 25 min, while cells were being prepared. Cells between 50-70% confluent were chosen for transfection, and medium was refreshed prior to transfection. Approximately 10 min before addition of samples, 10 µL of a transfection efficiency-increasing solution “QI” (Roche, USA) was added to each plate. Once 25 min elapsed, each sample was added drop-wise into cell culture plates. Cells were incubated with transfection buffer for 16 hrs, before medium was

removed, cells washed with PBS twice, and fresh medium replaced. After 24 hrs (40 hrs after transfection), whole cell protein was harvested from cells.

2.07 Stable Transfection Assay

H1299 or SAOS-2 cell plates (60-80% confluent) were transfected with 20 μg of one of the following: empty vector shRNA, CHIP shRNA1, 2, 3, or 4 (see transient transfection section for details). Medium was changed after 16 hrs, and 24 hrs after that (40 hrs after transfection), cells began drug selection. G418 (Geneticin) (Invitrogen, USA), a cytotoxic drug capable of inducing cell death by blocking polypeptide synthesis [242], was used to select for transfected cells (the PSUPER vector contains a G418 resistance gene). 1000 $\mu\text{g}/\text{mL}$ of G418 was added to the cell medium, and cells were cultured for four days before medium was changed, and fresh G418 added again. This process was repeated for two weeks until most of the cells were dead. Then, the concentration of G418 was decreased to 500 $\mu\text{g}/\text{mL}$ and cells continued treatment for another two weeks with medium being changed every four days until stable colonies of shRNA transfected cells formed. These cells were maintained at a G418 concentration of 500 $\mu\text{g}/\text{mL}$ and used in subsequent assays.

2.08 Whole-Cell Protein Extraction

Whole cell protein was extracted by putting culture plates on ice, removing medium, briefly rinsing cells with cold PBS before physically scraping cells from the plate, and suspending them in PBS. Cells were spun down into pellets (1 min at 15,000 $\times g$), and PBS was removed before adding 15 μL of a protease inhibitor and 120 μL of 1% NP40 Lysis Buffer (10% NP40 solution mixed in 50 mM Tris, 150 mM NaCl, 1 mM EDTA) (Sigma Aldrich, USA). Cell

samples were sonicated for 4-6 sec twice with a Sonic Dismembrator Model 100 (Fisher Scientific, USA) at 3 watts before resting on ice for 10 min, and then being spun down into pellets 15 min at 15, 000 x g) in a cold room (-4°C). Supernatant containing protein was collected for each sample and analyzed using Biorad Protein Dye Reagent (Biorad Laboratories, USA) – mixing 2 µL of protein sample with 200 µL of dye reagent and 800 µL of dH₂O, and then analyzing absorbance at 595 nm using a DU730 UV spectrophotometer (Beckman Coulter). Sample volume needed for a 40 µg amount of protein was calculated by dividing the absorbance by 2 (2 µL of protein sample used), and then dividing 40 (total protein amount in micrograms) by that number.

2.09 SDS PAGE/Transfer

In order to separate whole cell proteins, SDS PAGE was performed for all immunoblot assays. Proteins are separated through an acrylamide gel according to weight by an electric current (electrophoresis) [243]. 10-12% Acrylamide Gels were constructed (using 40% Acrylamide stock, 1.5 M Tris-8.8, H₂O, 10% SDS, 10% APS, and TEMED – Sigma Aldrich, USA), with a stacking gel composed of 5.1% Acrylamide, and immersed in gel tanks filled with 1 x Running Buffer composed of 25 mM Tris, 192 mM Glycine, and 1% SDS (Sigma Aldrich, USA) in dH₂O. Protein samples were mixed with an equal amount of 2 x loading buffer (0.1 M Tris pH 6.8, 20% Glycerol, 4% SDS, and 0.2% Bromophenol Blue) (Sigma Aldrich, USA), before being loaded into gels along with 2 µL of a Rec Protein Ladder (Fischer Bioreagents, USA), and run on a PowerPac 300 (Bio-Rad, USA) at 40 milliamps until the dye reached the bottom of the gel. Protein was transferred from gels to Immobilon nitrocellulose membranes (Millipore, USA) using a three buffer semidry transfer protocol: In a Transblot Semi-Dry Cell

(Bio-Rad, USA), two thick filter sheets were soaked in Anion Buffer 1 (0.3 M Tris, 15% methanol in dH₂O), and one thin sheet was soaked in Anion Buffer 2 (0.025 M Tris, 15% methanol in dH₂O) and stacked on the thick sheets. A section of nitrocellulose membrane, cut to match the size of the acrylamide gel, was soaked in methanol, and then Anion Buffer 2, and placed on the filter sheets. Then the acrylamide gel itself was soaked in Cation Buffer (0.025 M Tris, 15% methanol, 0.04 M Amino-N-Caproic Acid in dH₂O) (Sigma Aldrich, USA) and put on top of the nitrocellulose membrane. Bubbles were removed by gently wiping the membrane with a metal rod. Finally, one thin, and two thick filter sheets were soaked in Cation Buffer 3 and placed on top of the acrylamide gel. The transfer machine was then closed and plugged into a PS 500XT DC Power Supply (Hoeffer Scientific, USA), and the transfer was run at 75 milliamps per gel, for 1 hr, 15 min. Membranes were dried at 20°C for 4-18 hrs, and then stored at 4°C for subsequent immunoblot use.

2.10 Immunoblot Assay (IB)

In order to semi-quantitatively measure protein levels in cell lines, immunoblot assays were performed. Endogenous expression refers to native proteins already present in cell lines under normal culture conditions [244], while ectopic expression refers to proteins expressed in cells that are not normally expressed (proteins overexpressed by transfection for example) [245]. Nitrocellulose membranes were briefly rinsed in methanol, followed by 0.1 M TBS (Tris-buffered saline at pH 7.4) before being blocked by incubating membranes in 10 mL of TBST (0.1 M TBS with 1% Tween-20) (Uniqema Americas LLC, USA) and 4% powdered milk solution (Instant Skim Milk Powder – Smucker Foods, CA) for 1 hr at 20°C. Milk solution was removed and membranes washed in TBST for 5 min three times to remove excess milk, before being

incubated with 10 mL of the primary antibody/TBS solution, (see Table 3 – Primary Antibodies for a description of specific antibodies and concentrations used) for 1 hr, 30 min at 20°C. Membranes were washed with TBST for 5 min three times to remove excess primary antibody, and then incubated in 10 mL of the secondary antibody solution comprised of 2 µL of the secondary antibody specific to either mouse or rabbit (see Table 3), 1% powered milk, and TBST. Membranes were washed with TBST for 5 min three times to remove excess secondary antibody, brought into a dark room, and exposed to 400 µL of ECL solution (Western Lightning™ Plus-ECL – GE Healthcare, UK), comprised of equal parts oxidizing reagent (light solution), and enhanced luminol reagent (dark solution) for 1 min. Membranes were then gently blotted to remove excessive ECL solution, wrapped in Saran wrap, and enclosed in cassettes. In a developing room, Super RX-N X-Ray Films (Fuji Film Corporation, Japan) were placed over membranes, and exposed for 30 seconds to 10 min, before being developed in an Optimax X-Ray Film Producer (Protec, USA). Developed films were marked for protein size by matching the film up with the visible gel protein ladder on the nitrocellulose membrane, and then scanned at 600 dpi into *.tiff* files to generate immunoblot data. For multiple immunoblot assays on the same membrane, used membranes were stripped of old antibodies by briefly rinsing them in methanol, followed by washing in TBST for 5 min, and then incubating membranes at 50°C in glass tubes containing 50 mL of stripping buffer (mercaptoethanol, 10 mL of SDS, Tris pH 6.8, and dH₂O – Sigma Aldrich, USA). Membranes were then rinsed in dH₂O, and washed in TBST for 5 min three times before immunoblotting was repeated starting from the blocking step. Presence of a band at the appropriate molecule weights suggests that target protein is present in the sample. The protein β-Actin was immunoblotted as a loading control for this assay to ensure amount of protein is consistent between samples.

Table 3 - Antibodies

Protein Target	Primary Antibody	Dilution	Secondary Antibody
T7 epitope	Anti-human T7 (Novagen)	1:5000	Goat anti-mouse
p21 protein	Anti-human SC-817 (Santa-Cruz)	1:200	Goat anti-mouse
FLAG epitope	Anti-human M5 (Sigma Aldrich)	1:1000	Goat anti-mouse
FLAG epitope	Anti-human M2 (Sigma Aldrich)	1:1000	Goat anti-mouse
Mdm2 protein	Anti-human 2A10/SMP14 (Santa-Cruz)	1:200	Goat anti-mouse
Beta-Actin	Anti-human Actin (BD)	1:10000	Goat anti-mouse
Myc epitope	Anti-human Myc (Santa-Cruz)	1:100	Goat anti-mouse
His epitope	Anti-human His (Santa-Cruz)	1:100	Goat anti-mouse
HA epitope	Anti-human HA (Roche)	1:100	Goat anti-mouse
p63 protein	Anti-human 4A4 (Santa-Cruz)	1:200	Goat anti-mouse
CHIP protein	Anti-human CHIP (Santa-Cruz)	1:500	Goat anti-rabbit
AIP4 protein	Anti-human AIP4 (Abcam)	1:1000	Goat anti-mouse
p53 protein	Anti-human DO-1 (Santa-Cruz)	1:500	Goat anti-mouse

List of primary antibodies used in this study are shown in this table including the protein target, antibody name (and source), the working dilution used in immunoblot assays, and the secondary antibody used alongside the primary antibody during immunoblot analysis. Goat anti-mouse and goat anti-rabbit secondary antibodies were purchased from Jackson ImmunoResearch, USA.

2.11 - Co-Immunoprecipitation Assay

In order to test for protein-protein interactions, co-immunoprecipitation assays were performed. Target proteins are isolated by immunoprecipitation, alongside all substrates that interact with the target protein. The presence of a protein of interest in a co-immunoprecipitated protein fraction (analyzed by immunoblot) suggests interaction between the protein of interest and the immunoprecipitated protein [246]. Cell extracts were prepared using lysis buffer that contained 50 mM Tris-HCl (pH 7.4), 1 mM EDTA, 150 mM NaCl, 0.5% NP40, and 1 x protease inhibitor (Roche, USA). The protein concentration was balanced using the Bio-Rad Protein Assay. Approximately 500 µg to 1 mg of the lysates were immunoprecipitated with the indicated antibodies for 1 hr, incubated with protein A/G Plus-agarose (Santa Cruz Biotechnology) beads for 2 hrs at 4°C, and then washed three times with washing buffer containing 50 mM Tris-HCl (pH 7.4), 1 mM EDTA, 150 mM NaCl, and 0.2% NP40. The immunoprecipitated proteins underwent SDS-PAGE, nitrocellulose membrane transfer, and were analyzed by immunoblot. Whole cell lysates are immunoblotted for co-immunoprecipitated proteins and proteins of interest as a positive control.

2.12 – His-Ubiquitin Pull-Down Assay

To test for ubiquitination, a His-tagged ubiquitin construct was transfected into cells. Isolating His-tagged ubiquitin followed by subsequent immunoblotting for a protein of interest, can determine whether that protein has been ubiquitinated. Cells were transfected with His-tagged ubiquitin and the indicated expression plasmids. Thirty hours after transfection, cells were re-suspended in Buffer A (6 M guanidine HCl, 0.1 M Na₂HPO₄/NaH₂PO₄, 10 mM Tris-HCl (pH 8.0), and 10 mM imidazole (pH 8.0) and sonicated. Approximately 500 µg of cell

lysates were added to Ni-NTA (Nickel Nitrilotriacetic Acid) agarose, and were incubated at 20°C for 3 hr. Beads were then washed once with Buffer A, followed by two washes with Buffer A/TI (1 volume of Buffer A, 3 volumes of Buffer TI [25 mM Tris-Cl, 20 mM imidazole, pH 8.0]) and one wash with Buffer TI; all of the washes used 1 mL of buffer. After extensive washing, the precipitates were mixed with 2 x SDS loading buffer and boiled for 6 min. Samples then underwent SDS-PAGE and immunoblot analysis as normal. A known regulator of p63 ubiquitination, AIP4 is overexpressed by transfection in one sample as a positive control, while an empty vector (pcDNA3) is transfected into another sample as a negative control.

2.13 – MG132 Treatment

The proteasome blocker MG132 (Carbobenzyl-Leucine-Leucine-Leucine-Aldehyde) [247] (Sigma Aldrich, USA) was used in some transfection assays in order to visualize protein levels in the presence of an impaired proteasome. MG132 inhibits proteasome function by blocking both the chymotrypsin-like and caspase-like sites in the catalytic core of the proteasome [247]. MG132 solution was prepared in DMSO (Sigma Aldrich, USA) by adding 10 mM of MG132 to 0.8 mL of DMSO. After being incubated in transfection buffer for 16 hrs, transfected cells were washed with PBS twice as normal, then incubated in fresh medium at 37°C for 8 hrs, before 20 µM of MG132-DMSO solution was added. Cells were incubated in MG132 solution overnight for 16 hrs, before whole cell protein was harvested, and protein underwent SDS-PAGE and immunoblot as normal.

2.14 - Colony Forming Assay

In order to test for cell survival, a colony forming assay can be done where cells are allowed to grow in the presence of a selection agent. Cells that are viable form colonies, and survival can be measured by number of colonies formed, compared to a negative control. Colony forming assays were done after HEPES buffer transfection with the appropriate plasmids (either transient or stable transfection). Cell number from each transfection plate was estimated using a Bright Line Counting Chamber 3200 (Hausser Scientific, USA) using the following formula: # of cells per cubic millimeter = # cells counted per square millimeter x dilution factor x 10 (one milliliter = 1000 cubic millimeters). Cells were then sub-cultured into 6-well plates (using 1000 cells per well), and then cultured in the cytotoxic G418 (Geneticin) drug (Sigma Adrich, USA) at a concentration of 500 $\mu\text{g/mL}$ (used for transient transfections), or 1000 $\mu\text{g/mL}$ (used for stable transfections). Medium was changed every three days, and cells were cultured in this way for two weeks. After colony formation over this period of time, medium was removed and cells were washed twice in PBS. Cells were fixed in a 4% Formamide solution for 15 min, and then washed in crystal violet dye for 20 min. Tap water was used to rinse away excessive crystal violet dye until dyed colonies of cells were clearly visible. An IXUS70 Canon camera was used to take pictures of colonies, and number of colonies in each plate was counted. Experiments were repeated thrice (n=3) and run in triplicate, and the average number of colonies for each transfection regimen was calculated from three cell counts, and this data was plotted as a bar graph in Microsoft Excel. Error bars represent the standard deviation, and an unpaired Student's T-Test assuming unequal variance (also known as a Welch T-Test) was used to determine whether two average values were significantly different from each other (Microsoft, USA). An empty vector (pcDNA3) is transfected into one sample as a negative control.

2.15 - Luciferase Reporter Assay and β -Galactosidase Assay

In order to test for transcription of a target gene, a luciferase reporter gene containing luciferase and the gene of interest is transfected into cells, and cells are measured for bio-luminescence as luciferase converts luciferin to oxyluciferin to produce bio-luminescence [248]. Bio-luminescence is detected by a spectrophotometer, and absorbance is directly proportional to the amount of luciferase (and therefore the gene of interest as well) being transcribed. H1299 or SAOS2 cells (75-80% confluent) underwent transient transfection with a luciferase tagged-p21 promoter, a β -Galactosidase promoter, either T7-TAp63 α or T7-p53, and either Mdm2, FLAG-AIP4, or FLAG-CHIP (see Transfection section for details). After 40 hrs, cells were harvested using the Luciferase Assay System Protocol (Promega, USA), where a Luciferase Assay Buffer was diluted in dH₂O by a factor of 5 x, and 300 μ L was added to transfected cells after washing twice with PBS and removing all PBS solution. Cells were harvested using a cell scraper, and put in microfuge tubes on ice before being vortexed thoroughly for 30 sec, and spun down at 12,000 x g for 10 min at 4°C. Supernatant (cell lysate) was transferred to a fresh tube, and 20 μ L of cell lysate samples were put into Illuminometer Tubes (Promega, USA) and ran in a Lumat LB 9507 instrument (Berthold Technologies, USA) to measure bio-luminescence. Separately, 150 μ L of each cell lysate sample were used in a β -Galactosidase Assay (Promega). Cell lysate samples were transferred into microfuge tubes and 150 μ L of 2 x Buffer (Promega) was added to initiate detection reaction. Samples were briefly vortexed, before being incubated at 37°C for 30 min (or until samples turned a pale yellow). 500 μ L of 1 M sodium carbonate was added to each sample to stop the reaction and absorbance was read immediately at 420 nm using a DU-730 UV-Spectrophotometer (Beckman Coulter, USA). Each samples luciferase absorbance value was normalized by dividing it by the β -Galactosidase value to get a relative luciferase value that

was then used to calculate luciferase fold change normalized to the negative pcDNA3 transfected control cells. β -Galactosidase activity used as a transcriptional control between samples. Each experiment was repeated three times (n=3), and the average fold change was calculated, and this data plotted as a bar graph in Microsoft Excel. Error bars represent the standard deviation. Statistical significance between averages was determined in Microsoft Excel using an unpaired Student's T-Test without assuming equal variance (Microsoft, USA).

2.16 - Cell Scattering Assay

In order to test for epithelial to mesenchymal transition (EMT), a marker of invasion, cell scattering assays were performed. EMT involves cells losing cell-cell adhesion which results in cell scattering, and fewer colonies [249]. In three six well plates, 2.5×10^5 cells were seeded to sparsely cover the plate. Each plate represented six replicates of 10 μ g of the following transient transfection regimen: Empty vector, CHIP shRNA1, and CHIP shRNA4 (Volume of HEPES and CaCl_2 were halved from their normal amounts to accommodate the smaller sized plates). Cells were washed twice with PBS on the second day, and medium was changed. On the third day, medium was changed again and three replicates of each plate were treated with 10 ng/mL of the hepatocyte growth factor (HGF) hormone (Sigma Aldrich, USA) to promote cell scattering, while the other three replicates of each plate were left untreated. Cells were incubated for a further three days before five images for each well were taken using an Olympus CKX41 microscope (Olympus, USA) using the 40 x objective for 400 x total magnification. Once images were recorded, cells were harvested, whole protein extracted, and knockdowns confirmed by immunoblot. Scattered vs. non scattered cells were counted for each image where "scattered" cells were defined as cells within colonies of 4 cells or fewer, while "non-scattered" cells were

defined as cells within colonies of 5 cells or greater [250]. Number of scattered and non-scattered cells for all five images of each well was averaged, and then each of the three untreated and HGF triplicate average values were averaged. Cells stably transfected with the pSUPER empty vector were used as negative controls. Experiments were repeated three times (n=3) with five replicates, and averages for the untreated and HGF treated empty vector, CHIP shRNA1 and CHIP shRNA4 samples were plotted on a 2-D bar graph in Microsoft Excel (Microsoft, USA), with error bars representing the standard deviation. An unpaired Students T-Test assuming unequal variance was used to determine whether averages within treatment regimens were significantly different compared to the empty vector control of that regimen (HGF or non-HGF treated).

2.17 – Flow Cytometry for Apoptosis Analysis

In order to measure apoptosis, the AnnexinV-FITC apoptosis assay (BD Biosciences, USA) was used and then analyzed by flow cytometry. Viable cells cannot be stained by AnnexinV or 7-AAD, but cells undergoing early apoptosis have phosphatidylserine present on the outer leaflet of the plasma membrane [251] and can be labeled by the AnnexinV dye. Non-viable cells that do not have intact cell membranes can be labeled by the 7-AAD dye. Cells labeled with AnnexinV or AnnexinV and 7-AAD are considered by this assay to be apoptotic. H1299 cells underwent one of the following two experiments: either co-transfection with T7-TAp63 α or T7-p53, or either pcDNA3, Mdm2, FLAG-AIP4, or FLAG-CHIP; or transfection with increasing concentrations of FLAG-CHIP (and decreasing pcDNA3) and UV treated in an UV Cross-Linker Select-Series instrument (Spectroline, USA) with 4 mJ/cm² for 3 hrs. Cells were trypsinized gently using Trypsin that lacked EDTA, and washed twice in PBS. 10 x

Binding Buffer (0.1 M HEPES pH 7.4, 1.4 M NaCl, 25 mM CaCl₂) was diluted to 1 x Binding Buffer in dH₂O, and 5 mL were added to each cell sample. Cells were counted using a cell counter (Hausser Scientific, USA), and 1.5 x 10⁵ cells were added to a microfuge tube, one tube per sample. AnnexinV dye (10 µL) and 7-AAD dye (5 µL) were added to each tube, mixed gently by hand, and incubated for 15 min in the dark at 20°C. 400 µL of 1 x Binding Buffer was added to each sample and samples were analyzed by flow cytometry within 1 hr. Data from flow cytometry was analyzed using FlowJo (FlowJo LLC, USA), and plotted on a two dimensional graph where the x-axis represented cells stained with the green AnnexinV dye, and the y-axis represented cells stained with the red 7-AAD dye. This graph was separated into four quadrants with differently stained cells: No stain, red stained (only 7-AAD), green stained (only Annexin V), and yellow stained (both 7-AAD and Annexin V). Since AnnexinV stains cells in early apoptosis and dead cells, while 7-AAD can stain the DNA of dead cells, all signals positive for AnnexinV and double positive for AnnexinV and 7AAD was accepted as pro-apoptotic cells. Signals positive for 7-AAD were dismissed as false positives. The data was normalized to unstained cells as a negative control, giving a cellular apoptosis fraction by percentage value. Experiments were repeated three times (n=3), and percent apoptosis was calculated as an average between three values, bar graphs were generated on Microsoft Excel (Microsoft, USA), with error bars representing the standard deviation, and statistical significance was analyzed by an unpaired Student's T-Test with unequal variance.

2.18 - Flow Cytometry for Cell Cycle Analysis

In order to measure what fraction of cells is undergoing G1, S, and G2/M phases, cells are fixed and labeled with propidium iodide which labels DNA. Flow cytometry is used to sort fractions of cells undergoing different phases by differentiating how much DNA is being labeled (G2/M cells have twice the DNA as G1 cells, and S phase cells are in-between G1 and G2 DNA amounts) [252]. H1299 cells underwent one of the following two experiments repeated three times: either co-transfection with T7-TAp63 α or T7-p53, or either pcDNA3, Mdm2, FLAG-AIP4, or FLAG-CHIP; or transfection with CHIP shRNA1 or CHIP shRNA4 (and decreasing pcDNA3). Cells were harvested using trypsin (1-2 min exposure at 37°C) and re-suspended in cold (4°C) FCS (flow cytometry staining) wash buffer (0.5% FBS, 1 mM EDTA, and 0.05% sodium azide in PBS). Cell number from each transfection aliquot was estimated using a Bright Line Counting Chamber 3200 (Hausser Scientific, USA), and 1 mL of cells from each aliquot were transferred into a 15 mL culture tube at a density of 1 million cells/1 mL. Cold (-20°C) 70% ethanol was prepared prior to beginning experiment, and 3 mL was added drop-wise to each sample while vortexing samples to minimize cell death. Cells were fixed in 70% ethanol overnight at -20°C too allow for dye permeability. Once cells were fixed, they were centrifuged at 500 x g for 5 min and then re-suspended in FCS wash buffer. Cells were washed in FCS buffer for 5 min, and this process was repeated a second time. Once washing was complete, 1 mL of propidium iodide dye (50 μ g/ml PI, 3.8 mM sodium citrate) (Sigma Aldrich, USA) was added to stain cellular DNA. A stock solution of RNase A (10 μ g/ml RNase A) (Worthington Biochemicals, USA) was prepared prior to these experiments by boiling solution for 5 min and storing aliquots at -20°C), and 40 μ L of RNase A stock solution was added alongside the propidium iodide dye to each sample in order to eliminate RNA material. Cells were incubated

in the dye solution overnight at 4°C under a white light to ensure maximum dye staining efficiency. Once incubation was complete, cells were centrifuged at 800 x *g* for 5 min, and washed in FCS buffer for 5 min twice. Samples were re-suspended in 500 µL of FCS buffer in 1.5 mL tubes, and stored at 4°C in the dark until flow cytometry was conducted (done in the lab of Dr. Aja Rieger, University of Alberta). Once flow cytometry was done, data readouts were analyzed by FlowJo and propidium iodide absorbance averages for cell populations in G1, S, and G2/M phases were calculated. Averages were calculated for each experiment (n=3) and plotted in Microsoft Excel (Microsoft, USA), error bars represent the standard deviation, and statistical significance of averages between transfection regimens was analyzed by an unpaired Student's T-Test without assuming equal variance. Transfection efficiency was controlled for by immunoblotting transfected proteins (TAp63α, p53, CHIP, AIP4, and Mdm2) using whole cell lysates taken from each sample, while cycle variability was controlled for by transfecting H1299 cells split from the same culture with an equal passage number.

2.19 - Tissue Handling and Preparation

Benign and invasive prostate cancer tissues samples were acquired from the Alberta Cancer Research Biobank (Canada). Invasive prostate tissue samples were all adenocarcinomas biopsied from men between ages of 50 to 71. Use of these patient tissue samples was approved by the Health Research Ethics Board – Biomedical Panel (University of Alberta). Protein was extracted from tissues by suspending them in 1% NP40 Lysis Buffer, adding liquid nitrogen, and putting them into a 10 mL mashing tube (Wheaton, USA) on ice. Tissues were processed by physical shearing; and this was done by placing the mashing tube in a K41 Tri-R STIR-R instrument (tube was kept in ice for this procedure). Cells were mashed for 1 min on setting “4”

on this instrument, before shutting the instrument down and allowing the tube to cool on ice for 1 min (to avoid overheating). This process was repeated twice more, before solution was collected and put into microfuge tubes. Protein extracted continued as normal (starting just after the sonification step – see section 2.10). The Gleason score is often used to assess prognosis of prostate cancer patients. Gleason scores range from 2 to 10 with 2-4 having good prognosis, 5-6 being intermediate grade, 7 being moderate to poorly differentiated, and 8-10 being poorly differentiated tissues with poor prognosis [253, 254]. Gleason grades were unknown for all samples except Patient 2 (Score 7), and Patient 8 (Score 8), moderate-to-poor and poor prognosis respectively. Patients 2 and 3 had a family history of prostate cancer. All other information about these tissues samples is unknown.

2.20 – Statistical Analysis

Data for experiments (n=3) were plotted in Excel (Microsoft USA) as the mean \pm standard deviation. The standard deviation was used to satisfy the conditions needed for calculating an unpaired Student's T-Test with unequal variance (Welch T-Test). The test group was compared to the negative control group for each experiment using the Welch T-Test to determine statistical significance. A p-value of 0.05 or less was considered a statistically significant result between the sample and control group.

Chapter 3 – Results

3.01 – CHIP is a TAp63-Interacting Partner

The first aim of this study was to further test whether CHIP was a TAp63-interacting partner. A previous yeast-two hybrid study (unpublished data) was the impetus for testing this potential interaction. The objectives of this aim were to test if CHIP can bind to TAp63 and what domain of TAp63 was necessary for interaction. The H1299 lung carcinoma cell line was beneficial for these experiments, particularly the subsequent functional experiments performed in Section 3, because these cells are devoid of p53 expression (p53^{-/-}) [255], and therefore endogenous p53 is not present to account for any functional implications observed in these experiments. The H1299 lung carcinoma cell line was also chosen for these experiments because it is particularly easy to transfect with ectopic protein. In order to test whether ectopic CHIP binds with ectopic TAp63, co-immunoprecipitation was performed in H1229 cells. During co-immunoprecipitation, a protein of interest and all interacting partners are isolated. Interacting partners can be identified using immunoblot analysis, and the presence of an immunoblotted protein confirms interaction between that protein and the co-immunoprecipitated protein. Ectopic CHIP was found to co-immunoprecipitate with TAp63 α (Figure 10), the wild-type form of p63. This was confirmed both ways – CHIP was able to bind to immunoprecipitated TAp63, and TAp63 was able to bind to immunoprecipitated CHIP (Figure 10). Because this binding was characterizing ectopically expressed proteins, a co-immunoprecipitation assay was done to test binding between endogenous CHIP and endogenous p63 (Figure 11). The MCF10 α breast epithelium cell line was chosen for this experiment as it contains particularly high levels of endogenous TAp63 α compared to the H1299 cell line (which has endogenous TAp63 α , but the levels of this protein are much lower in H1299 compared to MCF10 α). Endogenous CHIP was able to bind to a protein complex immunoprecipitated with an antibody specific to p63, and endogenous p63 was able to bind to a protein complex immunoprecipitated with an antibody

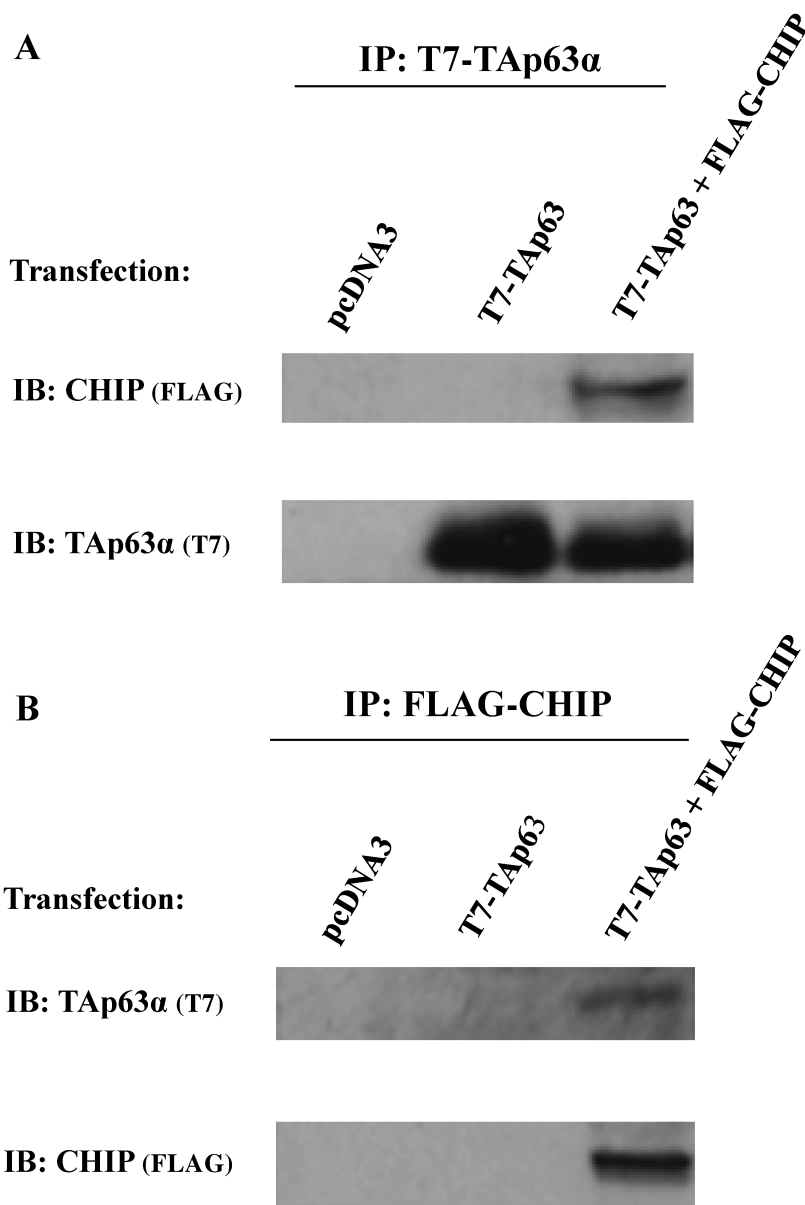


Figure 10 – Ectopic CHIP Binds to Ectopic TAp63 α .

H1299 cells were transfected with 4 μ g of T7-tagged TAp63 α DNA, and 20 μ g of either pcDNA3 empty vector, or FLAG-tagged CHIP. Whole cell protein extracts underwent immunoprecipitation (IP) for T7-TAp63 α (Panel A) or for FLAG-CHIP (Panel B), electrophoresis, and were analyzed for presence of CHIP and p63 by immunoblot (IB). This experiment was repeated twice (n=2).

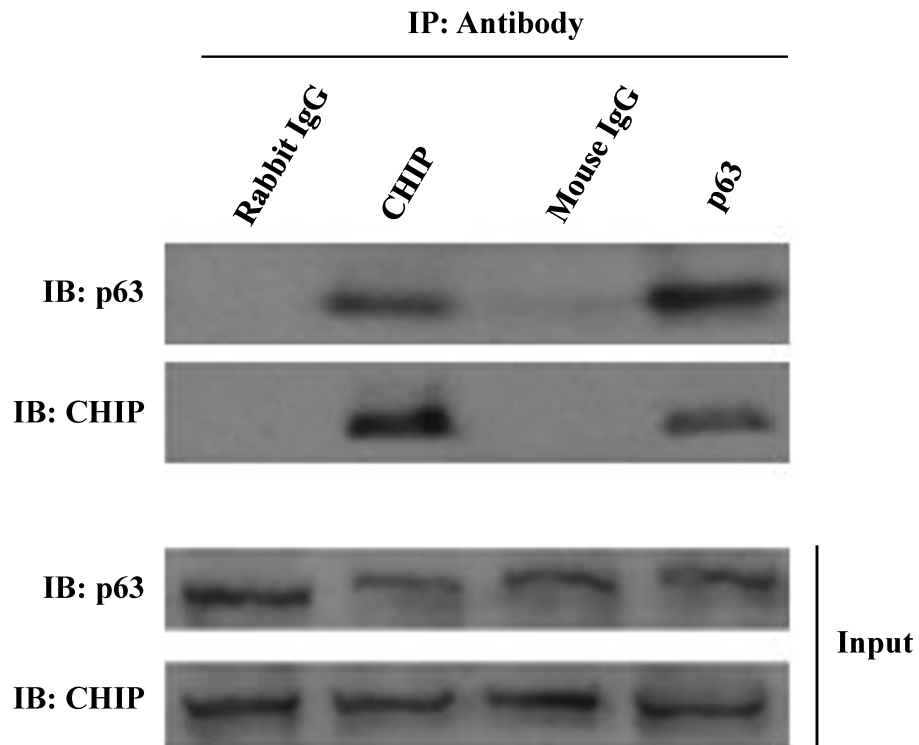


Figure 11 – Endogenous CHIP Binds to Endogenous p63.

Whole protein extracts from MCF10 α breast epithelial cells underwent immunoprecipitation with either anti-CHIP, anti-p63 “4A4”, anti-rabbit IgG (negative control for anti-CHIP), or anti-mouse IgG (negative control for anti-p63), underwent electrophoresis, and were analyzed for presence of CHIP and p63 by immunoblot. Non-immunoprecipitated fractions of the whole protein extracts were also analyzed for CHIP and p63 by immunoblot as a positive control. This experiment was repeated twice (n=2).

specific to CHIP (Figure 11). In order to test what domain of TAp63 was responsible for CHIP binding; five TAp63 α constructs were generated (Figure 12A) and ectopically transfected alongside wild-type CHIP. Co-immunoprecipitation of these constructs, followed by immunoblotting for CHIP determined which TAp63 domains were essential for CHIP interaction. CHIP was present when constructs C541, C393, and C108 were immunoprecipitated, but not constructs N362, or N540. The constructs C541, C393, and C108 all share the C-terminal SAM-domain in common, indicating that the SAM domain is required for CHIP binding (Figure 12A). Transfection of constructs was confirmed by immunoblot (Figure 12B). Arrows in Figure 12A and Figure 12B indicate the presence of each construct in the immunoprecipitated fraction (Figure 12A) and the whole cell lysate (Figure 12B) at the appropriate molecular weights. Domains contained in each construct are also shown (Figure 12C). In order to test whether TAp63 α is ubiquitinated in the presence of CHIP, a His-ubiquitin pull-down assay was performed. His-tagged ubiquitin with Ni-Agarose and all ubiquitinated proteins were isolated and TAp63 α was immunoblotted. TAp63 α is ubiquitinated in the presence of CHIP (Figure 13). When cell lysate underwent immunoblot for TAp63 α , a strong ubiquitination band is seen for TAp63 α when co-transfected with CHIP, similar to that seen when TAp63 α is co-transfected with the known p63 negative regulator AIP4 (Figure 13), suggesting that poly-ubiquitination of TAp63 α has occurred.

Figure 12 – Panel A

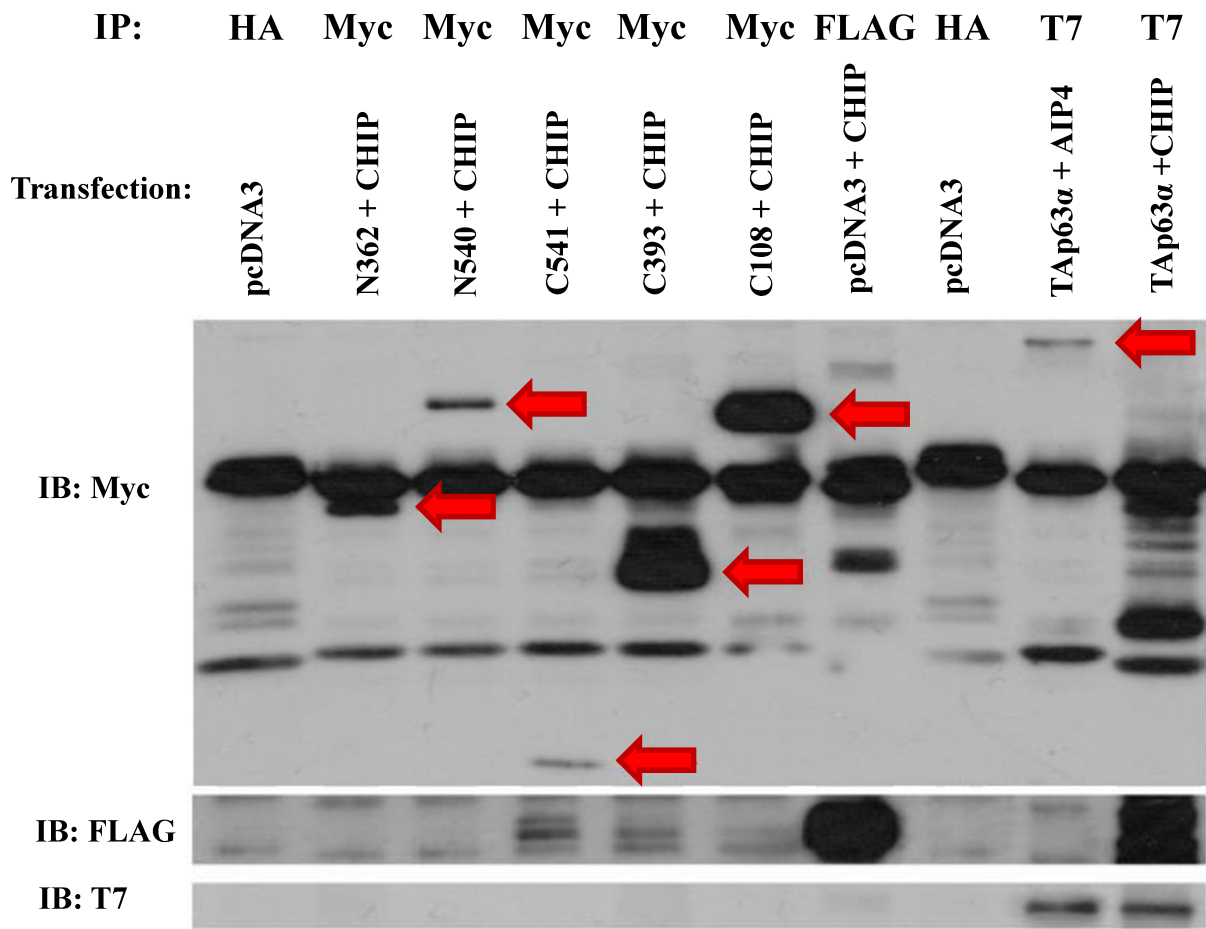


Figure 12, Panel B

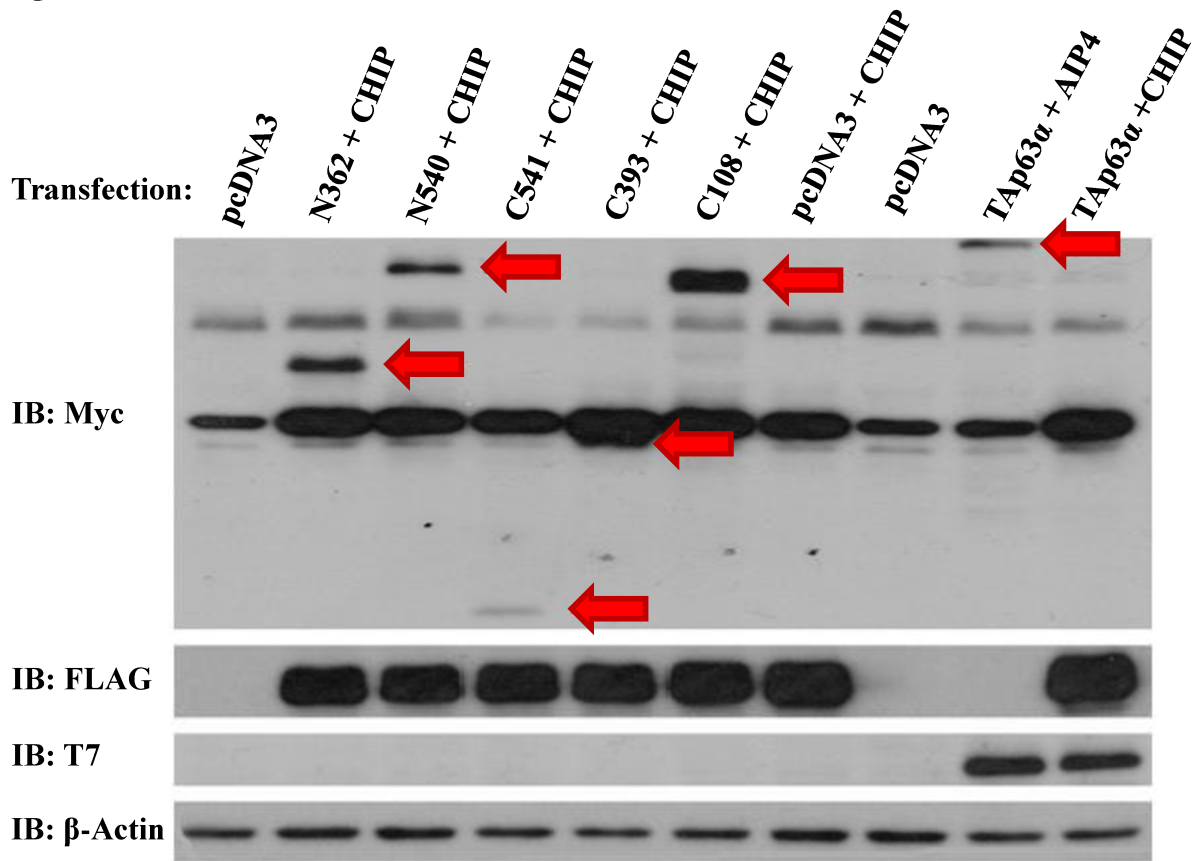


Figure 12, Panel C

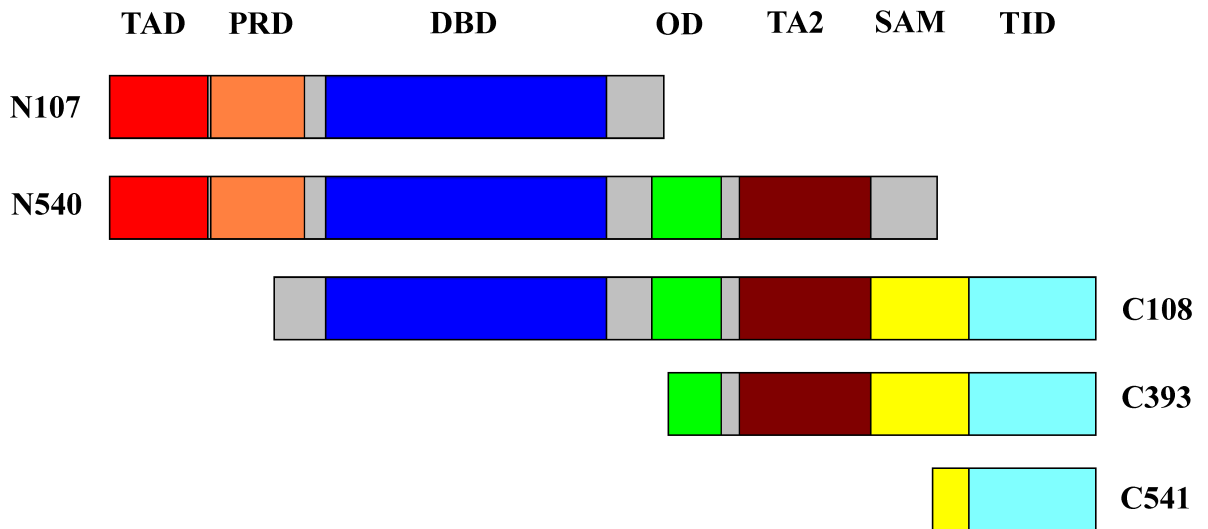


Figure 12 –The SAM Domain is Required for CHIP Binding to TAp63 α .

Five p63 deletion mutants (N terminus to AA (amino acid) 362; N terminus to AA 540; AA 393 to C-terminus; AA 541 to C-terminus; and AA 108 to C-terminus) (see Appendix A – constructs) were cloned into PCMV-Tag3B expression vectors with an N-terminal Myc epitope. H1299 cells were transfected with the following – Lane 1: 24 μ g of pcDNA3; Lanes 2-6: 4 μ g of one of the five p63 deletion mutants (N363, N540, C541, C393, C108 in order) and 20 μ g of FLAG-CHIP; Lane 7: 4 μ g pcDNA3, and 20 μ g FLAG-CHIP; Lane 8: 24 μ g pcDNA3; Lane 9: 4 μ g T7-TAp63 α and 20 μ g Myc-AIP4; and Lane 10: 4 μ g T7-TAp63 α and 20 μ g FLAG-CHIP (Panel A). Whole cell lysate were immunoprecipitated for either Myc, HA, M5, or T7, underwent SDS-PAGE and immunoblot. Whole cell lysate fractions were also analyzed by immunoblot to confirm transfection (Panel B). A picture modified from Figure 5 shows the domains contained in each deletion construct (Panel C). This experiment was repeated twice (n=2).

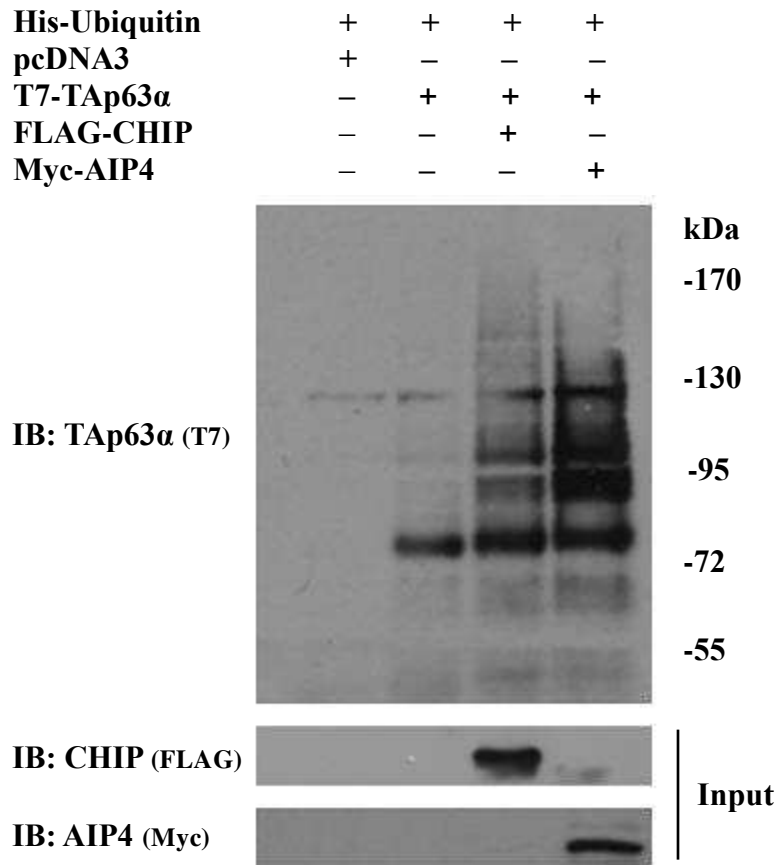


Figure 13 – TAp63 α is Ubiquitinated in the Presence of CHIP.

H1299 cells were transfected with 2 μ g of His-tagged Ubiquitin, and the following plasmids in order of lane (from left to right): Lane 1 – 24 μ g of pcDNA3, Lane 2 – 4 μ g of T7-TAp63 α and 20 μ g of pcDNA3, Lane 3 – 4 μ g of T7-TAp63 α and 20 μ g of FLAG-CHIP, and Lane 4 – 4 μ g of T7-TAp63 α and 20 μ g of Myc-AIP4. Whole cell protein was analyzed using a His pull-down assay, and then underwent SDS-PAGE and immunoblotting for p63. This experiment was repeated twice (n=2).

3.02 – CHIP Negatively Regulates TAp63 α Protein Levels

The second aim of the study was to test if CHIP negatively regulates TAp63 α protein levels. The objectives of this aim were to test if ectopic CHIP, and endogenous CHIP reduced TAp63 α protein levels, whether ablation of CHIP restored endogenous levels of TAp63 α , whether the proteasome was required for reduction in endogenous levels of TAp63 α in the presence of CHIP, and whether CHIP could also negatively regulate levels of the Δ Np63 α isoform. In order to test whether ectopic TAp63 α levels are reduced in the presence of ectopic CHIP, TAp63 α was co-transfected alongside CHIP in H1299 cells. The empty vector pcDNA3 and Mdm2 were used as negative controls, as neither the empty vector nor Mdm2 should be able to induce proteasome degradation of ectopic TAp63 α . TAp63 α was co-transfected with the positive control AIP4, which has been previously demonstrated to ubiquitinate and induce proteasome-mediated degradation of p63 [208]. When ectopic TAp63 α was co-transfected with ectopic CHIP, TAp63 α protein levels were reduced compared to when TAp63 α was co-transfected with the empty pcDNA3 vector or Mdm2, which cannot induce degradation of p63 isoforms (Figure 14). This reduction in protein level is comparable to that seen when TAp63 α is co-transfected with its negative regulator AIP4. In order to test whether endogenous p63 levels were also affected by ectopic CHIP, H1299 cells were transfected with increasing concentrations of CHIP. As CHIP levels increase, endogenous TAp63 α decreases (Figure 15). In order to determine whether endogenous levels of CHIP can affect endogenous TAp63 levels, CHIP was ablated in H1299 cells and endogenous TAp63 α levels were measured. H1299 cells with stably knocked-down CHIP were generated, and endogenous p63 protein was measured by immunoblot (Figure 16). Three out of four knockdowns were successful in visibly knocking down endogenous CHIP protein, and two out of those three knockdowns (CHIP shRNA1, and CHIP

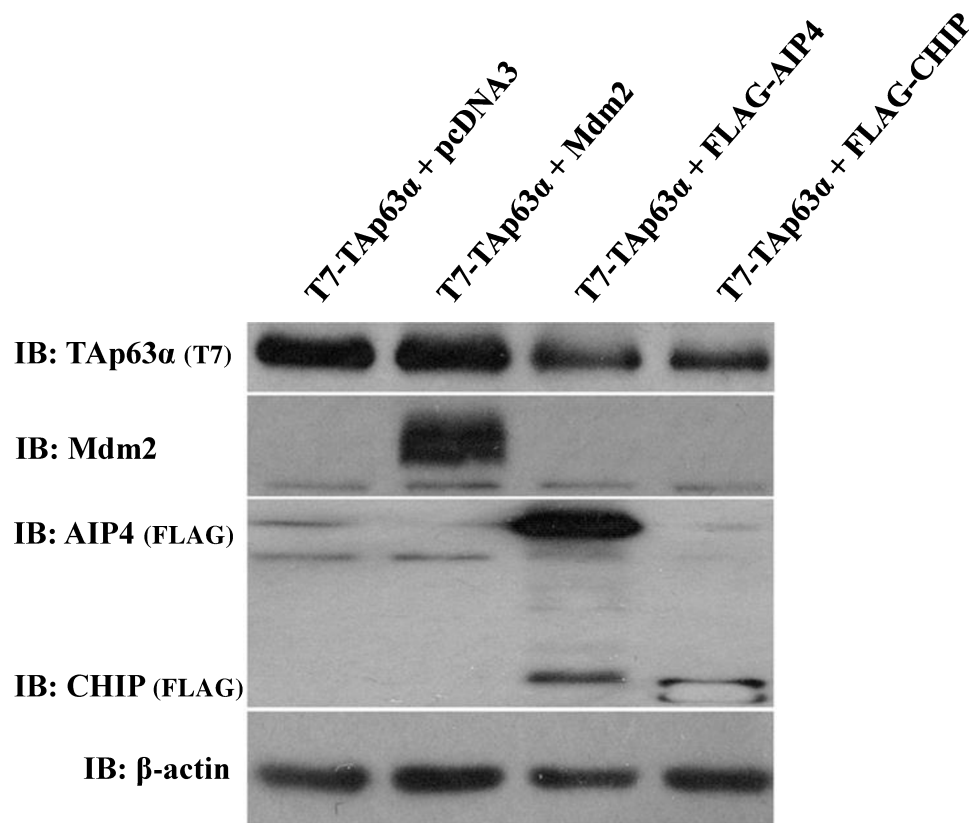


Figure 14 – Ectopic TAp63α is Negatively Impacted in the Presence of CHIP.

H1299 cells were co-transfected with 4 μg of T7-TAp63α and 20 μg of one of the following: pcDNA3, Mdm2, FLAG-AIP4, or FLAG-CHIP. Whole cell protein was extracted, underwent SDS-PAGE, and was analyzed by immunoblot. This experiment was repeated three times (n=3).

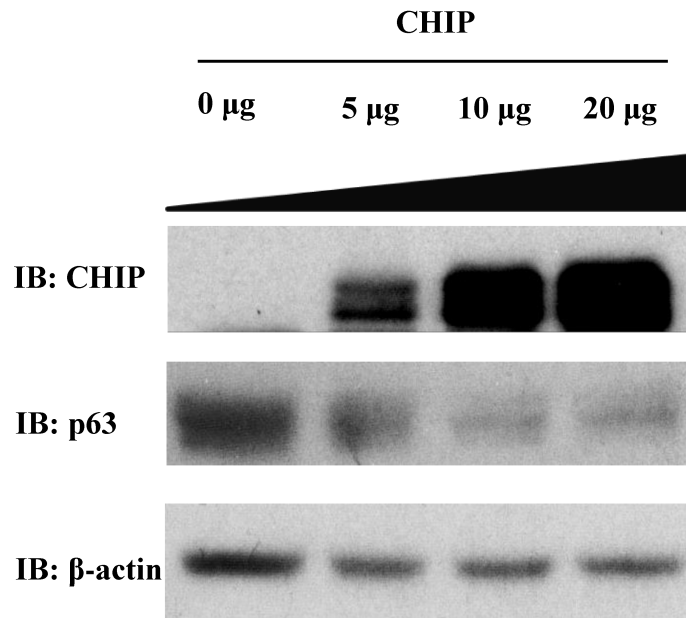


Figure 15 – Increasing Ectopic CHIP Expression Reduces Endogenous p63 Levels.

H1299 cells were transfected with 0 μ g, 5 μ g, 10 μ g, or 20 μ g of FLAG-CHIP. Whole cell lysate was extracted, underwent SDS-PAGE and analyzed by immunoblot. This experiment was repeated three times (n=3).

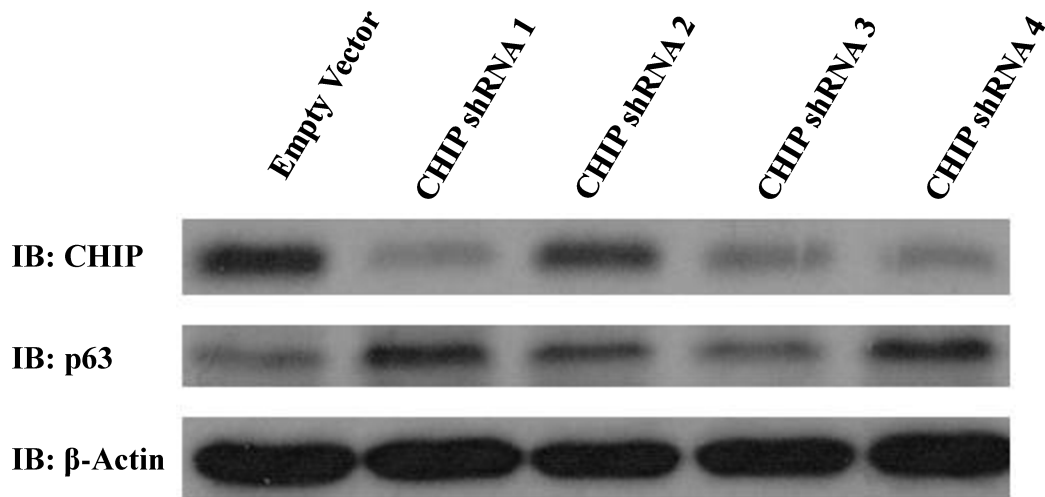


Figure 16 – Ablation of Endogenous CHIP Restores Endogenous p63.

H1299 cells were transfected with 20 μ g of one of the following: the empty vector, or one of the four CHIP shRNA vectors. Cells underwent clonal selection by subjecting them to continuous culture in the presence of the cytotoxic drug G418. Cells surviving selection were maintained in G418, and whole cell lysate from subcultures of these clones were extracted, underwent SDS-PAGE and analyzed by immunoblot. Stable selection of H1299 cells was repeated twice (n=2).

shRNA4) were accompanied by a visible increase in endogenous TAp63 protein (Figure 16), indicating that CHIP knockdown can restore endogenous TAp63 levels. The third construct succeeded in knocking down CHIP, but was not accompanied by an increase in endogenous TAp63, and therefore was unused in subsequent experiments. Lack of endogenous TAp63 in cells knocked down by CHIP shRNA3 might be explained by an off target effect. The previous data strongly suggest that CHIP is a negative regulator of TAp63 protein stability, and since CHIP is an E-3 ligase, targeting many substrates for proteasome-mediated degradation, it was determined whether the proteasome was necessary for this negative regulation, as it is with AIP4. In order to test whether the proteasome is necessary for CHIP-mediated degradation of TAp63 α , H1299 cells were transfected with CHIP, and either treated with the proteasome inhibitor MG132, or left untreated. In untreated cells transfected with ectopic CHIP, endogenous TAp63 levels were reduced as previously observed, but when cells treated with the proteasome inhibitor MG132, and transfected with ectopic CHIP, endogenous TAp63 was not reduced, indicating that when the proteasome is inhibited, TAp63 levels are stabilized (Figure 17). This stabilization was also observed in cells transfected with ectopic AIP4 (Figure 17). It is likely that like AIP4, CHIP also relies on the proteasome for TAp63 degradation. Endogenous levels of the TAp63 transcriptional target p21 were measured in these cells, and its protein levels were also stabilized when the proteasome was inhibited by MG132, and reduced when cells were untreated (Figure 17). Besides TAp63 α , Δ Np63 α expression was also measured by immunoblot in the presence of CHIP to see if CHIP can negative regulated the dominant-negative isoform. In the presence of ectopic CHIP, ectopic Δ Np63 α is reduced by a similar margin to TAp63 α (Figure 18). These data suggest that CHIP is a negative regulator of both TAp63 α and Δ Np63 α , and that this reduction in protein levels is dependent on proteasome function.

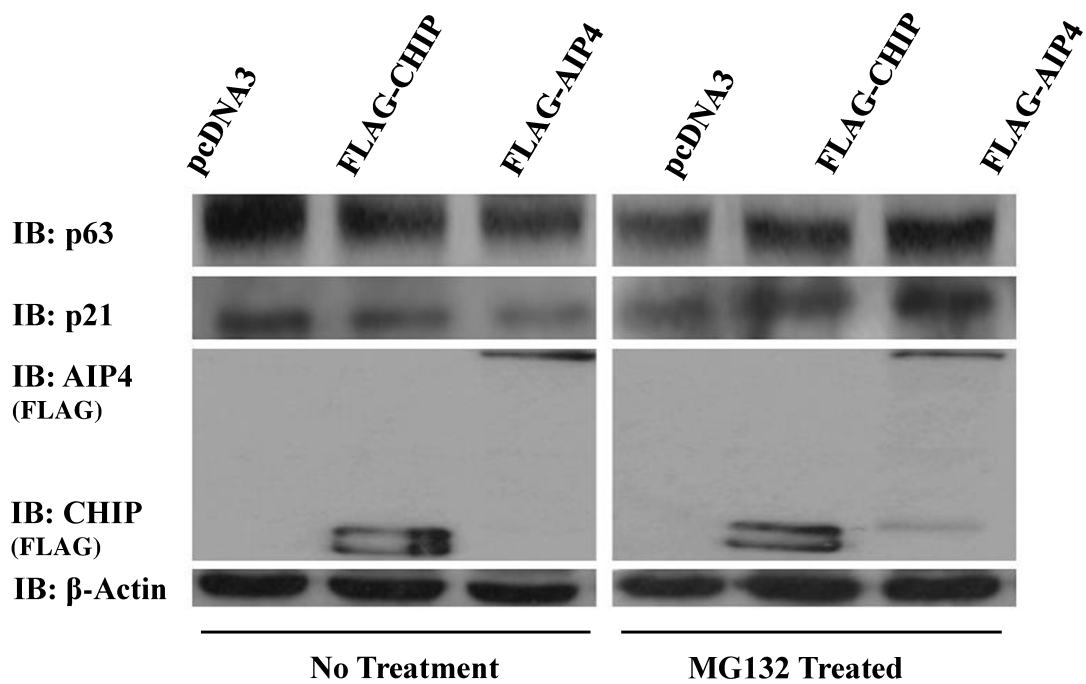


Figure 17 – Inhibition of the Proteasome Stabilizes Endogenous p63.

Two groups of H1299 cells were transfected with 20 μg of pcDNA3, FLAG-CHIP, or FLAG-AIP4. One group was treated as normal, and the second was treated with 10 $\mu\text{g}/\mu\text{L}$ of the proteasome inhibitor MG132. Whole cell lysate from both groups was extracted, underwent SDS-PAGE, and analyzed by immunoblot. This experiment was repeated twice (n=2).

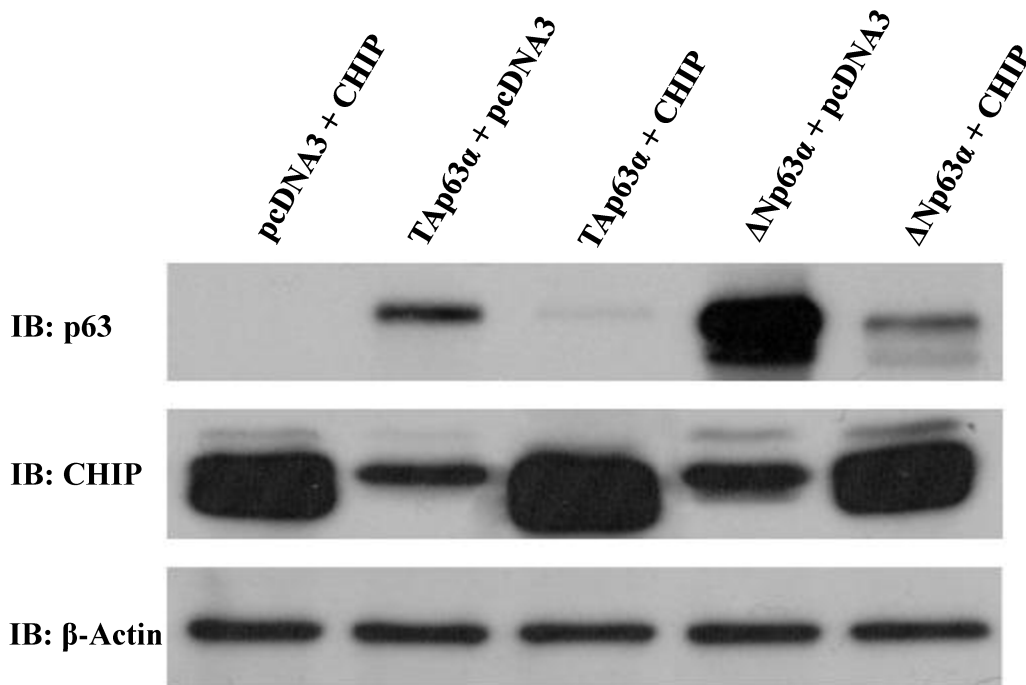


Figure 18 – Increasing Expression of Ectopic CHIP Reduces the Levels of Both Alpha Isoforms of p63 (TAp63 α and Δ Np63 α).

H1299 cells were transfected with the following plasmids (from left to right): Lane 1 – 4 μ g of pcDNA3, 20 μ g of FLAG-CHIP; Lane 2 – 4 μ g of T7-TAp63 α + 20 μ g of pcDNA3; Lane 3 – 4 μ g T7-TAp63 α + 20 μ g of FLAG-CHIP; Lane 4 – 4 μ g of Δ Np63 α + 20 μ g of pcDNA3; and Lane 5 – 4 μ g of Δ Np63 α + 20 μ g of FLAG-CHIP. Whole cell protein was extracted, underwent SDS-PAGE, and was analyzed by immunoblot. This experiment was repeated twice (n=2).

3.03 – CHIP Negatively Regulates TAp63 α Function

The third aim of this study was to investigate CHIP's role in negatively regulating TAp63 function. The objectives of this aim were to test to what degree CHIP impacts the apoptotic, cell cycle arrest, and anti-invasion functions of TAp63 and compare it with how CHIP impacts those functions of p53. In order to test whether CHIP is associated with increased cell survival, colony forming assays were performed using transfected H1299 cells. Cell death was induced by culturing transfected cells in the cytotoxic drug G418. G418 exerts its toxic effects by inhibiting protein synthesis. This is done by binding to the 80S ribosome, and interfering with translation. This drug results in cytotoxic effects with a slow onset [256]. TAp63 α was transfected alone and colonies were compared to those transfected with just the pcDNA3 empty vector, and cell death induced by G418 selection was more pronounced in the presence of TAp63 α (Figure 19B), with cell survival reduced compared to the pcDNA3 control by 60% (from 100% to roughly 40%). However, when CHIP is co-transfected with TAp63 α , the survival fraction is increased, from 40% to 70% (Figure 19B), while when co-transfected with p53, the survival fraction is also increased, from 30% to 50% (Figure 19A). The increase in cell survival observed with TAp63 α and CHIP is equivalent to that seen when TAp63 α is co-transfected with its known negative regulator AIP4 (Figure 19B). Mdm2 is not as effective at preventing cell death in conjunction with TAp63 α , but is very effective at increasing cell survival when co-transfected with p53, increasing it to almost 90% (Figure 19A). Transfection of plasmids in this assay was confirmed by western blot (Figure 19C). The increase in cell survival associated with CHIP is visibly apparent when looking at the number of colonies in each plate for both cases (Figure 19D). In order to test whether endogenous CHIP also promotes cell survival, CHIP was knocked down in H1299 cells with the two most effective CHIP shRNA constructs, 1 and 4 (Figure 16), either

Figure 19 – Panel A

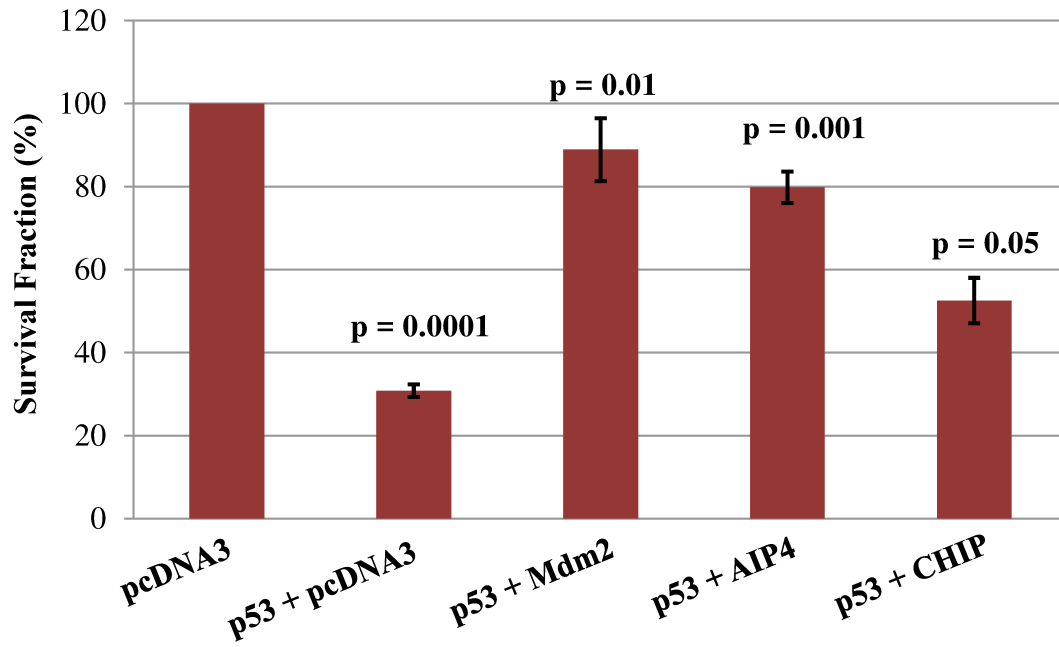


Figure 19 – Panel B

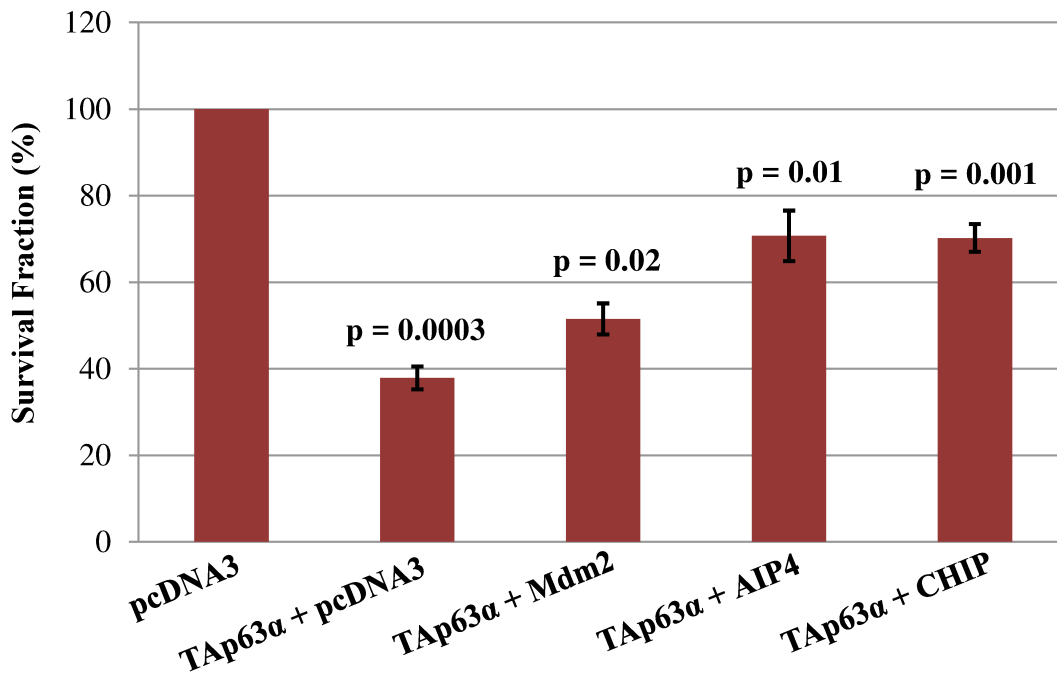


Figure 19 – Panel C

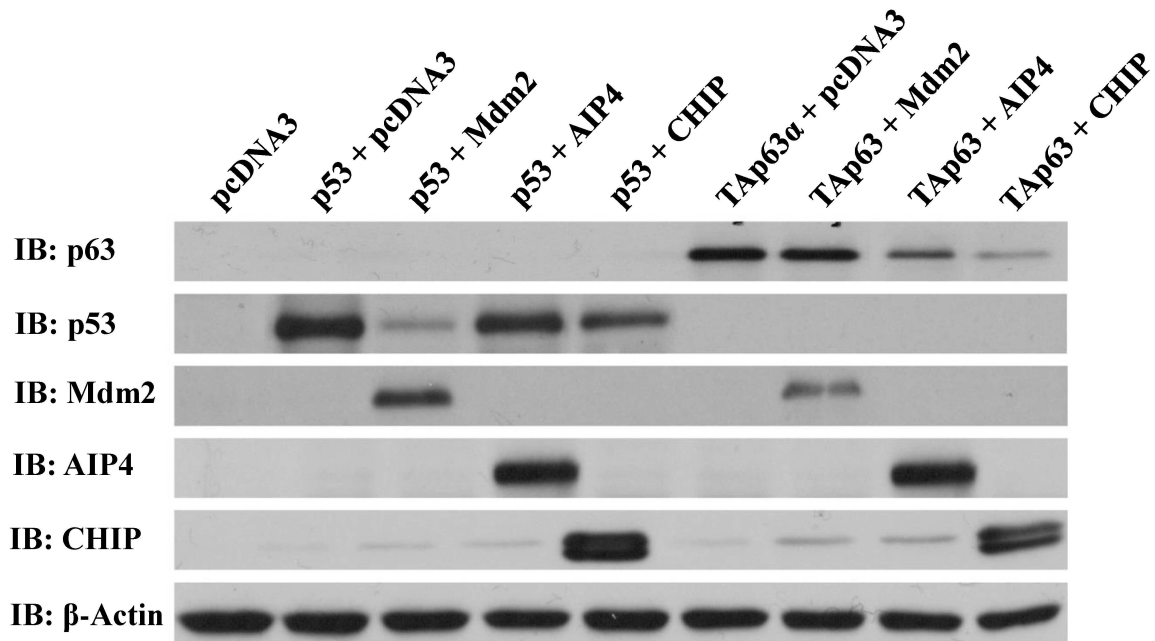


Figure 19 – Panel D

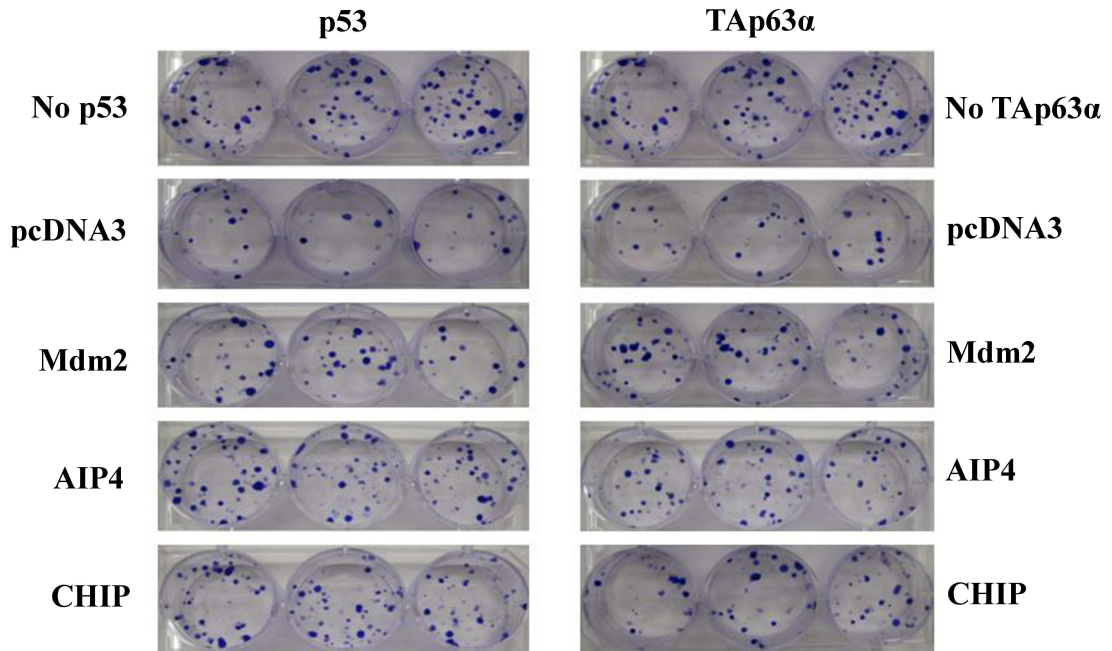


Figure 19 – Ectopic CHIP is Associated with Increased Cell Survival.

H1299 cells were transfected in triplicate with 4 μg of either p53 (Panel A) or p63 (Panel B) and one of the following: 20 μg of pcDNA3 (empty vector), 20 μg of Mdm2, 20 μg of Myc-AIP4, or 20 μg of FLAG-CHIP. Negative controls lacking p53 or p63 were transfected with 24 μg of pcDNA3 (“no p53” and “no TAp63 α ” plates). Transfected cells were sub-cultured into six-well plates, and treated with the cytotoxic drug G418 for clonal selection. Whole cell lysate from remaining cells not sub-cultured underwent SDS-PAGE and were analyzed by immunoblot to confirm transfection (Panel C). Drug selection continued for two weeks until colonies formed. Cells were fixed with formamide and stained with crystal violet dye (Panel D). Number of colonies per well were manually counted, and an average was calculated for each triplicate. A percent survival fraction was calculated for each average, normalized to the average of the pcDNA3 negative control, graphed in Microsoft Excel. P-values were calculated by comparing cell counts of cells transfected with p53 + pcDNA3 and TAp63 α + pcDNA3 were compared to the pcDNA3 negative control cell counts. All other p-values were compared to the cell counts of the p53 + pcDNA3 or TAp63 α + pcDNA3 containing cells (Panel A, and Panel B). These experiments were repeated three times (n=3) with each experiment done in triplicate.

transiently (Figure 20A), or stably (Figure 20B), and cells underwent selection in G418 until colonies grew. Cell survival in transiently transfected cells decreased from 100% to 70% and 75% in the presence of CHIP shRNA1 and CHIP shRNA4 respectively (Figure 20A). Cell survival in stably transfected cells decreased from 100% to 40% and 70% for CHIP shRNA1 and CHIP shRNA4 respectively (Figure 20B). Ablation of CHIP by knock-down was confirmed by immunoblot (Figure 20C, Figure 20D). Reductions in survival are visibly apparent in the stained colony photographs taken of the cell groups for transient (Figure 20E) and stable (Figure 20F) transfected cells. In order to test whether CHIP protects cells from TAp63 α -induced apoptosis, H1299 cells were transfected with CHIP and TAp63 α , and an AnnexinV-FITC apoptotic assay was performed. The percent of apoptotic cells was calculated for both TAp63 α or p53 co-transfected with CHIP by measuring cells dyed with AnnexinV and 7-AAD using flow cytometry. Since AnnexinV can label phosphatidylserine, normally present on the inner leaflet of the plasma membrane but also present on the outer membrane during early apoptosis where the dye can label it, and 7-AAD can label DNA of non-viable cells, then cells dyed with AnnexinV or AnnexinV and 7-AAD together were considered apoptotic [257]. When TAp63 α is co-transfected with pcDNA3, the apoptotic percent increases from just above 1% (pcDNA3 empty vector control) to just above 6% (Figure 21B). This is reduced to 4% when TAp63 α is co-transfected with CHIP. Similarly, CHIP's effect on p53-induced apoptosis was also tested by measuring the apoptotic percent of cells co-transfected with p53 and CHIP. When p53 is transfected in H1299 cells alone, the apoptotic fraction rises from 1% in the presence of the pcDNA3 empty vector to roughly 10% in the presence of p53 (Figure 21A). Presence of CHIP reduces the apoptotic fraction to 6% (Figure 21A) compared to cells transfected with p53 alone. CHIP is not as effective at reducing apoptosis in cells transfected with p53 as Mdm2 is (Mdm2 is

Figure 20 – Panel A

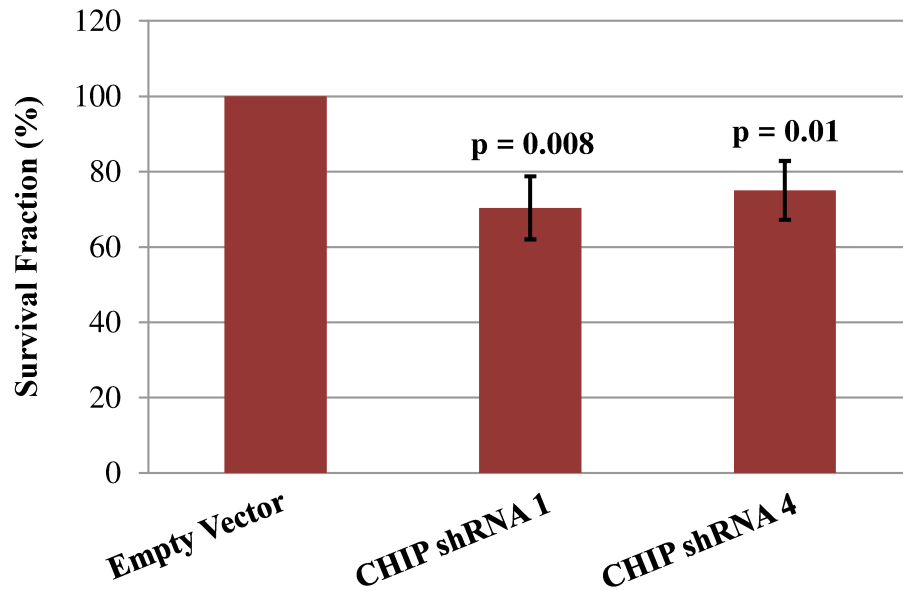


Figure 20 – Panel B

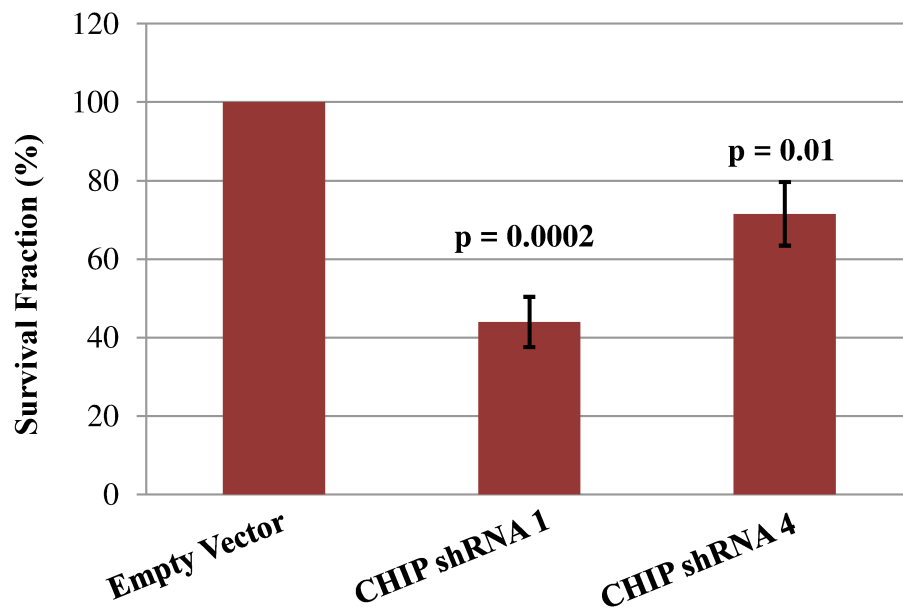


Figure 20 – Panel C

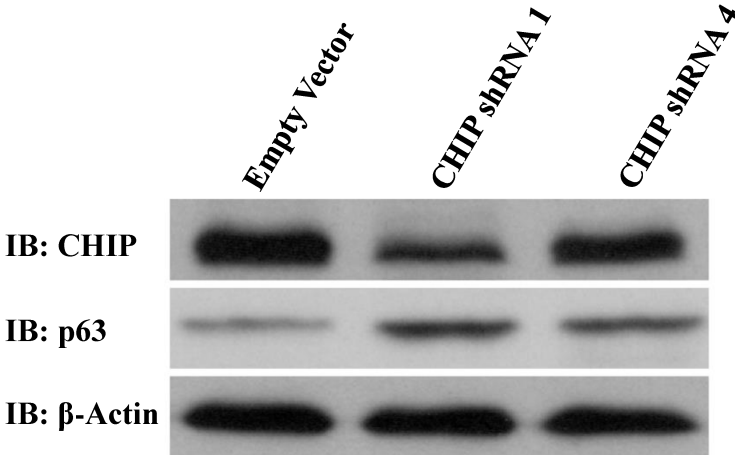


Figure 20 – Panel D

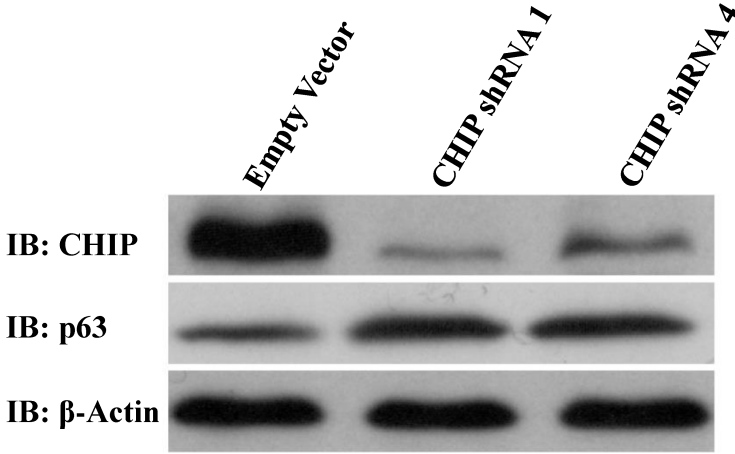


Figure 20 – Panel E

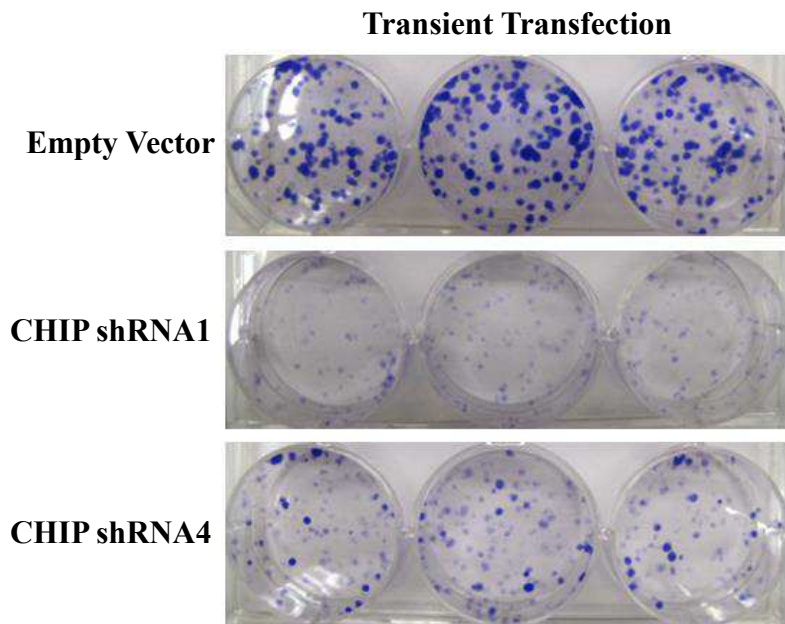


Figure 20 – Panel F

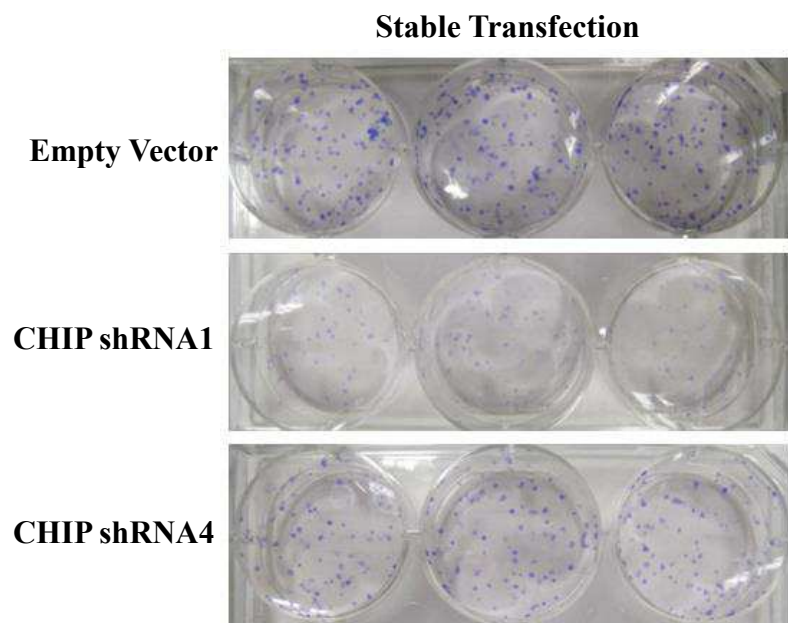


Figure 20 – Ablation of Endogenous CHIP is Associated with Decreased Cell Survival.

H1299 cells were transiently transfected in triplicate with 20 µg of empty vector, CHIP shRNA1, or CHIP shRNA4 (Panel A). Transient cells and previously transfected stable cells (Panel B) were sub-cultured into six-well plates, and treated with the cytotoxic drug G418 for clonal selection. Whole cell lysate from remaining cells not sub-cultured underwent SDS-PAGE and were analyzed by immunoblot to confirm transfection (Panel C, Panel D). Drug selection continued for two weeks until colonies formed. Twenty four hours after selection, cells were fixed with formamide and stained with crystal violet (Panel E, Panel F). Number of colonies per well were manually counted, and an average was calculated for each triplicate. A percent survival fraction was calculated for each average, normalized to the average of the empty vector control, and graphed in Microsoft Excel (Panel A and Panel B). P-values were calculated by comparing the cell counts from CHIP shRNA1 or CHIP shRNA2 and comparing them with the cell counts from the empty vector control (Panel A, and Panel B). These experiments were repeated three times (n=3) with each experiment done in triplicate.

Figure 21 – Panel A

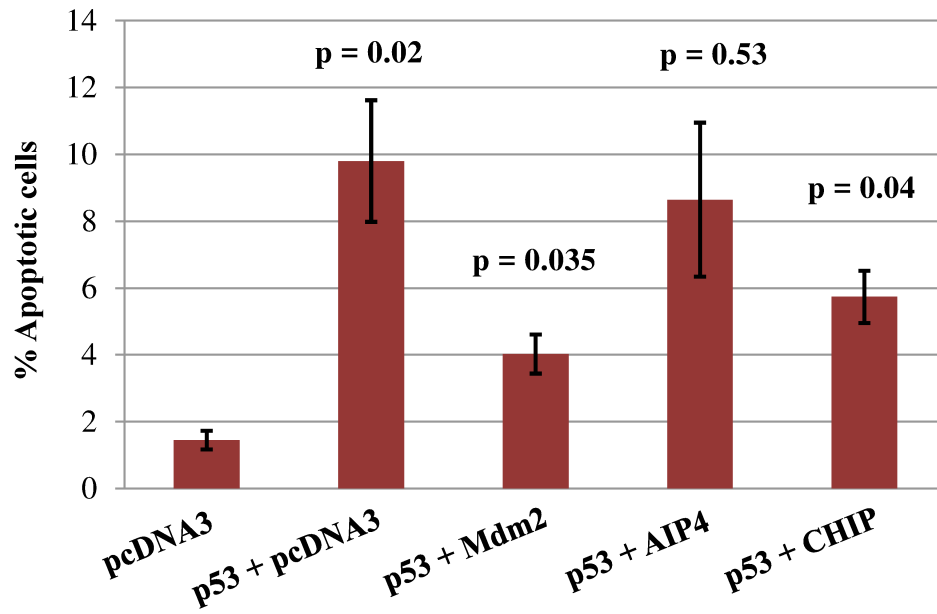


Figure 21 –Panel B

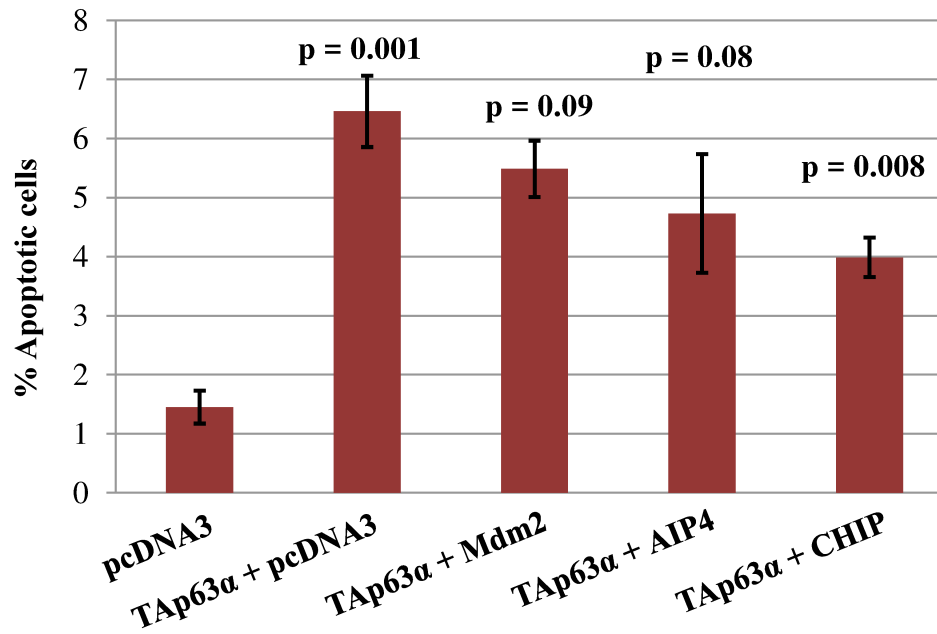


Figure 21 – Panel C

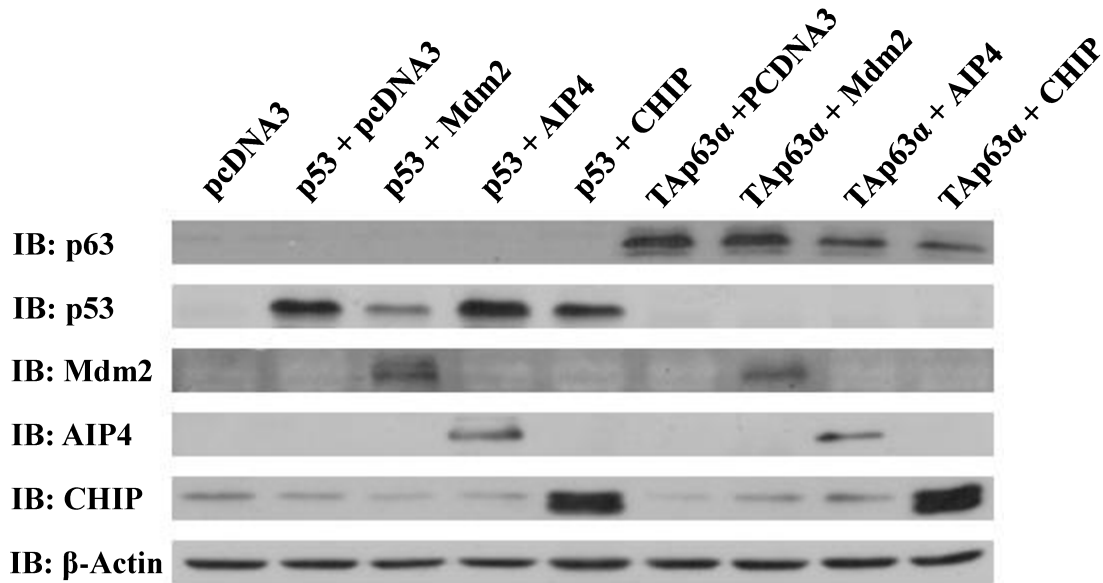


Figure 21 – Both TAp63 α -Induced and p53-Induced Apoptosis is Inhibited in the Presence of Ectopic CHIP.

H1299 cells were transfected in triplicate with 4 μ g of either p53 or T7-TAp63 α , and 20 μ g of either pcDNA3, Mdm2, FLAG-AIP4, or FLAG-CHIP (negative control was transfected with 24 μ g of pcDNA3) (Panel C). Cells were harvested, dyed with AnnexinV and 7-AAD, and flow cytometry was performed. FlowJo software analyzed the green AnnexinV signals, and the red 7-AAD signals and plotted them on a two dimensional graph. Signals for AnnexinV (green) or both AnnexinV and 7-AAD (yellow) were considered positive for apoptotic cells, while 7-AAD signals (red) were considered false positives. Apoptotic cell fractions were calculated as a percent of yellow and green stained cells normalized to the total cells, and averages of these percent values were graphed in Excel (Microsoft, USA). P-values were calculated by comparing the apoptotic percent values of cells transfected with p53 + pcDNA3 and T7-TAp63 α + pcDNA3 to those transfected with pcDNA3. All other p-values were compared to the percent values of the p53 + pcDNA3 or T7-TAp63 α + pcDNA3 transfected cells (Panel A, and Panel B). This experiment was repeated thrice (n=3) with each experiment done in triplicate.

accompanied by a reduction of apoptotic cells to 4% from 10%) (Figure 21A), however, in TAp63-transfected cells, CHIP is more effective than both Mdm2 and AIP4 at reducing apoptosis, both proteins failing to decrease apoptotic cells by a statistically significant amount (Figure 21B). Transfection was confirmed for this assay by immunoblot (Figure 21C). The fraction of apoptotic cells does not increase very highly when TAp63 α is transfected alone, and so an assay was conducted where cells were transfected with increasing concentrations of CHIP and exposed to UV radiation to induce apoptosis. When ectopic CHIP is absent from cells, the apoptotic fraction is 15%, but as the amount of CHIP transfected in cells increases (to 5 μ g, 10 μ g, and 20 μ g), this apoptotic fraction is reduced, reaching just below 3% when 20 μ g of CHIP is transfected into cells (Figure 22A). This reduction in apoptotic percent is accompanied by a reduction in endogenous TAp63 levels, as confirmed by an immunoblot (Figure 22B). In order to test whether CHIP affected TAp63-induced cell cycle arrest, a luciferase reporter assay was conducted using a p21 promoter driven luciferase. The ability of TAp63 and p53 to induce cell-cycle arrest was measured by co-transfecting H1299 cells or SAOS-2 cells with a luciferase tagged p21 reporter, TAp63 α or p53, and CHIP, and measuring bio-luminescence. The SAOS-2 osteosarcoma cell line was also used alongside the H1299 cell line for the luciferase reporter assays as it is devoid of both p53 and p73 expression (p53^{-/-}; p73^{-/-}) [130]. When TAp63 α was transfected in H1299 cells alongside pcDNA3, p21 transcription increased 14-fold compared to the empty vector pcDNA3 control. This change was reduced to just below 4-fold in the presence of CHIP (Figure 23B), a greater decrease than either Mdm2 or AIP4. When p53 was transfected alongside pcDNA3, p21 transcription increased by almost 65-fold, and the presence of CHIP was able to reduce this to just above 10-fold, almost as much as the negative regulator Mdm2 (at just above 5-fold (Figure 23A). Similar results were observed in SAOS-2 cells. When TAp63 α was

Figure 22 – Panel A

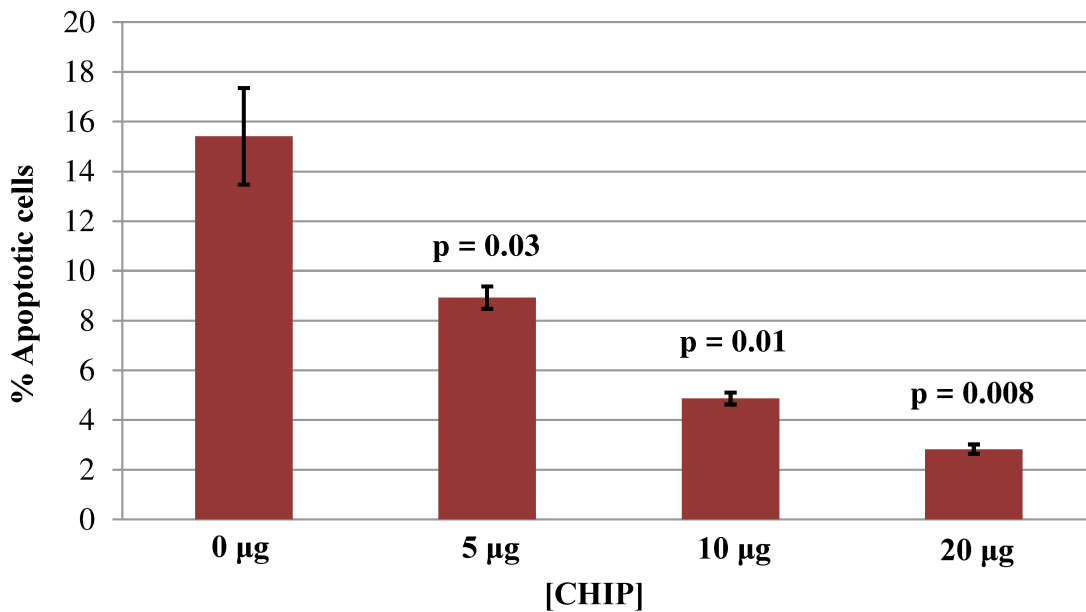


Figure 22 – Panel B

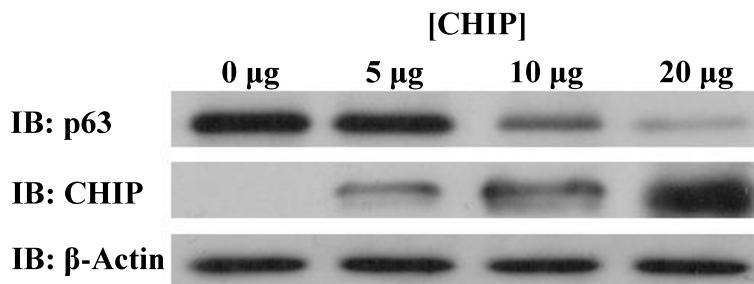


Figure 22 – UV-Induced Apoptosis is Reduced as Ectopic CHIP Expression Increases.

H1299 cells were transfected with 0 µg, 5 µg, 10 µg, or 20 µg of FLAG-CHIP, before undergoing UV treatment (250 nm, 4 mJ/cm²) for 3 hrs. Cells were trypsinized, and stained with AnnexinV and 7-AAD dyes before being analyzed by flow cytometry. Signals for AnnexinV (green) or both AnnexinV and 7-AAD (yellow) were considered positive for apoptotic cells, while 7-AAD signals (red) were considered false positives. Apoptotic cell fractions were calculated as a percent of AnnexinV⁺ 7-AAD⁺ and AnnexinV⁺ 7-AAD⁻ stained cells normalized to the total cell fraction, and averages of these percent values were graphed in Excel (Microsoft, USA) (Panel A). P-values were calculated by comparing the apoptotic percent values of cells

transfected with FLAG-CHIP to apoptotic percent values of cells transfected without FLAG-CHIP. Whole cell lysate was extracted, and underwent SDS-PAGE before being analyzed by immunoblot to confirm CHIP transfection (Panel B). This experiment was repeated thrice (n=3).

Figure 23 – Panel A

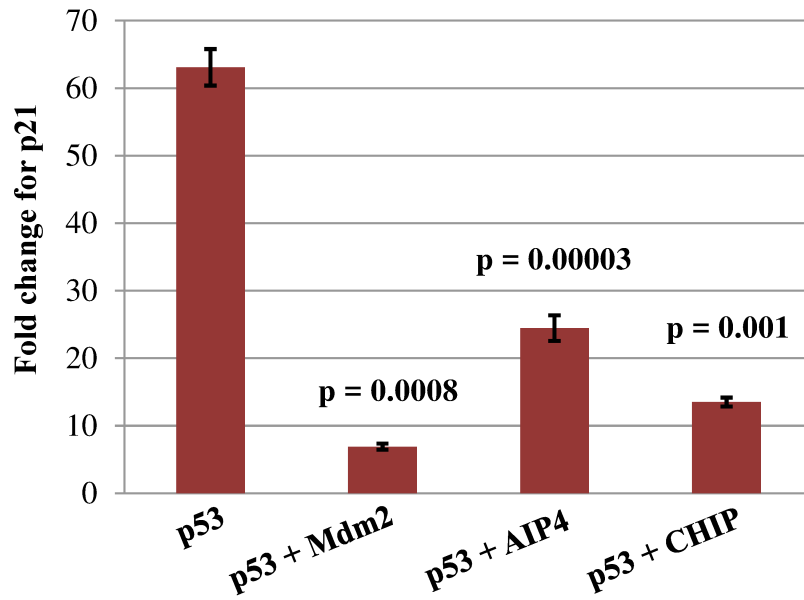


Figure 23 – Panel B

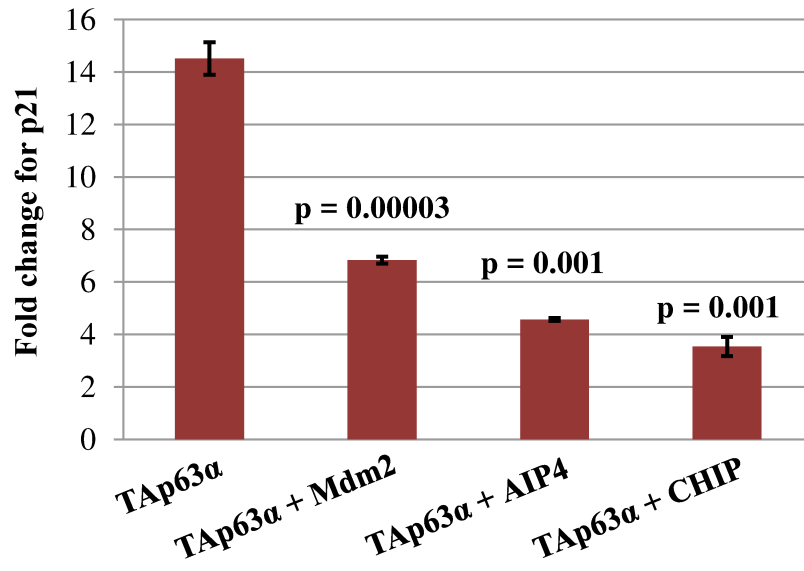


Figure 23 – Panel C

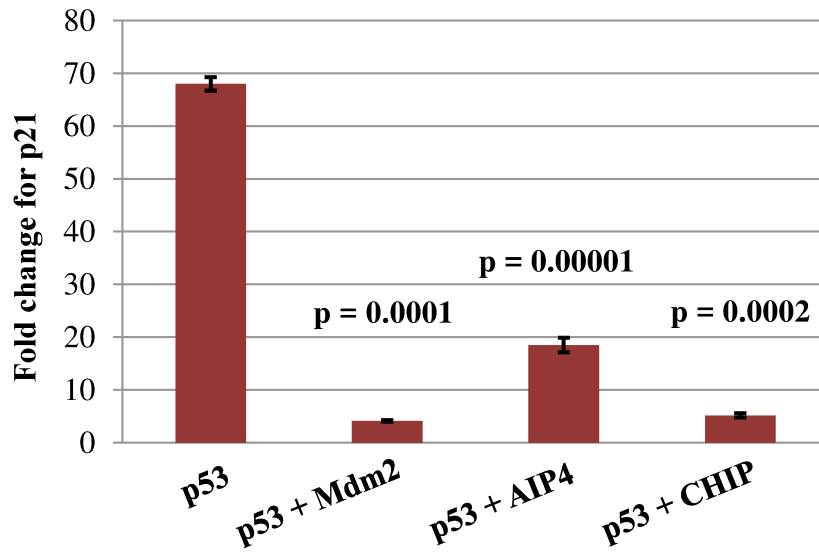


Figure 23 – Panel D

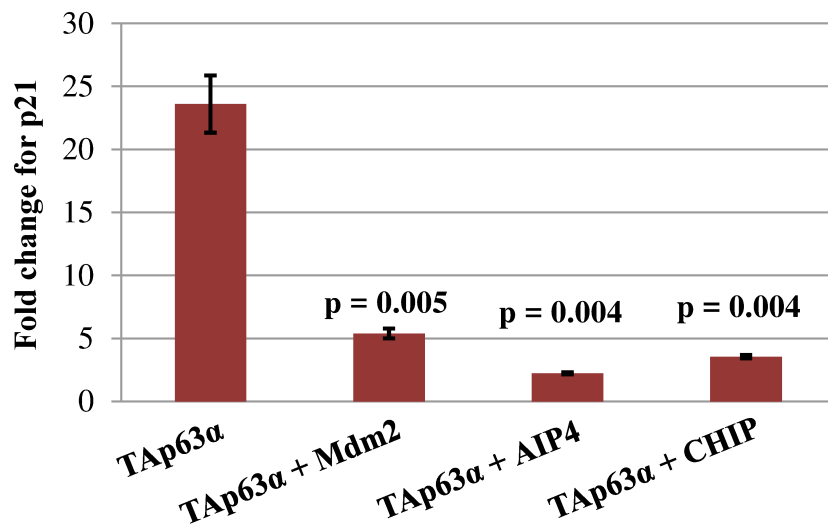


Figure 23 – Panel E

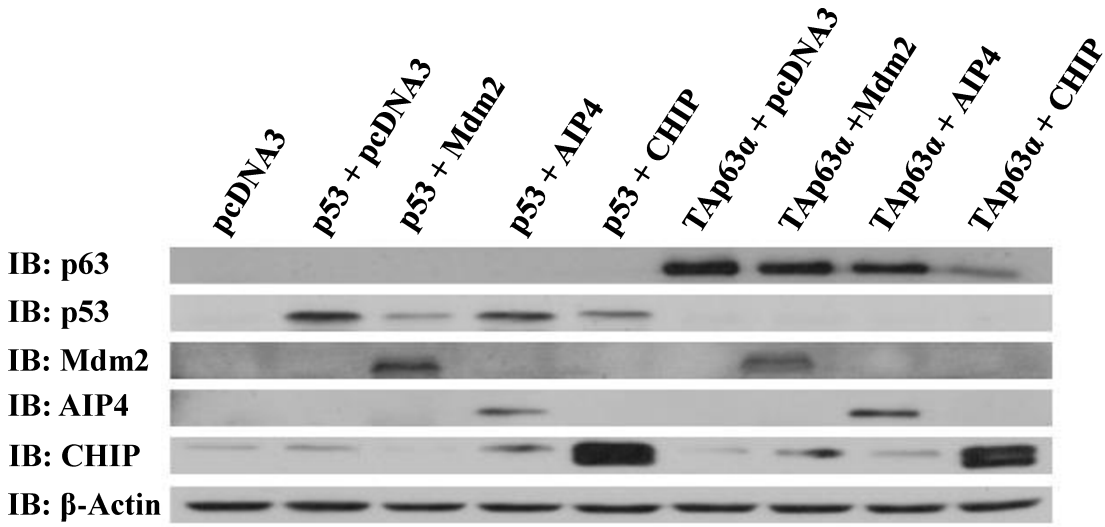


Figure 23 – Panel F

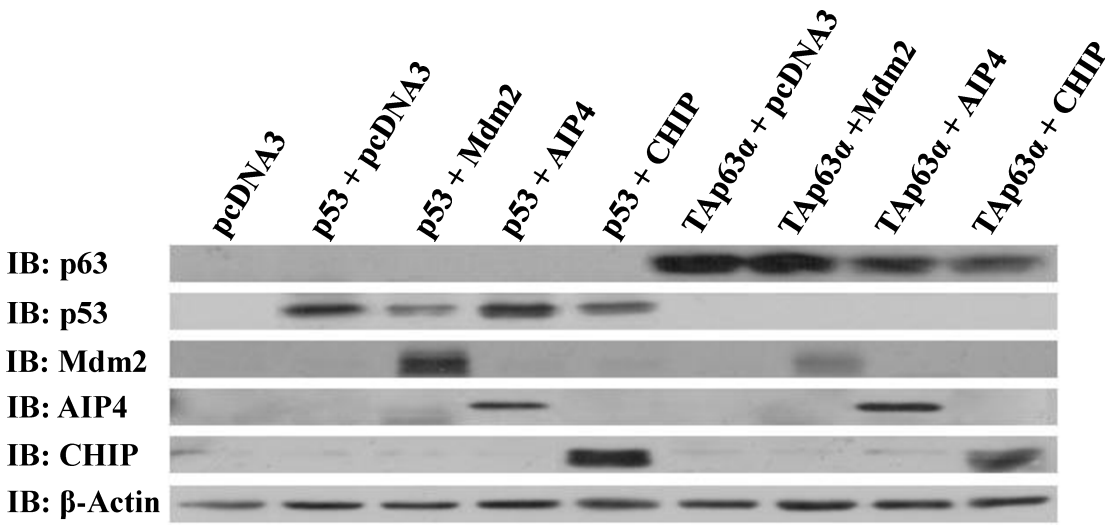


Figure 23 – Both TAp63 α -Induced and p53-Induced Transcription of p21 is Inhibited in the Presence of Ectopic CHIP.

H1299 and SAOS-2 cells were transiently transfected in triplicate with 2 μ g of a p21-luciferase promoter, 2 μ g of a β -galactosidase promoter, and one of the following: 20 μ g of pcDNA3; 4 μ g of p53 + 16 μ g pcDNA3; 4 μ g of p53 + 16 μ g Mdm2; 4 μ g of p53 + 16 μ g of Myc-AIP4; 4 μ g of p53 + 16 μ g of FLAG-CHIP; 4 μ g of TAp63 α + 16 μ g of pcDNA3; 4 μ g of TAp63 α + 16 μ g of Mdm2; 4 μ g of TAp63 α + 16 μ g of Myc-AIP4; or 4 μ g of TAp63 α + 16 μ g of FLAG-CHIP (Panel E, and Panel F). Cells were harvested and a luciferase assay was done measuring bioluminescence absorbance. Absorbance values were normalized to measured β -galactosidase values. Averages were compared as a fraction to the pcDNA3 control to get the relative fold change for p21, and averages of each triplicate were plotted on a bar graph using Excel (Microsoft, USA), and p-values were calculated for the p53 + pcDNA3 and TAp63 α + pcDNA3 values by comparing them to pcDNA3 values, while all other p-values were calculated by comparing their values against those of either p53 + pcDNA3 (Panel A, and Panel C) or TAp63 α + pcDNA3 (Panel B and Panel D) (Microsoft, USA). Assays done with H1299 cells are shown in Panels A and B and assays done with SAOS-2 cells are shown in Panels C and D. These experiments were repeated three times (n=3).

transfected alongside pcDNA3, p21 transcription increased by nearly 25-fold compared to transfection with only the pcDNA3 control, and the presence of transfected CHIP was able to reduce p21 transcription to just under 5-fold, almost as much as the negative regulator AIP4 (just under 3-fold) (Figure 23D). In SAOS-2 cells, when p53 was transfected alongside pcDNA3, p21 transcription increased to roughly 70-fold compared to the pcDNA3 control, and when CHIP was co-transfected with p53, p21 transcription was reduced to roughly 5-fold, to about the same degree as Mdm2 (just under 5-fold) (Figure 23C). Fold change reduction for p21 in the presence of Mdm2, AIP4, and CHIP negative regulators was accompanied by a reduction in ectopic levels of both TAp63 α and p53 for H1299 cells (Figure 23E), and SAOS-2 cells (Figure 23F), confirmed by immunoblot. In order to test whether CHIP was associated with fewer cells in G1 phase, propidium iodide was used to stain H1299 cells. Dye absorbance is directly proportional to how much DNA is being labeled by PI in fixed H1299 cells. Cells in G2/M have twice the amount of DNA than cells in G1, and cells in S have intermediate amounts. Flow cytometry was used to measure cell fractions undergoing different cell cycle phases (G1, S and G2/M) in cells co-transfected with TAp63 α or p53 and CHIP (Figure 24A, 24B). When cells are transfected with either TAp63 α or p53 alongside pcDNA3, the percent of cells in the G1 phase increases by about 10% in both cases compared to the pcDNA3 control (Figure 24A). In the presence of Mdm2, AIP4, or CHIP, both TAp63 α and p53 transfected cells have a 10% reduction of cells in the G1 phase. Levels of cells in G1 are indistinguishable from the pcDNA3 control cell population (Figure 24A). Transfection was confirmed by immunoblot (Figure 24B). To test for association of endogenous TAp63 with fraction of cells in G1, stably transfected cells with CHIP shRNA1 or 2 were assayed by flow cytometry. When CHIP is knocked-down, percent of cells in G1 increases by 10% in the presence of both CHIP shRNA sequences (Figure 25A).

Figure 24 – Panel A

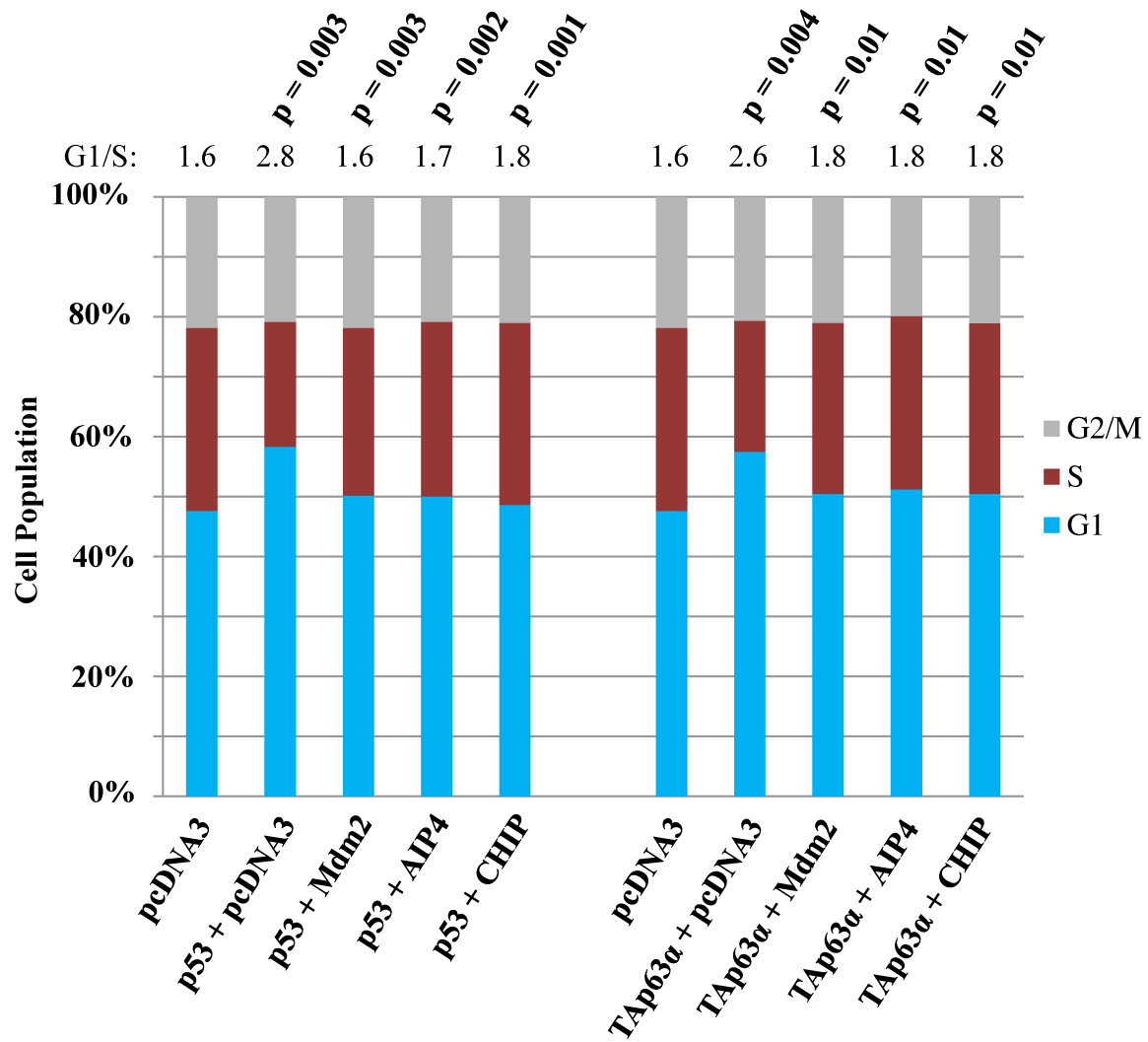


Figure 24 – Panel B

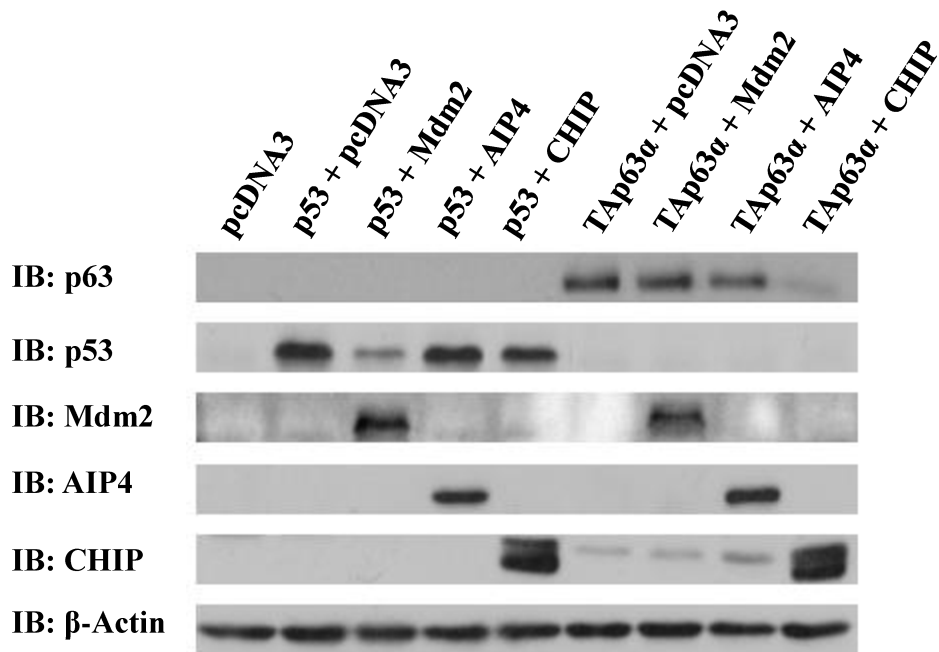


Figure 24 – p53 and TAp63α-Induced G1 Arrest is Reduced in the Presence of Ectopic CHIP.

H1299 cells were transiently transfected in triplicate with 4 μ g of either p53 or T7-TAp63 α , and 20 μ g of either pcDNA3, Mdm2, FLAG-AIP4, or FLAG-CHIP (negative control was transfected with 24 μ g of pcDNA3). Cells were harvested, dyed with propidium iodide, and analyzed by flow cytometry. Data was analyzed using FlowJo (FlowJo, USA) to determine G1, S, and G2/M cell values. Averages of these values were calculated, and plotted in Microsoft Excel (Microsoft, USA), and a G1/S ratio was calculated by dividing G1 values by S values and calculating an average (Panel A). P-values for G1/S ratio averages of p53 + pcDNA3 and TAp63 α + pcDNA3 were calculated by comparing G1/S values from cells transfected with pcDNA3 to p53 + pcDNA3 and TAp63 α + pcDNA3. All other p-values were compared to the G1/S values of p53 + pcDNA3 and TAp63 α + pcDNA3 (Panel A). Whole cell lysates taken from fractions of each group of harvested cells underwent SDS-PAGE and were analyzed by immunoblot to confirm transfection (Panel B). This experiment was repeated three times (n=3).

Figure 25 – Panel A

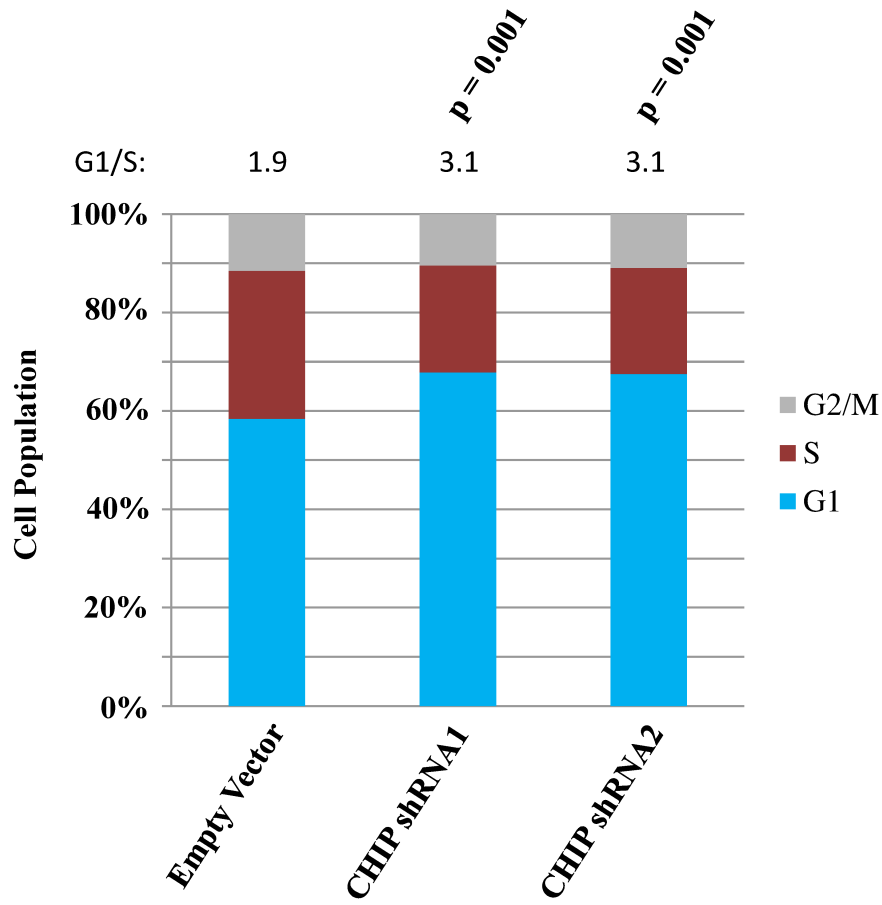


Figure 25 – Panel B

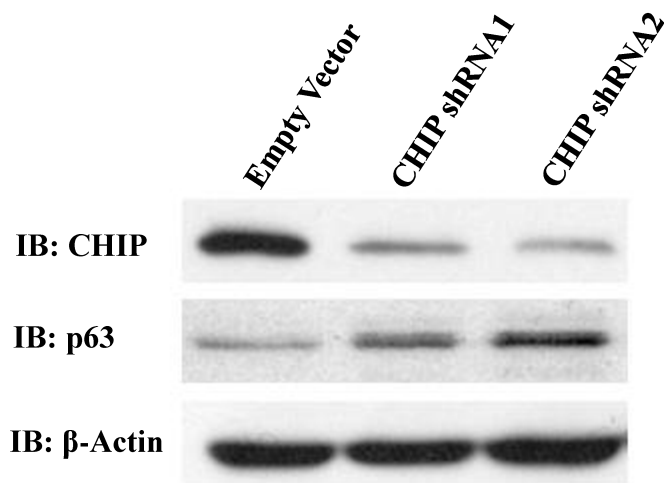


Figure 25 – Ablation of Endogenous CHIP is Associated with Increased Percentage of Cells in the G1 Phase.

H1299 cells were transfected with 20 µg of empty vector control, CHIP shRNA1, or CHIP shRNA2. Cells were harvested, dyed with propidium iodide, and analyzed by flow cytometry. Data was analyzed using FlowJo (FlowJo, USA) to determine G1, S, and G2/M cell values. Averages of these values were calculated, and plotted in Microsoft Excel (Microsoft, USA), and a G1/S ratio was calculated by dividing G1 values by S values and calculating an average (Panel A). P-values were calculated by comparing the G1/S values of CHIP shRNA1 and CHIP shRNA2 with those of the empty vector control (Panel A). Whole cell lysates taken from fractions of each harvested cell group underwent SDS-PAGE, and were analyzed by immunoblot to confirm transfection (Panel B). This experiment was repeated three times (n=3).

This increase in percent of G1 cells is associated with a decrease in endogenous CHIP levels, and an increase in endogenous TAp63 levels, confirmed by immunoblot (Figure 25B). In order to test whether CHIP affects anti-malignant properties of TAp63, a cell scattering assay was performed. Cell invasion can be indirectly tested for using a cell scattering assay on cells with endogenous CHIP knocked down. This assay measures the dispersion of epithelial colonies induced by the hepatocyte growth factor. Cell migration results in scattered cells, and since this is characteristic of epithelial to mesenchymal transition (EMT), including loss of cell to cell adhesion, this assay is used to identify factors that promote EMT and cell migration, both indirect markers of invasion [258]. Percent of cells scattered in the presence of the empty vector control is about 55%. This scattering fraction decreases to just over 30% in presence of CHIP shRNA1 and just over 40% in the presence of CHIP shRNA2 (Figure 26A). When hepatocyte growth factor (HGF) is added to increase cell scattering, cells transfected with the empty vector control have an increase in cell scattering percent from 55% to nearly 80%. In cells transfected with CHIP shRNA1, addition of HGF is associated with an increase of scattered cells from just over 30% to only 50%, far less than the empty vector control. Similarly, when the HGF hormone is added to cells transfected with CHIP shRNA2, cell scattering increases from just over 40% to just over 55% (Figure 26A). Reduction in cell scattering is associated with reduction in endogenous CHIP, and an increase in endogenous TAp63, as confirmed by immunoblot (Figure 26B). Cell scattering is also less visibly apparent in cell populations where CHIP is being knocked down as seen in the photographs taken for counting scattered cells (Figure 26C).

Figure 26 – Panel A

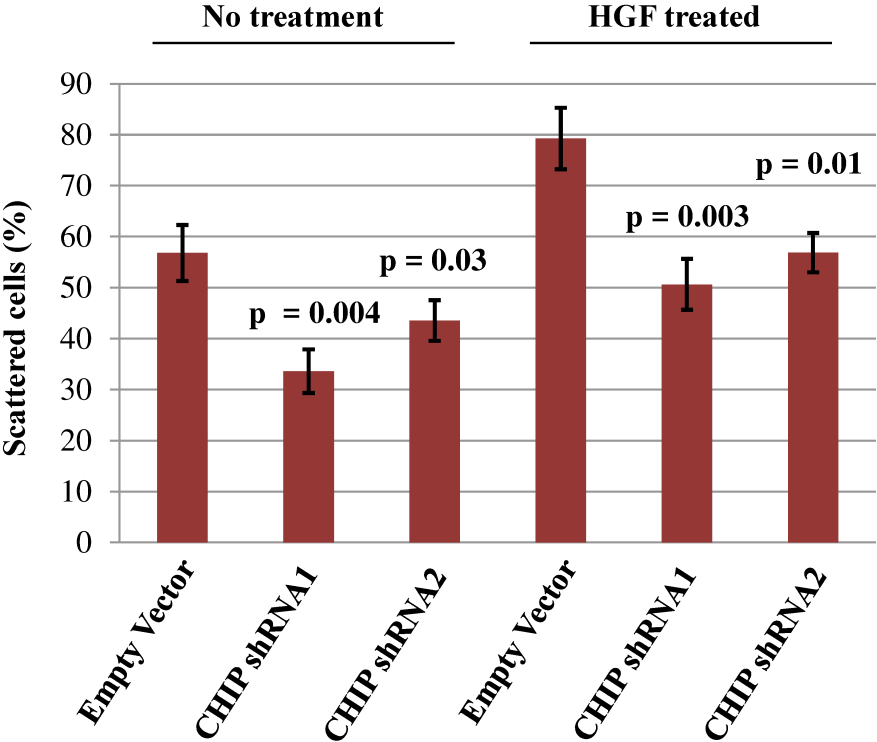


Figure 26 – Panel B

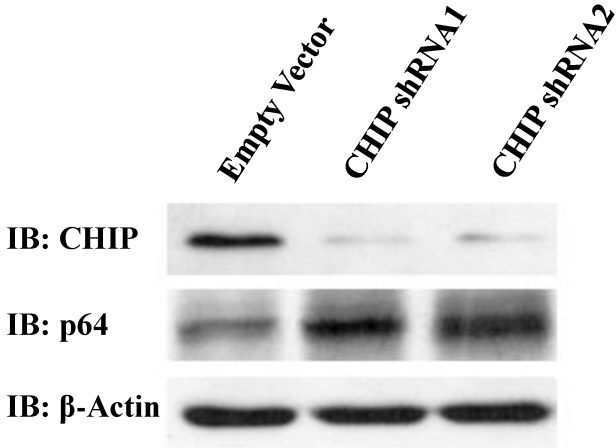


Figure 26 – Panel C

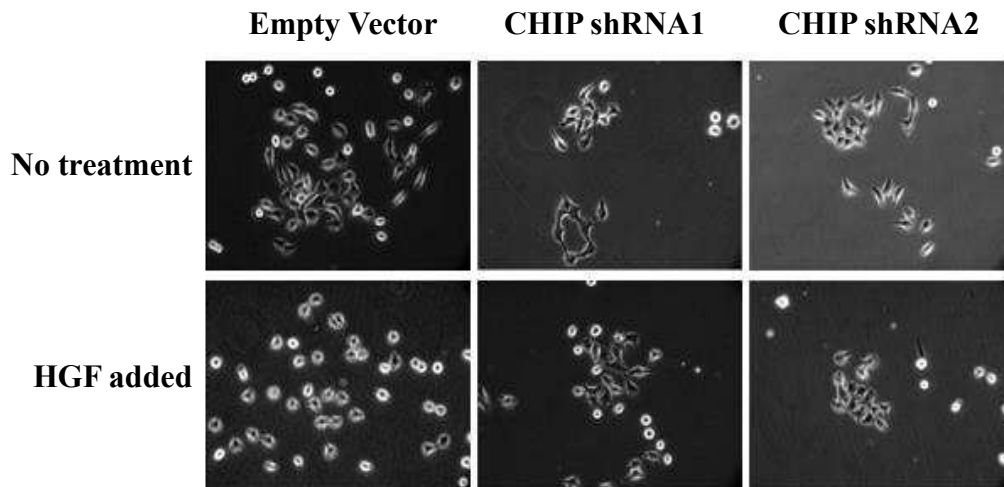


Figure 26 – Ablation of CHIP Reduces Cell Scattering.

H1299 stably transfected cells (Empty vector control, CHIP shRNA1, and CHIP shRNA2) were cultured in two triplicate groups. A cell scattering assay was conducted on these groups where one triplicate was treated with HGF (10 ng/L), while the other was left untreated. Cells were photographed (Panel C) and counted as grouped or scattered, and scattered cells were calculated as a percent of total cells counted and averages of these percent values were plotted in Excel (Microsoft, USA) (Panel A). P-values were calculated using a Student's T-Test (unpaired, unequal variance) between the percent values of cells transfected with the empty vector control and percent values of cells transfected with either CHIP shRNA1 or CHIP shRNA2. Whole cell lysates taken from a fraction of each cell group underwent SD-PAGE, and were analyzed by immunoblot to confirm transfection (Panel B). This experiment was repeated three times (n=3) with five replicates for each experiment.

3.04 – Endogenous CHIP and TAp63 Levels are Negatively Correlated in Carcinoma Cell Lines and Patient Tissue Samples

The final aim of the study was to look for negative correlations between endogenous p63 and CHIP expression in various carcinoma cell lines, and patient tissue samples. One normal fibroblast cell line (BJ) was used, alongside five squamous cell carcinoma cell lines (Figure 27A), and six invasive melanoma cell lines (Figure 27B). Negative correlation between CHIP and p63 levels was observed in three out of five squamous cell carcinoma cell lines (SCC9, FADU, and SCC15) (Figure 27A), and three out of six invasive melanoma cell lines (M2, Mewo, Hs895T) (Figure 27B). Surprisingly, no negative correlation was observed for either AIP4 or Mdm2 in any of these cell lines. Nine invasive prostate carcinoma tissue samples were also tested for endogenous CHIP and TAp63. These tissues were obtained from males aged 55 to 71 years of age, and were all adenocarcinomas. Compared to two benign prostate neoplasm tissue samples, all nine invasive carcinoma tissue samples had decreased endogenous TAp63 levels, and at least five out of nine had increased endogenous CHIP levels (Figure 28). Not one invasive prostate carcinoma tissue sample had greater levels of endogenous p63 than the benign prostate neoplasms, or lower levels of CHIP than the benign tissues (Figure 28). Negative correlation between TAp63 and CHIP was especially evident in invasive prostate carcinoma tissues 2, 3, and 4 (Figure 28).

Figure 27 – Panel A

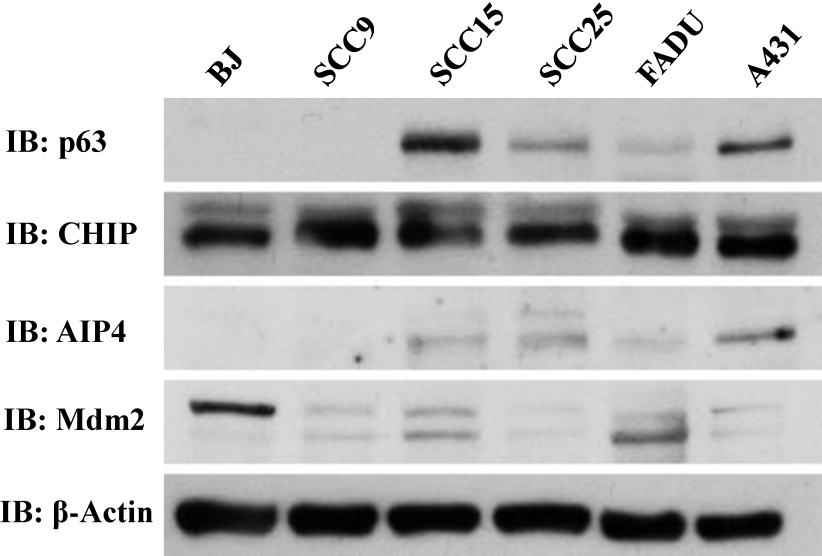


Figure 27 – Panel B

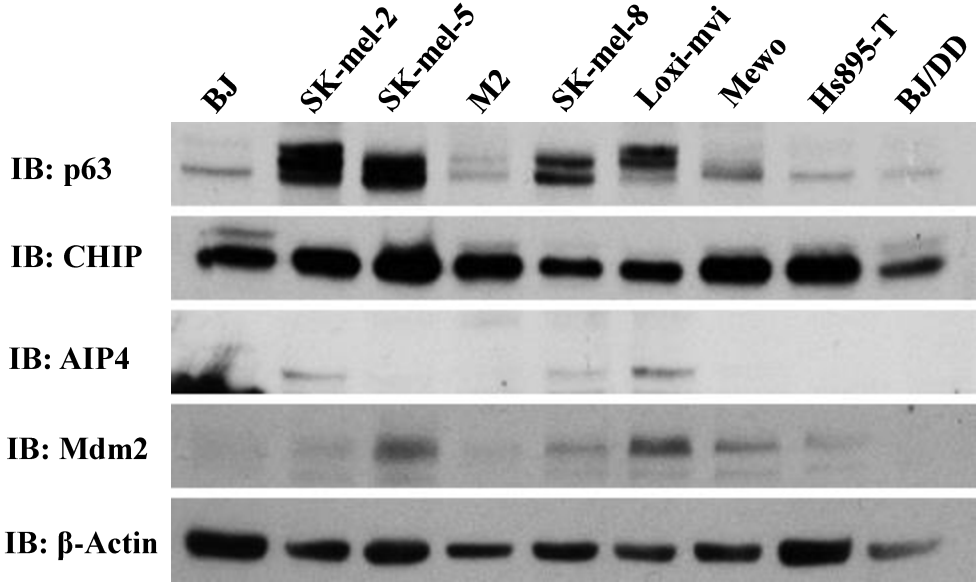


Figure 27 – Endogenous TAp63 and CHIP Levels in Selected Squamous Cell Carcinoma Cell Lines.

All cell lines were cultured under typical conditions (see Section 2.05) grown to 80-100% confluence and whole cell lysate was harvested, underwent SDS-PAGE, and analyzed by immunoblot. The first panel shows squamous cell carcinoma cell lines (Panel A). The second panel shows invasive melanoma cell lines (Panel B). This experiment was repeated twice (n=2).

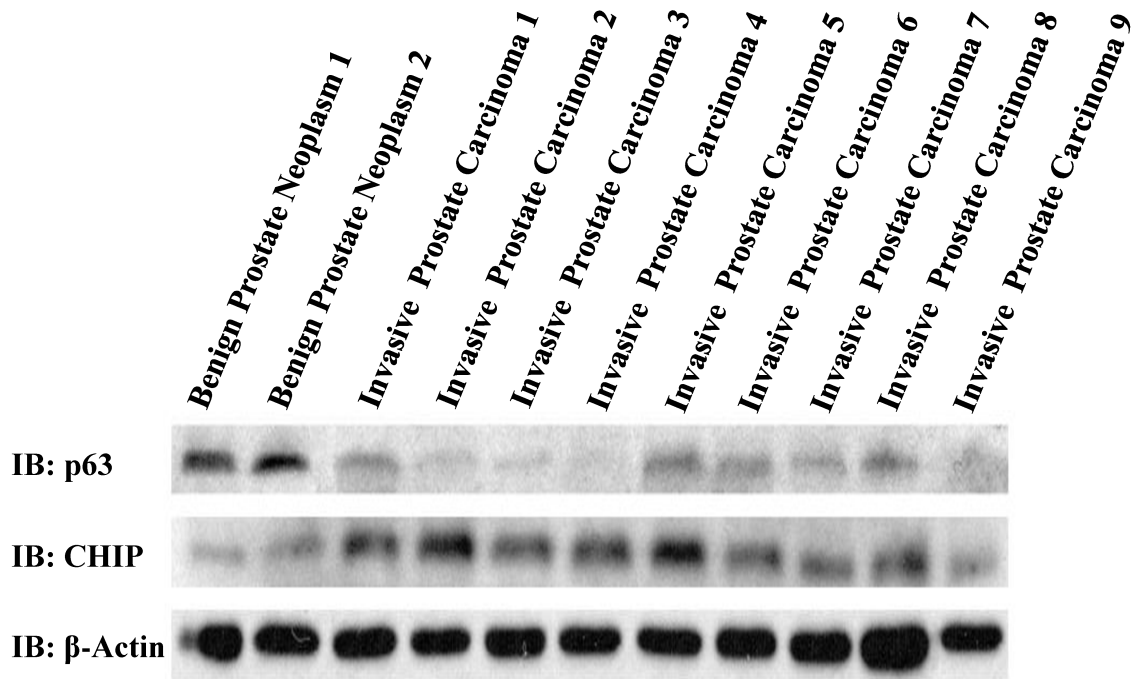


Figure 28 – Endogenous TAp63 and CHIP Levels in Nine Invasive Prostate Carcinoma Tissue Samples.

Whole cell lysates from nine invasive prostate carcinoma tissue samples and two benign prostate neoplasm samples underwent SDS-PAGE and were analyzed by immunoblot. Gleason scores for Patients 2 and 8 were 7 and 8 respectively. No Gleason scores are known for the other patients.

Chapter 4 – Discussion and Conclusions

4.01 – Discussion

The goal of this study was to determine whether CHIP negatively regulates TAp63 levels and function by targeting TAp63 for ubiquitin-mediated proteasome degradation. The first result demonstrated that CHIP is able to bind to TAp63 (Section 3.01), thereby being a TAp63-interacting partner supporting the Yeast 2-hybrid data (unpublished data).

Not only does CHIP bind to ectopic TAp63 (Figure 10), but it also can bind to endogenous p63 in MCF10 α breast epithelial cells (Figure 11). MCF10 α cells have high TAp63 α expression (data not shown), making these cells a good model for testing endogenous binding. Since CHIP can also degrade p53, it would be interesting to determine whether p73 is also a CHIP binding partner, if so then CHIP would be able to target the entire p53 family for proteasome degradation. CHIP binds to p53 near its TAD, and it was thought that it would also bind to a similar area on TAp63; however the construct binding assay showed otherwise. Based on C108, C393, and C541 constructs in a co-immunoprecipitation assay, CHIP requires the C-terminal region containing the SAM domain to bind with TAp63 (Figure 12). However, the binding is weaker in the three constructs than wild-type TAp63. This could be for many reasons including different protein shape (constructs lack a large portion of the TAp63 protein that might be necessary for proper folding), or perhaps another part of the protein such as the N-terminal PRD or TAD domain is required in cooperation for binding. It could also be that a different epitope tag (T7) was used for the full length wild-type TAp63 α than the deletion mutants, which used the Myc tag. Repeating this experiment using the same epitope tag would be necessary to eliminate this possibility.

It is interesting that the section containing the SAM domain is necessary for TAp63-CHIP binding since p53 does not contain one. The SAM domain is present in alpha isoforms of

p63 and p73, and has been implicated in protein-protein interactions with other SAM domains, being involved in forming large protein complexes [99]. It might be that CHIP is unable to bind to other p63 isoforms that lack the SAM domain (beta, gamma), or perhaps it binds to different areas of these proteins. It could also be that CHIP does not directly bind to p63: CHIP requires Hsp70/Hsc70 to bind many client substrates using its TPR domain to interact with the chaperone protein, and its U-box domain to ubiquitinate the client substrate. There are no data available for direct binding between p53 and CHIP, however, CHIP's U-box is observed to require Hsp70 or Hsc70 binding for its ubiquitination effect [259]. This may mean that CHIP does not directly bind to p53 or to TAp63, and that it requires the chaperone heat shock protein Hsp70. The p53 protein has many sites recognized by molecular chaperones including Hsp70, located on the N-terminal PRD domain, the DBD, and near the carboxyl terminus [240]. Of these, the N-terminal PRD domain is unfolded and exposed, making it possible to associate with Hsp70. A mutation in the PRD domain (R175H) increases association with Hsp70 and also increases degradation by CHIP [240]. If TAp63 associates with Hsp70 in a similar fashion as p53, this area might be important for increased binding with CHIP. Although wild-type p53 forms transient complexes with Hsc70 (a type of constitutively expressed Hsp70 protein), when CHIP is overexpressed, p63-Hsc70 complexes become more stable as p53 is locked into the CHIP-mediated degradation pathway [240]. TAp63 may follow a similar pathway where it can transiently associate with Hsc70 or other chaperone proteins and overexpression of CHIP can stabilize its association, resulting in its targeting for proteasome degradation. Proteins with the U-box domain like CHIP often interact with chaperone client proteins [260], further supporting the idea that this negative regulation of p53 family members by CHIP can be linked to the heat shock system. This interaction would involve CHIP binding to Hsp70/Hsc70 using its TPR domain, which is

recognized by Hsp70/Hsc70's C-terminal Glu-Glu-Val-Asp motif [261]. Once bound, CHIP can ubiquitinate Hsp70-bound client proteins, or Hsp70 itself if it is not bound to a client protein, by recruiting UbH5 E-2 conjugation family members using its U-box domain, and catalyzing the direct transfer of ubiquitin to the client protein. CHIP's E-4 ligase ability then catalyzes the attachment of Lys 48 linked poly-ubiquitin chains rendering the substrate recognizable by the proteasome. CHIP's role as tumor suppressor protein or proto-oncogene is in contention with controversial data, but Hsp70 proteins are largely agreed to have oncogenic function, being overexpressed in many invasive carcinomas including bladder, breast, colorectal, melanoma, and ovarian carcinomas [261]. It is possible from the ubiquitination study (Figure 13) that CHIP fulfills both E-3 and E-4 roles with respect to TAp63 ubiquitination; however, it is also possible that CHIP recruits another protein to enact the E-4 function. One limitation of this study is the lack of an ubiquitin mutant to ensure TAp63 is being poly-ubiquitinated rather than multi-ubiquitinated. To confirm Lys 48 poly-ubiquitination of TAp63, this experiment could be repeated using ubiquitin with a Lys 48 to arginine mutation rendering Lys 48 ubiquitin chain formation inactive. Other lysine mutants could be tested as well, but Lys 48 chains are considered to be the primary pattern of poly-ubiquitination recognized by the proteasome (Lys 63 linked chains for instance are not recognized) [190, 191].

This study has also defined CHIP as a negative regulator of p63 stability (Section 3.02), being associated with both ectopic (Figure 14) and endogenous (Figure 15) protein degradation that is dependent on proteasome function. CHIP knockdown cells have stabilized endogenous p63 (Figure 16), and may indicate that like AIP4, CHIP is a major regulator of TAp63. This same phenomenon was observed with endogenous p53 as well when CHIP was knocked down (covered in Section 3.03). This negative regulation of TAp63 by CHIP is consistent with the Lys

48 linkage model of CHIP with E-2 members of the UbcH5 family. CHIP can also interact with the E-2 enzyme Ubc13 to make Lys 68 linked poly-ubiquitin chains [224], but since Lys 68 chains are not recognized by the proteasome, it is unlikely that this is the type of ubiquitination by CHIP that is affecting TAp63 protein stability, since a functioning proteasome is necessary for the degradation effect (Figure 17), and in fact it seems that CHIP instead stabilizes TAp63 levels when proteasome function is blocked.

Importantly, the TAp63 α isoform is not the only variant of p63 able to be targeted by CHIP. The most commonly expressed of all p63 isoforms, Δ Np63 α , is also degraded in the presence of CHIP (Figure 18). Since Δ Np63 α has oncogenic function, this observation is consistent with CHIP having a context-dependent role between tumor suppressor and oncogenic function, just as it can target both wild-type and mutant p53 for degradation [240]. It would be interesting to determine whether CHIP can also affect the stability of p63 isoforms that lack the SAM domain, since both TAp63 α and Δ Np63 α contain it, but not the other isoforms.

In the third aim of this study, how the functional ability of TAp63 was affected by the presence of CHIP was investigated (Section 3.03). Both p53 and TAp63 individual transfections into these cells decrease cell survival by roughly the same amount (60-65% reduction in survival), consistent with their roles in promoting cell death. Mdm2, AIP4, and CHIP are all able to restore cell survival (Figure 19), but the magnitude of effect they have depends on what tumor suppressor protein they are co-transfected with. As expected, Mdm2 is able to almost completely reverse the decrease in cell survival observed when p53 is transfected alone into H1299 cells (recovers survival to roughly 90%). Since Mdm2 is considered to be the major regulator of p53, this is consistent with the previous research. Mdm2 cannot target any p63 isoform alone for degradation, but in one study, it was reported that it can target the Δ Np63

variants for degradation in the presence of the E-3 ligase Fbw7 [177]. Although this would not seem to account for the minimal increase in cell survival observed when Mdm2 is co-transfected with TAp63 in H1299 cells, since Δ Np63 is a tumor suppressor, there may be another explanation besides protein degradation to explain an increase in cell survival when TAp63 is co-transfected with Mdm2. One study did highlight other ways Mdm2 can negatively affect p63 function either by physically blocking TAp63's transactivation ability or facilitating export of TAp63 out of the nucleus into the cytoplasm where it would have to be imported back into the nucleus to resume any transactivation ability [202]. The small increase in cell survival (from roughly 40% to 50%) might then be due to a weak inhibitory effect of Mdm2 on TAp63. However, other studies have found that Mdm2 either has no effect on p63 function or that it can stabilize p63 levels and enhance p63 function [201], providing conflicting data, indicating that Mdm2's interaction with p63 is not fully understood.

Considered to be the major negative protein regulator of TAp63 (and p73 as well), AIP4 when co-transfected with TAp63 increased cell survival by a greater extent than Mdm2 (to 70%). Although this is consistent with the literature, interestingly, AIP4 was also associated with a considerable increase in cell survival when co-transfected with p53 (from 35% to 80%). This is surprising, as to my knowledge no study has ever reported AIP4 able to target p53 for degradation. Also interesting with regards to the previous observation is that AIP4 is not associated with a decrease in p53 levels in any of co-transfection immunoblot assays (Figure 3A). To explain this functional change, it may be possible that AIP4 indirectly interferes with p53 function by targeting endogenous TAp63 for degradation. The p53 protein has been reported to rely on either p63 or p73 to promote apoptosis, while the other two proteins can induce apoptosis independent of p53 status [131], and so if AIP4 is interfering with native p63

(or p73) levels in H1299 cells then this might account for the increase in survival. This has interesting implications involving p63 and p73; possibly supporting the idea that they are more important to the initiation of apoptosis in mature cells than traditionally thought.

CHIP was also associated with an increase in cell survival when co-transfected with TAp63, and to virtually the same degree as TAp63's primary negative regulator AIP4 (increasing cell survival to 70%). This is consistent with the degree it affects TAp63 levels, assayed by immunoblot, and is supporting evidence that CHIP is at least as important as AIP4 in negatively regulating TAp63. Knocking down CHIP with the two selected CHIP shRNA sequences was effective at reducing cell survival in stably transfected cells (Figure 20), although the two sequences did not have the same magnitude of effect. Decrease in cell survival may be accounted for by many different phenomena including apoptosis, autophagy, and necrosis [81]. Save for the latter (which can sometimes be regulated by internal cellular processes in the case of "programmed necrosis", but classically refers to conventional/environmental cell death), these are all considered regulated processes, and both p53 and TAp63 can target the transcription of genes that produce proteins affecting these pathways [60, 101, 262-264]. The major limitation of the survival studies is the lack of single transfection regimens for CHIP, AIP4, and Mdm2. While it is clear that the three E-3 ligase regulators interfere with TAp63 and p53-induced cell death, promoting survival, repeating the experiment using single transfection CHIP, AIP4, and Mdm2 controls would determine whether they promote higher levels of survival compared to the pcDNA3 control. Adding these positive controls to the experiment would ensure that CHIP and the other two E-3 ligases had pro-survival effects on endogenous levels of TAp63 (but not p53, since that protein is not expressed endogenously in the H1299 cell line).

In addition to cell survival assays, cell death assays were also performed. TAp63 can induce cell death through apoptosis, and target the transcription of many genes involved with encoding proteins involved in intrinsic apoptosis such as bax, PUMA, and *Noxa*; and extrinsic apoptosis inducing TRAIL-R, TNFR, and CD95-Fas [91, 108, 265]. Fascinatingly, the apoptosis pathway itself potentiates TAp63 α -induced transcriptional activity resulting in a positive feedback loop: Caspases 3, 6, 7, and 8 are all able to cleave off the TI domains located on TAp63 α , and Δ Np63 α [265]. When TAp63 α loses its TI domain, it becomes more transcriptionally active, able to increase the transcription of a higher amount of pro-apoptotic targets (and thereby promoting apoptosis), and when Δ Np63 α loses its TI domain, its dominant-negative inhibitory effect against TAp63 α is weakened [265]. When measuring percent of cells undergoing death using flow cytometry, Mdm2 and AIP4 co-transfected with TAp63 did not significantly decrease percentage of apoptotic cells (Figure 21), which was surprising in the case of AIP4, since it is regarded as the primary regulator of TAp63. This could be due to the fact that the cells were unstressed, and the apoptotic fraction was not very high to begin with (co-transfection with TAp63 and p53 increases apoptotic cell fraction independent of cellular stress by 6.5% and 10% respectively). Mdm2 did significantly decrease the apoptotic fraction when co-transfected with p53, in agreement with its role as the primary p53 negative regulator. CHIP was able to significantly reduce the apoptotic cell fraction when co-transfected with both TAp63 and p53 (Figure 21). This reduction in the apoptotic fraction by CHIP was even more pronounced when H1299 cells were stressed with UV radiation, resulting in an increase of the fraction of apoptotic cells to 15% (Figure 22). At the highest transfection concentration, CHIP reduced the apoptotic fraction almost entirely (to fewer than 3%) and this was accompanied by a reduction in endogenous TAp63, further supporting the idea that CHIP is one of the primary

regulators of p63. Also of note, since CHIP was shown to degrade the Δ Np63 α isoform as well as the TAp63 isoform, it seems that despite also targeting the oncogenic Δ Np63 α isoform for degradation, the presence of CHIP overall seems to have an oncogenic effect in these assays by being associated with a decrease in apoptosis. It may be that degrading TAp63 has a more pronounced effect on promoting cell survival than degrading the dominant-negative Δ Np63 isoform has on preventing cell survival.

CHIP is also associated with preventing p21 induction, a marker of cell cycle arrest. It is not known whether CHIP can target p73 for proteasome degradation or negatively affect p73 function, however, p73 is another protein able to target the p21 gene for transcription, so without p53 and p73, p63 remains as the only p53 family member able to target p21 for transcription, once transfected into this cell line. TAp63 α is not able to induce the same levels of p21 transcription as p53 (shown in this study where p53 has a much higher effect on promoting p21 expression) or other more transcriptionally active isoforms like TAp63 γ [60], however, it can still induce p21 expression in both H1299 and SAOS-2 cells by a fold change of 14 and 24 respectively (Figure 23). All three E-3 ligases are associated with a reduction in p21 transcription with the presence of CHIP acting as the most powerful inhibitor in H1299 cells and the second most powerful inhibitor in SAOS-2 cells (second to AIP4), although it was very close to AIP4 in terms of p21 transcriptional reduction in these assays. Consistent with promoting cell survival and inhibiting apoptosis, these data suggest that CHIP also inhibits transcription of p21 and therefore discourages cell cycle arrest. The influence of CHIP on the cell cycle was also examined. Percent of cells in G1 increases by a fraction of 10% when H1299 cells are transfected with either p53 or TAp63 α , and this increase in G1 percent is abolished in the presence of any of the three negative regulators for p53 and TAp63 α transfected cells (Figure

24). Both proteins likely can promote cell cycle arrest by targeting p21 for transcription. Interestingly despite being able to promote a much higher transcription of p21, p53 does not induce a higher percentage of G1 cells than TAp63 α , so perhaps other negative regulatory pathways of cell cycle arrest are at play in these cells, or maybe TAp63 α 's modest increase of p21 transcription compared to p53 is sufficient to induce a meaningful increase in cells undergoing G1 arrest. Ablation of CHIP is also associated with an increase in the percentage of cells in G1 (Figure 25), supporting the evidence that CHIP inhibits cell cycle arrest mediated by p63.

Not only is CHIP involved in negatively regulating the primary tumor suppressive function of TAp63, but it is also involved in inhibiting secondary tumor suppressive functions as well: When CHIP is knocked-down in H1299 cells, cell scattering is reduced, and this reduction is correlated with an increase in endogenous TAp63 (Figure 26). Cell scattering is associated with transition from epithelial to mesenchymal morphology, a marker of invasion [266]. By degrading TAp63, CHIP may have an oncogenic role in promoting secondary malignant characteristics. It might be able to promote cell scattering by epithelial to mesenchymal transition, and therefore invasion ability by affecting TAp63's transactivation of dicer, the endonuclease capable of processing precursor RNA into miRNA and siRNA molecules [267]. Dicer is thought to be able to suppress metastasis by processing certain miRNA molecules that inhibit metastasis pathways including miR-31, miR-126, miR-130b, miR-206, and miR-335 [268]. It would be very interesting to determine whether CHIP reduces TAp63-mediated dicer transactivation to support this idea. Since the cell scattering assay shows migration of cells rather than invasion, this assay is only an indirect method of assessing invasive capacity. Another way to test invasion would include Matrigel assays that test for cell penetration through

a semi-solid medium rather than cell migration. 3D assays using this principle can also be employed which better reflect tumor invasion than 2D migration assays can [269-271]. Even though it is not a direct marker of invasion, epithelial to mesenchymal transition can be confirmed in this experiment by measuring epithelial markers such as E-cadherin [272], and mesenchymal biomarkers such as N-cadherin, and vimentin [273, 274].

The final aim of the study looked at CHIP and TAp63 levels in various invasive carcinoma cell lines and patient tissue samples (Section 3.04). Lack of TAp63 is associated with highly invasive cancers [119, 275], so it was interesting to look for association between loss of endogenous p63 and presence of CHIP. Established cell lines are known to acquire additional mutations as they are passaged [276], and since some of these mutations may be related to continuous culture and not carcinogenesis, it cannot be expected that CHIP and p63 levels are always negatively correlated. Furthermore, CHIP and p63 levels (either TA or Δ N) are often conflicting with each other when measured in cancers (reviewed in Section 1.04), and rarely is consistent from cancer to cancer. However, no study to my knowledge has looked at an association between CHIP and p63 expression. When measuring levels of these proteins in squamous cell carcinoma and melanoma cell lines (Figure 27), chosen because these cell lines are examples of epithelial-derived carcinomas that have inactivated p53, some of these lines including Mewo, Hs895-T, M2, SCC25, FADU, and A341 demonstrated very high levels of CHIP in association with very low levels of TAp63. Not all of these cell lines demonstrated this association, however, when looking for patterns between the other two E-3 ligases used in this study (AIP4 and Mdm2), no negative association between endogenous levels of either of these two proteins and TAp63 could be observed at all. This is very surprising in the case of AIP4, as we expected the major p63 regulator to be associated with low TAp63 levels in at least some of

these cell lines. It is interesting that CHIP does show some negative association in these assays, further supporting the idea that it is one of the major protein regulators of TAp63, and therefore has oncogenic function; although this negative association could be due to coincidence (Section 5.0 provides examples on how to confirm whether these observations are supporting a CHIP oncogenic function). Mdm2 and p53 associate with the chaperone protein Hsp90, and CHIP may be able to indirectly interact with Mdm2 through its binding partner Hsp90 to coordinate degradation of p53 [240]. To my knowledge, there is no evidence that AIP4 can cooperate with Hsp90 in this fashion, but perhaps some other unidentified interaction links it to one of the p53 negative regulators. An Mdm2-CHIP “cross-talk” through Hsp90 could also be important for regulating TAp63 stability as well. Mdm2 is not associated with a reduction in TAp63 levels and yet previous research has demonstrated that it can bind to p63 [202]. Perhaps then Mdm2-p63 can also interact with chaperone proteins like Hsp90 and therefore Mdm2 can regulate p63 stability by cross talk with the heat shock-CHIP pathway. However, these associations could be coincidental, and to test whether CHIP is endogenously responsible for the lower expression of TAp63 in these cell lines, knock down studies would be necessary for confirmation. Even more interesting than the negative correlation between CHIP and TAp63 levels observed in carcinoma cell lines is the levels of CHIP and TAp63 in the invasive prostate cancer tissue samples. All nine invasive tissue samples have lower TAp63 levels compared to the two benign prostate neoplasm samples (Figure 28). Furthermore, at least seven out of nine of these invasive samples also have higher CHIP levels than the benign samples. Since patient tissue samples have not been continuously cultured, this negative association between CHIP and TAp63 levels may indicate the possibility of clinical relevance in this observed association.

4.02 – Conclusions

In this study, it is concluded that CHIP binds to, ubiquitinates, and targets TAp63 for proteasome-mediated degradation. This study strongly supports the idea that CHIP is a prime regulator of TAp63 protein stability and function with a similar strength to AIP4, the previously characterized primary p63 regulator. This also heavily implies that CHIP has oncogenic roles in relation to its negative regulation of TAp63 including suppression of apoptosis, cell cycle arrest, while promoting cell survival and cell scattering. This study supports CHIP as a possible proto-oncogene with respect to the TAp63 and p53 tumor suppressor proteins. However, CHIP is most often implicated as a tumor suppressor in many papers as it can also target proto-oncogenes for degradation, and therefore it is likely that CHIP has context dependent roles in cancer development. An increased understanding of these context dependent roles could help determine under what conditions CHIP acts as a tumor suppressor or oncogene in invasive carcinomas.

Chapter 5 – Future Directions

5.01 – Further Characterizing CHIP’s Negative Regulation of TAp63 Stability

In order to fully characterize how CHIP binds to the TAp63, a series of FLAG-tagged CHIP-deletion mutants could be generated including one lacking the N-terminal TPR domain (CHIP Δ TPR), one lacking the central CC domain (CHIP Δ CC), and one lacking the C-terminal U-box domain (CHIP Δ U-box). Co-transfecting each of these constructs with wild-type TAp63 α in H1299 lung carcinoma cells followed by immunoprecipitating the FLAG-tag and immunoblotting for TAp63 would reveal what domain of CHIP is necessary for TAp63 binding. Whether CHIP can directly bind to TAp63 alone or requires the Hsp70 chaperone protein can be tested in in-vitro studies, where GST-tagged TAp63 α , FLAG-tagged CHIP, and Hsp70 proteins are purified in bacteria. A GST pull down assay could be performed where GST-tagged TAp63 α is pulled down and then immunoblotted for FLAG-CHIP in the presence or absence of Hsp70. If the presence of Hsp70 is required for binding, then ablating Hsp70 expression through Hsp70 shRNA or small-molecule inhibitors of Hsp70 such as the small molecule ATP analog Ver-155008 (which can inhibit both Hsp70 and Hsc70) [277] should prevent CHIP mediated TAp63 degradation. Ubiquitination of TAp63 α could also be tested in the presence of the CHIP Δ U-box mutant to ensure that CHIP is responsible for both E-3 and E-4 ligase abilities for ubiquitinating TAp63. Lack of ubiquitination here would support the hypothesis that CHIP is solely responsible for ubiquitinating TAp63 without the help of any other E-3/E-4 ligases. Finally, co-transfecting TAp63 γ (the shortest of the TA variants) with CHIP would determine whether or not CHIP can degrade p63 isoforms lacking the SAM domain. Lys 48 ubiquitin mutants could also be introduced as negative controls in these experiments to ensure that CHIP is responsible for Lys 48 poly-ubiquitination of TAp63, thereby targeting it for proteasome-mediated degradation.

5.02 – Further Investigating CHIP’s Negative Regulation of TAp63 Function

To investigate how CHIP is promoting cell scattering, CHIP could be transfected into H1299 lung carcinoma cells alongside TAp63 α , and a dicer-luciferase reporter gene. A luciferase reporter assay would then be conducted and relative dicer expression would be compared between CHIP and empty vector samples to see if dicer expression is reduced in the presence of CHIP. It would also be interesting to overexpress CHIP alongside either an empty vector or dicer, and perform a cell scattering assay to see whether cell scattering is reduced in the presence of dicer. These experiments could also be performed using maspin, another invasion and metastasis suppressor instead of dicer. Furthermore, direct invasion assays could be performed that test penetration of cells into a semi-solid medium such as Matrigel that approximates the extracellular matrix coating the basement membrane dividing the epithelium from the stromal tissues [270, 271].

In carcinoma cell lines that show a negative correlation between CHIP and p63 levels (such as Mewo, Hs895-T, M2, SCC25, FADU, and A431) it would be interesting to overexpress CHIP, and see if endogenous p63 is further reduced. Furthermore, in cell lines that demonstrated high concentrations of TAp63, such as (Sk-mel-2, Sk-mel-5, and Sk-mel-8), overexpressing CHIP may also reduce TAp63 levels (this might be easier to observe than the cell lines that start with low endogenous TAp63). CHIP Δ U-box could possibly be used as a negative control if that mutant is unable to negatively regulate TAp63 stability. Also in the cell lines with low TAp63 levels (ex. Mewo, Hs895-T), CHIP could be knocked down using CHIP shRNA and then endogenous p63 levels could be measured to see if there is an increase. This would provide a strong negative link between CHIP and TAp63 levels in multiple carcinoma cell lines. Alternatively, an assay making use of the new CRISPR/Cas9 (Clustered Regularly Interspaced

Short Palindromic Repeats)-associated protein 9 system to edit the genomic DNA [278] could be effective for knocking out CHIP, completely ablating CHIP expression in these cells (rather than just reducing it through shRNA interference). If knockdown/knockout of CHIP is successful in re-establishing TAp63 stability and function, then CHIP could also be the therapeutic target for E-3 ligase inhibitors in future of cancer treatment.

Bibliography

1. Greenfield, L., K. Oldham, G. Zelenock, and K. Lillemoe. Essentials of Surgery - Scientific Principles and Practice. New York, USA: Lippincott Williams & Wilkins; 1997.
2. Weinberg, R.A. The Biology of Cancer. 1st ed. New York: Garland Science; 2007.
3. Sembulingham, K. Essentials of Medical Physiology. 6th ed. New Delhi, India: JP Medical Ltd; 2012.
4. Montgomery, B.E., G.S. Daum, and C.J. Dunton. Endometrial hyperplasia: a review. Obstet Gynecol Surv, 2004. **59**(5): p. 368-78.
5. Franks, L.M. Benign nodular hyperplasia of the prostate; a review. Ann R Coll Surg Engl, 1953. **14**(2): p. 92-106.
6. Hong W., H.W., Holland Frei. Cancer Medicine. 8th ed. Shelton, USA: People's Medical Publishing House; 2010.
7. Siegel, R.L., K.D. Miller, and A. Jemal. Cancer statistics 2015. CA Cancer J Clin, 2015. **65**(1): p. 5-29.
8. Bromfield G, D.D., De P, Newman K, Rahal R, Shaw A, Weir H, Woods R, Xie L, Demers A, Ellison L, Semenciw R, and Daigle J. Canadian Cancer Statistics 2015: Predictions of the future burden of cancer in Canada. Canadian Cancer Society, 2015. p.1-151
9. Rosenwald, I.B. The role of translation in neoplastic transformation from a pathologist's point of view. Oncogene, 2004. **23**(18): p. 3230-47.
10. Todd, R. and D.T. Wong. Oncogenes. Anticancer Res, 1999. **19**(6A): p. 4729-46.

11. Weinberg, R.A. Oncogenes and the Molecular-Biology of Cancer. *Journal of Cell Biology*, 1983. **97**(6): p. 1661-1662.
12. Boylan, J.F., et al. Role of the Ha-ras (RasH) oncogene in mediating progression of the tumor cell phenotype (review). *Anticancer Res*, 1990. **10**(3): p. 717-24.
13. Goodsell, D.S. The molecular perspective: the ras oncogene. *Stem Cells*, 1999. **17**(4): p. 235-6.
14. Sun, W. and J. Yang. Functional mechanisms for human tumor suppressors. *J Cancer*, 2010. **1**: p. 136-40.
15. Knudson, A.G., Jr. Mutation and cancer: statistical study of retinoblastoma. *Proc Natl Acad Sci U S A*, 1971. **68**(4): p. 820-3.
16. Giacinti, C. and A. Giordano. RB and cell cycle progression. *Oncogene*, 2006. **25**(38): p. 5220-7.
17. Bignon, Y.J. and P. Rio. The retinoblastoma gene: will therapeutic use of its tumor suppressive properties be possible?. *Bull Cancer*, 1993. **80**(8): p. 704-12.
18. Marino-Enriquez, A. and C.D. Fletcher. Shouldn't we care about the biology of benign tumours? *Nat Rev Cancer*, 2014. **14**(11): p. 701-2.
19. Allred, D.C. Ductal carcinoma in situ: terminology, classification, and natural history. *J Natl Cancer Inst Monogr*, 2010. **2010**(41): p. 134-8.
20. McDougall, S.R., A.R. Anderson, and M.A. Chaplain. Mathematical modelling of dynamic adaptive tumour-induced angiogenesis: clinical implications and therapeutic targeting strategies. *J Theor Biol*, 2006. **241**(3): p. 564-89.
21. Pointillart V, R.A., A. Ravaund, and J. Palussiere. *Vertebral Metastases*. Bordeaux, France: Springer-Verlag; 2002.

22. Berman, J.J. Tumor taxonomy for the developmental lineage classification of neoplasms. *BMC Cancer*, 2004. **4**: p. 88.
23. Sastry K, and V. Shukul. *Developmental Biology*. 1st ed. Meerut, India: Rastogi Publications; 2007.
24. Wenig, B.M. Squamous cell carcinoma of the upper aerodigestive tract: precursors and problematic variants. *Mod Pathol*, 2002. **15**(3): p. 229-54.
25. Harvey, J.C., and E.J Beattie. *Cancer Surgery*. Philadelphia, USA: Saunders; 1996.
26. Houssami, N., et al. Early detection of second breast cancers improves prognosis in breast cancer survivors. *Ann Oncol*, 2009. **20**(9): p. 1505-10.
27. Brenner, D.E. and D.P. Normolle. Biomarkers for cancer risk, early detection, and prognosis: the validation conundrum. *Cancer Epidemiol Biomarkers Prev*, 2007. **16**(10): p. 1918-20.
28. Nun-Anan, P. and R.K. Vilaichone. Late stage and grave prognosis of esophageal cancer in Thailand. *Asian Pac J Cancer Prev*, 2015. **16**(5): p. 1747-9.
29. Longuespee, R., et al. Ovarian cancer molecular pathology. *Cancer Metastasis Rev*, 2012. **31**(3-4): p. 713-32.
30. Dasari, S. and P.B. Tchounwou. Cisplatin in cancer therapy: molecular mechanisms of action. *Eur J Pharmacol*, 2014. **740**: p. 364-78.
31. Horwitz, S.B. Taxol (paclitaxel): mechanisms of action. *Ann Oncol*, 1994. **5 Suppl 6**: p. S3-6.
32. Das, G.C., et al. Taxol-induced cell cycle arrest and apoptosis: dose-response relationship in lung cancer cells of different wild-type p53 status and under isogenic condition. *Cancer Lett*, 2001. **165**(2): p. 147-53.

33. Markman, M. Pharmaceutical management of ovarian cancer : current status. *Drugs*, 2008. **68**(6): p. 771-89.
34. Links, M. and C. Lewis. Chemoprotectants: a review of their clinical pharmacology and therapeutic efficacy. *Drugs*, 1999. **57**(3): p. 293-308.
35. Kelley, M.R., et al. Role of the DNA base excision repair protein, APE1 in cisplatin, oxaliplatin, or carboplatin induced sensory neuropathy. *PLoS One*, 2014. **9**(9): p. e106485.
36. Schippinger, W., et al. Frequency of febrile neutropenia in breast cancer patients receiving epirubicin and docetaxel/paclitaxel with colony-stimulating growth factors: a comparison of filgrastim or lenograstim with pegfilgrastim. *Oncology*, 2006. **70**(4): p. 290-3.
37. Markman, M. The promise and perils of 'targeted therapy' of advanced ovarian cancer. *Oncology*, 2008. **74**(1-2): p. 1-6.
38. Shen, D.W., et al. Cisplatin resistance: a cellular self-defense mechanism resulting from multiple epigenetic and genetic changes. *Pharmacol Rev*, 2012. **64**(3): p. 706-21.
39. Yusuf, R.Z., et al. Paclitaxel resistance: molecular mechanisms and pharmacologic manipulation. *Curr Cancer Drug Targets*, 2003. **3**(1): p. 1-19.
40. Chien, J., et al. Platinum-sensitive recurrence in ovarian cancer: the role of tumor microenvironment. *Front Oncol*, 2013. **3**: p. 251.
41. Saraswathy, M. and S. Gong. Different strategies to overcome multidrug resistance in cancer. *Biotechnol Adv*, 2013. **31**(8): p. 1397-407.
42. Kalyn, R. Overview of targeted therapies in oncology. *J Oncol Pharm Pract*, 2007. **13**(4): p. 199-205.

43. Guo, X.E., et al. Targeting tumor suppressor networks for cancer therapeutics. *Curr Drug Targets*, 2014. **15**(1): p. 2-16.
44. Slamon, D.J., et al. Human breast cancer: correlation of relapse and survival with amplification of the HER-2/neu oncogene. *Science*, 1987. **235**(4785): p. 177-82.
45. Faltus, T., et al. Silencing of the HER2/neu gene by siRNA inhibits proliferation and induces apoptosis in HER2/neu-overexpressing breast cancer cells. *Neoplasia*, 2004. **6**(6): p. 786-95.
46. Singh, J.C., K. Jhaveri, and F.J. Esteva. HER2-positive advanced breast cancer: optimizing patient outcomes and opportunities for drug development. *Br J Cancer*, 2014. **111**(10): p. 1888-98.
47. Slamon, D.J., et al. Use of chemotherapy plus a monoclonal antibody against HER2 for metastatic breast cancer that overexpresses HER2. *N Engl J Med*, 2001. **344**(11): p. 783-92.
48. Goldman, J.M. and J.V. Melo. Chronic myeloid leukemia--advances in biology and new approaches to treatment. *N Engl J Med*, 2003. **349**(15): p. 1451-64.
49. American Cancer Society. *Cancer Facts & Figures 2015*. Atlanta: American Cancer Society; 2015.
50. Green, M.R. Targeting targeted therapy. *N Engl J Med*, 2004. **350**(21): p. 2191-3.
51. Philip, P.A. Development of targeted therapies for pancreatic cancer. *Lancet Oncol*, 2011. **12**(3): p. 206-7.
52. De Laurenzi, V. and G. Melino. Evolution of functions within the p53/p63/p73 family. *Ann N Y Acad Sci*, 2000. **926**: p. 90-100.
53. Hollstein, M., et al. p53 mutations in human cancers. *Science*, 1991. **253**(5015): p. 49-53.

54. Khoury, M.P. and J.C. Bourdon. p53 Isoforms: An Intracellular Microprocessor? *Genes Cancer*, 2011. **2**(4): p. 453-65.
55. Melino, G., et al. Functional regulation of p73 and p63: development and cancer. *Trends Biochem Sci*, 2003. **28**(12): p. 663-70.
56. Augustin, M., et al. Cloning and chromosomal mapping of the human p53-related KET gene to chromosome 3q27 and its murine homolog Ket to mouse chromosome 16. *Mamm Genome*, 1998. **9**(11): p. 899-902.
57. Kaghad, M., et al. Monoallelically expressed gene related to p53 at 1p36, a region frequently deleted in neuroblastoma and other human cancers. *Cell*, 1997. **90**(4): p. 809-19.
58. Osada, M., et al. Cloning and functional analysis of human p51, which structurally and functionally resembles p53. *Nat Med*, 1998. **4**(7): p. 839-43.
59. Trink, B., et al. A new human p53 homologue. *Nat Med*, 1998. **4**(7): p. 747-8.
60. Yang, A., et al. p63, a p53 homolog at 3q27-29, encodes multiple products with transactivating, death-inducing, and dominant-negative activities. *Mol Cell*, 1998. **2**(3): p. 305-16.
61. Schmale, H. and C. Bamberger. A novel protein with strong homology to the tumor suppressor p53. *Oncogene*, 1997. **15**(11): p. 1363-7.
62. Zeng, X., Y. Zhu, and H. Lu. NBP is the p53 homolog p63. *Carcinogenesis*, 2001. **22**(2): p. 215-9.
63. Soussi, T. The history of p53. A perfect example of the drawbacks of scientific paradigms. *EMBO Rep*, 2010. **11**(11): p. 822-6.

64. Mowat, M., et al. Rearrangements of the cellular p53 gene in erythroleukaemic cells transformed by Friend virus. *Nature*, 1985. **314**(6012): p. 633-6.
65. Oren, M. and V. Rotter. Mutant p53 gain-of-function in cancer. *Cold Spring Harb Perspect Biol*, 2010. **2**(2): p. a001107.
66. Soussi, T. The humoral response to the tumor-suppressor gene-product p53 in human cancer: implications for diagnosis and therapy. *Immunol Today*, 1996. **17**(8): p. 354-6.
67. Colman, M.S., C.A. Afshari, and J.C. Barrett. Regulation of p53 stability and activity in response to genotoxic stress. *Mutat Res*, 2000. **462**(2-3): p. 179-88.
68. Moll, U.M. The Role of p63 and p73 in tumor formation and progression: coming of age toward clinical usefulness. *Clin Cancer Res*, 2003. **9**(15): p. 5437-41.
69. Shiloh, Y. and Y. Ziv. The ATM protein kinase: regulating the cellular response to genotoxic stress, and more. *Nat Rev Mol Cell Biol*, 2013. **14**(4): p. 197-210.
70. Shiotani, B. and L. Zou. Single-stranded DNA orchestrates an ATM-to-ATR switch at DNA breaks. *Mol Cell*, 2009. **33**(5): p. 547-58.
71. Powers, J.T., et al. E2F1 uses the ATM signaling pathway to induce p53 and Chk2 phosphorylation and apoptosis. *Mol Cancer Res*, 2004. **2**(4): p. 203-14.
72. Mirzayans, R., et al. New insights into p53 signaling and cancer cell response to DNA damage: implications for cancer therapy. *J Biomed Biotechnol*, 2012. **2012**: p. 170325.
73. Vermeulen, K., D.R. Van Bockstaele, and Z.N. Berneman. The cell cycle: a review of regulation, deregulation and therapeutic targets in cancer. *Cell Prolif*, 2003. **36**(3): p. 131-49.
74. Frade, J.M. and M.C. Ovejero-Benito. Neuronal cell cycle: the neuron itself and its circumstances. *Cell Cycle*, 2015. **14**(5): p. 712-20.

75. Munoz-Espin, D. and M. Serrano. Cellular senescence: from physiology to pathology. *Nat Rev Mol Cell Biol*, 2014. **15**(7): p. 482-96.
76. Pellegata, N.S., et al. DNA damage and p53-mediated cell cycle arrest: a reevaluation. *Proc Natl Acad Sci U S A*, 1996. **93**(26): p. 15209-14.
77. Harris, S.L. and A.J. Levine. The p53 pathway: positive and negative feedback loops. *Oncogene*, 2005. **24**(17): p. 2899-908.
78. Zhang, X.P., et al. Cell fate decision mediated by p53 pulses. *Proc Natl Acad Sci U S A*, 2009. **106**(30): p. 12245-50.
79. Fridman, J.S. and S.W. Lowe. Control of apoptosis by p53. *Oncogene*, 2003. **22**(56): p. 9030-40.
80. Elmore, S. Apoptosis: a review of programmed cell death. *Toxicol Pathol*, 2007. **35**(4): p. 495-516.
81. Ouyang, L., et al. Programmed cell death pathways in cancer: a review of apoptosis, autophagy and programmed necrosis. *Cell Prolif*, 2012. **45**(6): p. 487-98.
82. Efeyan, A. and M. Serrano. p53: guardian of the genome and policeman of the oncogenes. *Cell Cycle*, 2007. **6**(9): p. 1006-10.
83. Lane, D.P. Cancer. p53, guardian of the genome. *Nature*, 1992. **358**(6381): p. 15-6.
84. Hagiwara, K., et al. Mutational analysis of the p63/p73L/p51/p40/CUSP/KET gene in human cancer cell lines using intronic primers. *Cancer Res*, 1999. **59**(17): p. 4165-9.
85. Hibi, K., et al. AIS is an oncogene amplified in squamous cell carcinoma. *Proc Natl Acad Sci U S A*, 2000. **97**(10): p. 5462-7.
86. Yang, A., et al. On the shoulders of giants: p63, p73 and the rise of p53. *Trends Genet*, 2002. **18**(2): p. 90-5.

87. Irwin, M.S. and W.G. Kaelin, Jr. Role of the newer p53 family proteins in malignancy. *Apoptosis*, 2001. **6**(1-2): p. 17-29.
88. Moll, U.M. and N. Slade. p63 and p73: roles in development and tumor formation. *Mol Cancer Res*, 2004. **2**(7): p. 371-86.
89. Shin, J.S., et al. Structural convergence of unstructured p53 family transactivation domains in MDM2 recognition. *Cell Cycle*, 2015. **14**(4): p. 533-43.
90. Levrero, M., et al. The p53/p63/p73 family of transcription factors: overlapping and distinct functions. *J Cell Sci*, 2000. **113** (Pt 10): p. 1661-70.
91. Petitjean, A., et al. Properties of the six isoforms of p63: p53-like regulation in response to genotoxic stress and cross talk with DeltaNp73. *Carcinogenesis*, 2008. **29**(2): p. 273-81.
92. Yang, A. and F. McKeon. P63 and P73: P53 mimics, menaces and more. *Nat Rev Mol Cell Biol*, 2000. **1**(3): p. 199-207.
93. Melino, G. p63 is a suppressor of tumorigenesis and metastasis interacting with mutant p53. *Cell Death Differ*, 2011. **18**(9): p. 1487-99.
94. Helton, E.S., J. Zhang, and X. Chen. The proline-rich domain in p63 is necessary for the transcriptional and apoptosis-inducing activities of TAp63. *Oncogene*, 2008. **27**(20): p. 2843-50.
95. Coppari, E., et al. A nanotechnological, molecular-modeling, and immunological approach to study the interaction of the anti-tumorigenic peptide p28 with the p53 family of proteins. *Int J Nanomedicine*, 2014. **9**: p. 1799-813.
96. Wright, J.D. and C. Lim. Mechanism of DNA-binding loss upon single-point mutation in p53. *J Biosci*, 2007. **32**(5): p. 827-39.

97. McGrath, J.A., et al. Hay-Wells syndrome is caused by heterozygous missense mutations in the SAM domain of p63. *Hum Mol Genet*, 2001. **10**(3): p. 221-9.
98. Kim, C.A. and J.U. Bowie. SAM domains: uniform structure, diversity of function. *Trends Biochem Sci*, 2003. **28**(12): p. 625-8.
99. Thanos, C.D. and J.U. Bowie. p53 Family members p63 and p73 are SAM domain-containing proteins. *Protein Sci*, 1999. **8**(8): p. 1708-10.
100. Ghioni, P., et al. Complex transcriptional effects of p63 isoforms: identification of novel activation and repression domains. *Mol Cell Biol*, 2002. **22**(24): p. 8659-68.
101. Dohn, M., S. Zhang, and X. Chen. p63alpha and DeltaNp63alpha can induce cell cycle arrest and apoptosis and differentially regulate p53 target genes. *Oncogene*, 2001. **20**(25): p. 3193-205.
102. Serber, Z., et al. A C-terminal inhibitory domain controls the activity of p63 by an intramolecular mechanism. *Mol Cell Biol*, 2002. **22**(24): p. 8601-11.
103. Deutsch, G.B., et al. DNA damage in oocytes induces a switch of the quality control factor TAp63alpha from dimer to tetramer. *Cell*, 2011. **144**(4): p. 566-76.
104. King, K.E., et al. Unique domain functions of p63 isotypes that differentially regulate distinct aspects of epidermal homeostasis. *Carcinogenesis*, 2006. **27**(1): p. 53-63.
105. Thurfjell, N., et al. Complex p63 mRNA isoform expression patterns in squamous cell carcinoma of the head and neck. *Int J Oncol*, 2004. **25**(1): p. 27-35.
106. Nylander, K., et al. Differential expression of p63 isoforms in normal tissues and neoplastic cells. *J Pathol*, 2002. **198**(4): p. 417-27.

107. King, K.E., et al. deltaNp63alpha functions as both a positive and a negative transcriptional regulator and blocks in vitro differentiation of murine keratinocytes. *Oncogene*, 2003. **22**(23): p. 3635-44.
108. Amelio, I., et al. p63 the guardian of human reproduction. *Cell Cycle*, 2012. **11**(24): p. 4545-51.
109. Hutt, K., et al. How to best preserve oocytes in female cancer patients exposed to DNA damage inducing therapeutics. *Cell Death Differ*, 2013. **20**(8): p. 967-8.
110. Marchbank, A., et al. The CUSP DeltaNp63alpha isoform of human p63 is downregulated by solar-simulated ultraviolet radiation. *J Dermatol Sci*, 2003. **32**(1): p. 71-4.
111. Liefer, K.M., et al. Down-regulation of p63 is required for epidermal UV-B-induced apoptosis. *Cancer Res*, 2000. **60**(15): p. 4016-20.
112. Yamaguchi, K., et al. Frequent gain of the p40/p51/p63 gene locus in primary head and neck squamous cell carcinoma. *Int J Cancer*, 2000. **86**(5): p. 684-9.
113. Massion, P.P., et al. Significance of p63 amplification and overexpression in lung cancer development and prognosis. *Cancer Res*, 2003. **63**(21): p. 7113-21.
114. Koga, F., et al. Impaired p63 expression associates with poor prognosis and uroplakin III expression in invasive urothelial carcinoma of the bladder. *Clin Cancer Res*, 2003. **9**(15): p. 5501-7.
115. Hibi, K., et al. AIS overexpression in advanced esophageal cancer. *Clin Cancer Res*, 2001. **7**(3): p. 469-72.
116. Pelosi, G., et al. p63 immunoreactivity in lung cancer: yet another player in the development of squamous cell carcinomas? *J Pathol*, 2002. **198**(1): p. 100-9.

117. Park, B.J., et al. Frequent alteration of p63 expression in human primary bladder carcinomas. *Cancer Res*, 2000. **60**(13): p. 3370-4.
118. Park, H.R., et al. Low expression of p63 and p73 in osteosarcoma. *Tumori*, 2004. **90**(2): p. 239-43.
119. Urist, M.J., et al. Loss of p63 expression is associated with tumor progression in bladder cancer. *Am J Pathol*, 2002. **161**(4): p. 1199-206.
120. Chen, Y.K., S.S. Hsue, and L.M. Lin. Expression of p63 (TA and deltaN isoforms) in human primary well differentiated buccal carcinomas. *Int J Oral Maxillofac Surg*, 2004. **33**(5): p. 493-7.
121. Pruneri, G., et al. p63 in laryngeal squamous cell carcinoma: evidence for a role of TA-p63 down-regulation in tumorigenesis and lack of prognostic implications of p63 immunoreactivity. *Lab Invest*, 2002. **82**(10): p. 1327-34.
122. Deyoung, M.P. and L.W. Ellisen. p63 and p73 in human cancer: defining the network. *Oncogene*, 2007. **26**(36): p. 5169-83.
123. Irwin, M., et al. Role for the p53 homologue p73 in E2F-1-induced apoptosis. *Nature*, 2000. **407**(6804): p. 645-8.
124. Yang, A., et al. p63 is essential for regenerative proliferation in limb, craniofacial and epithelial development. *Nature*, 1999. **398**(6729): p. 714-8.
125. Ianakiev, P., et al. Split-hand/split-foot malformation is caused by mutations in the p63 gene on 3q27. *Am J Hum Genet*, 2000. **67**(1): p. 59-66.
126. Celli, J., et al. Heterozygous germline mutations in the p53 homolog p63 are the cause of EEC syndrome. *Cell*, 1999. **99**(2): p. 143-53.

127. Tan, E.H., et al. Functions of TAp63 and p53 in restraining the development of metastatic cancer. *Oncogene*, 2014. **33**(25): p. 3325-33.
128. Guo, X., et al. TAp63 induces senescence and suppresses tumorigenesis in vivo. *Nat Cell Biol*, 2009. **11**(12): p. 1451-7.
129. Su, X., et al. TAp63 is a master transcriptional regulator of lipid and glucose metabolism. *Cell Metab*, 2012. **16**(4): p. 511-25.
130. D'Alessandro, A., et al. Metabolic effect of TAp63alpha: enhanced glycolysis and pentose phosphate pathway, resulting in increased antioxidant defense. *Oncotarget*, 2014. **5**(17): p. 7722-33.
131. Flores, E.R., et al. p63 and p73 are required for p53-dependent apoptosis in response to DNA damage. *Nature*, 2002. **416**(6880): p. 560-4.
132. Flores, E.R., et al. Tumor predisposition in mice mutant for p63 and p73: evidence for broader tumor suppressor functions for the p53 family. *Cancer Cell*, 2005. **7**(4): p. 363-73.
133. Su, X., D. Chakravarti, and E.R. Flores. p63 steps into the limelight: crucial roles in the suppression of tumorigenesis and metastasis. *Nat Rev Cancer*, 2013. **13**(2): p. 136-43.
134. Su, X., et al. TAp63 suppresses metastasis through coordinate regulation of Dicer and miRNAs. *Nature*, 2010. **467**(7318): p. 986-90.
135. Jacobs, W.B., et al. p63 is an essential proapoptotic protein during neural development. *Neuron*, 2005. **48**(5): p. 743-56.
136. Katoh, I., et al. p51A (TAp63gamma), a p53 homolog, accumulates in response to DNA damage for cell regulation. *Oncogene*, 2000. **19**(27): p. 3126-30.

137. Sasaki, Y., et al. Adenovirus-mediated transfer of the p53 family genes, p73 and p51/p63 induces cell cycle arrest and apoptosis in colorectal cancer cell lines: potential application to gene therapy of colorectal cancer. *Gene Ther*, 2001. **8**(18): p. 1401-8.
138. Rocco, J.W., et al. p63 mediates survival in squamous cell carcinoma by suppression of p73-dependent apoptosis. *Cancer Cell*, 2006. **9**(1): p. 45-56.
139. Perez, C.A., et al. p63 consensus DNA-binding site: identification, analysis and application into a p63MH algorithm. *Oncogene*, 2007. **26**(52): p. 7363-70.
140. Ortt, K. and S. Sinha. Derivation of the consensus DNA-binding sequence for p63 reveals unique requirements that are distinct from p53. *FEBS Lett*, 2006. **580**(18): p. 4544-50.
141. Gressner, O., et al. TAp63alpha induces apoptosis by activating signaling via death receptors and mitochondria. *EMBO J*, 2005. **24**(13): p. 2458-71.
142. Ishida, M., et al. The PMAIP1 gene on chromosome 18 is a candidate tumor suppressor gene in human pancreatic cancer. *Dig Dis Sci*, 2008. **53**(9): p. 2576-82.
143. Davies, L., et al. PERP expression stabilizes active p53 via modulation of p53-MDM2 interaction in uveal melanoma cells. *Cell Death Dis*, 2011. **2**: p. e136.
144. Sun, R., et al. Toll-like receptor 3 (TLR3) induces apoptosis via death receptors and mitochondria by up-regulating the transactivating p63 isoform alpha (TAP63alpha). *J Biol Chem*, 2011. **286**(18): p. 15918-28.
145. He, G., et al. Induction of p21 by p53 following DNA damage inhibits both Cdk4 and Cdk2 activities. *Oncogene*, 2005. **24**(18): p. 2929-43.
146. Momii, Y., et al. p73gamma transactivates the p21 promoter through preferential interaction with the p300/CBP-associated factor in human prostate cancer cells. *Oncol Rep*, 2007. **18**(2): p. 411-6.

147. Johnson, J., et al. p73 expression modulates p63 and Mdm2 protein presence in complex with p53 family-specific DNA target sequence in squamous cell carcinogenesis. *Oncogene*, 2008. **27**(19): p. 2780-7.
148. Spiesbach, K., et al. TAp63gamma can substitute for p53 in inducing expression of the maspin tumor suppressor. *Int J Cancer*, 2005. **114**(4): p. 555-62.
149. Flores-Jasso, C.F., et al. First step in pre-miRNAs processing by human Dicer. *Acta Pharmacol Sin*, 2009. **30**(8): p. 1177-85.
150. Muller, P.A., et al. Mutant p53 regulates Dicer through p63-dependent and -independent mechanisms to promote an invasive phenotype. *J Biol Chem*, 2014. **289**(1): p. 122-32.
151. Zou, Z., et al. Maspin, a serpin with tumor-suppressing activity in human mammary epithelial cells. *Science*, 1994. **263**(5146): p. 526-9.
152. Khalkhali-Ellis, Z. Maspin: the new frontier. *Clin Cancer Res*, 2006. **12**(24): p. 7279-83.
153. Bose, P., et al. Tumor cell apoptosis mediated by cytoplasmic ING1 is associated with improved survival in oral squamous cell carcinoma patients. *Oncotarget*, 2014. **5**(10): p. 3210-9.
154. Abad, M., et al. The tumor suppressor ING1 contributes to epigenetic control of cellular senescence. *Aging Cell*, 2011. **10**(1): p. 158-71.
155. Thakur, S., et al. Stromal ING1 expression induces a secretory phenotype and correlates with breast cancer patient survival. *Mol Cancer*, 2015. **14**: p. 164.
156. Senoo, M., Y. Matsumura, and S. Habu. TAp63gamma (p51A) and dNp63alpha (p73L), two major isoforms of the p63 gene, exert opposite effects on the vascular endothelial growth factor (VEGF) gene expression. *Oncogene*, 2002. **21**(16): p. 2455-65.

157. Carmeliet, P. VEGF as a key mediator of angiogenesis in cancer. *Oncology*, 2005. **69 Suppl 3**: p. 4-10.
158. Yuan, M., et al. c-Abl phosphorylation of DeltaNp63alpha is critical for cell viability. *Cell Death Dis*, 2010. **1**: p. e16.
159. Gonfloni, S., et al. Inhibition of the c-Abl-TAp63 pathway protects mouse oocytes from chemotherapy-induced death. *Nat Med*, 2009. **15**(10): p. 1179-85.
160. Bergamaschi, D., et al. ASPP1 and ASPP2: common activators of p53 family members. *Mol Cell Biol*, 2004. **24**(3): p. 1341-50.
161. MacPartlin, M., S.X. Zeng, and H. Lu. Phosphorylation and stabilization of TAp63gamma by IkappaB kinase-beta. *J Biol Chem*, 2008. **283**(23): p. 15754-61.
162. Wang, N., et al. Cables1 protects p63 from proteasomal degradation to ensure deletion of cells after genotoxic stress. *EMBO Rep*, 2010. **11**(8): p. 633-9.
163. Li, C., et al. Pin1 modulates p63alpha protein stability in regulation of cell survival, proliferation and tumor formation. *Cell Death Dis*, 2013. **4**: p. e943.
164. Bernassola, F., et al. The promyelocytic leukaemia protein tumour suppressor functions as a transcriptional regulator of p63. *Oncogene*, 2005. **24**(46): p. 6982-6.
165. Joseph, C.G., et al. Association of the autoimmune disease scleroderma with an immunologic response to cancer. *Science*, 2014. **343**(6167): p. 152-7.
166. Humphries, L.A., et al. Pro-apoptotic TP53 homolog TAp63 is repressed via epigenetic silencing and B-cell receptor signalling in chronic lymphocytic leukaemia. *Br J Haematol*, 2013. **163**(5): p. 590-602.
167. Stindt, M.H., et al. Functional interplay between MDM2, p63/p73 and mutant p53. *Oncogene*, 2015. **34**(33): p. 4300-10.

168. Adorno, M., et al. A Mutant-p53/Smad complex opposes p63 to empower TGFbeta-induced metastasis. *Cell*, 2009. **137**(1): p. 87-98.
169. Schwab, M. *Encyclopedia of Cancer*, 3rd ed. Berlin: Springer-Verlag; 2009. p. 3235.
170. Sager, R. Expression genetics in cancer: shifting the focus from DNA to RNA. *Proc Natl Acad Sci U S A*, 1997. **94**(3): p. 952-5.
171. Di Costanzo, A., et al. Homeodomain protein Dlx3 induces phosphorylation-dependent p63 degradation. *Cell Cycle*, 2009. **8**(8): p. 1185-95.
172. Jung, Y.S., et al. Pirh2 E3 ubiquitin ligase modulates keratinocyte differentiation through p63. *J Invest Dermatol*, 2013. **133**(5): p. 1178-87.
173. Fomenkov, A., et al. RACK1 and stratifin target DeltaNp63alpha for a proteasome degradation in head and neck squamous cell carcinoma cells upon DNA damage. *Cell Cycle*, 2004. **3**(10): p. 1285-95.
174. Bakkers, J., et al. Destabilization of DeltaNp63alpha by Nedd4-mediated ubiquitination and Ubc9-mediated sumoylation, and its implications on dorsoventral patterning of the zebrafish embryo. *Cell Cycle*, 2005. **4**(6): p. 790-800.
175. Huang, Y., et al. ATM kinase is a master switch for the Delta Np63 alpha phosphorylation/degradation in human head and neck squamous cell carcinoma cells upon DNA damage. *Cell Cycle*, 2008. **7**(18): p. 2846-55.
176. Lazzari, C., et al. HIPK2 phosphorylates DeltaNp63alpha and promotes its degradation in response to DNA damage. *Oncogene*, 2011. **30**(48): p. 4802-13.
177. Galli, F., et al. MDM2 and Fbw7 cooperate to induce p63 protein degradation following DNA damage and cell differentiation. *J Cell Sci*, 2010. **123**(Pt 14): p. 2423-33.

178. Hildesheim, J., et al. Gadd45a regulates matrix metalloproteinases by suppressing DeltaNp63alpha and beta-catenin via p38 MAP kinase and APC complex activation. *Oncogene*, 2004. **23**(10): p. 1829-37.
179. Komatsu, S., et al. Plk1 regulates liver tumor cell death by phosphorylation of TAp63. *Oncogene*, 2009. **28**(41): p. 3631-41.
180. Kornitzer, D. and A. Ciechanover. Modes of regulation of ubiquitin-mediated protein degradation. *J Cell Physiol*, 2000. **182**(1): p. 1-11.
181. Jung, T., B. Catalgol, and T. Grune. The proteasomal system. *Mol Aspects Med*, 2009. **30**(4): p. 191-296.
182. Shi, D. and W. Gu. Dual Roles of MDM2 in the Regulation of p53: Ubiquitination Dependent and Ubiquitination Independent Mechanisms of MDM2 Repression of p53 Activity. *Genes Cancer*, 2012. **3**(3-4): p. 240-8.
183. Li, C. and Z.X. Xiao. Regulation of p63 protein stability via ubiquitin-proteasome pathway. *Biomed Res Int*, 2014. **2014**: p. 175721.
184. Glickman, M.H. and A. Ciechanover. The ubiquitin-proteasome proteolytic pathway: destruction for the sake of construction. *Physiol Rev*, 2002. **82**(2): p. 373-428.
185. Herrmann, J., L.O. Lerman, and A. Lerman. Ubiquitin and ubiquitin-like proteins in protein regulation. *Circ Res*, 2007. **100**(9): p. 1276-91.
186. Sadowski, M., et al. Protein monoubiquitination and polyubiquitination generate structural diversity to control distinct biological processes. *IUBMB Life*, 2012. **64**(2): p. 136-42.

187. Ikeda, F. and I. Dikic. Atypical ubiquitin chains: new molecular signals. 'Protein Modifications: Beyond the Usual Suspects' review series. *EMBO Rep*, 2008. **9**(6): p. 536-42.
188. Mukhopadhyay, D. and H. Riezman. Proteasome-independent functions of ubiquitin in endocytosis and signaling. *Science*, 2007. **315**(5809): p. 201-5.
189. Adams, J. The proteasome: a suitable antineoplastic target. *Nat Rev Cancer*, 2004. **4**(5): p. 349-60.
190. Thrower, J.S., et al. Recognition of the polyubiquitin proteolytic signal. *EMBO J*, 2000. **19**(1): p. 94-102.
191. Dammer, E.B., et al. Polyubiquitin linkage profiles in three models of proteolytic stress suggest the etiology of Alzheimer disease. *J Biol Chem*, 2011. **286**(12): p. 10457-65.
192. Wong, B.R., et al. Drug discovery in the ubiquitin regulatory pathway. *Drug Discov Today*, 2003. **8**(16): p. 746-54.
193. Hoppe, T. Multiubiquitylation by E4 enzymes: 'one size' doesn't fit all. *Trends Biochem Sci*, 2005. **30**(4): p. 183-7.
194. Hochstrasser, M. Lingering mysteries of ubiquitin-chain assembly. *Cell*, 2006. **124**(1): p. 27-34.
195. Melino, G., et al. Itch: a HECT-type E3 ligase regulating immunity, skin and cancer. *Cell Death Differ*, 2008. **15**(7): p. 1103-12.
196. Metzger, M.B., V.A. Hristova, and A.M. Weissman. HECT and RING finger families of E3 ubiquitin ligases at a glance. *J Cell Sci*, 2012. **125**(Pt 3): p. 531-7.

197. Wu, H. and R.P. Leng. UBE4B, a ubiquitin chain assembly factor, is required for MDM2-mediated p53 polyubiquitination and degradation. *Cell Cycle*, 2011. **10**(12): p. 1912-5.
198. Moll, U.M. and O. Petrenko. The MDM2-p53 interaction. *Mol Cancer Res*, 2003. **1**(14): p. 1001-8.
199. Kussie, P.H., et al. Structure of the MDM2 oncoprotein bound to the p53 tumor suppressor transactivation domain. *Science*, 1996. **274**(5289): p. 948-53.
200. Fang, S., et al. Mdm2 is a RING finger-dependent ubiquitin protein ligase for itself and p53. *J Biol Chem*, 2000. **275**(12): p. 8945-51.
201. Calabro, V., et al. The human MDM2 oncoprotein increases the transcriptional activity and the protein level of the p53 homolog p63. *J Biol Chem*, 2002. **277**(4): p. 2674-81.
202. Kadakia, M., C. Slader, and S.J. Berberich. Regulation of p63 function by Mdm2 and MdmX. *DNA Cell Biol*, 2001. **20**(6): p. 321-30.
203. Little, N.A. and A.G. Jochemsen. Hdmx and Mdm2 can repress transcription activation by p53 but not by p63. *Oncogene*, 2001. **20**(33): p. 4576-80.
204. Barak, Y., et al. mdm2 expression is induced by wild type p53 activity. *EMBO J*, 1993. **12**(2): p. 461-8.
205. Badciong, J.C. and A.L. Haas. MdmX is a RING finger ubiquitin ligase capable of synergistically enhancing Mdm2 ubiquitination. *J Biol Chem*, 2002. **277**(51): p. 49668-75.
206. Ongkeko, W.M., et al. MDM2 and MDMX bind and stabilize the p53-related protein p73. *Curr Biol*, 1999. **9**(15): p. 829-32.

207. Bergamaschi, D., et al. Mdm2 and mdmX prevent ASPP1 and ASPP2 from stimulating p53 without targeting p53 for degradation. *Oncogene*, 2005. **24**(23): p. 3836-41.
208. Rossi, M., et al. Itch/AIP4 associates with and promotes p63 protein degradation. *Cell Cycle*, 2006. **5**(16): p. 1816-22.
209. Melino, G., R.A. Knight, and G. Cesareni. Degradation of p63 by Itch. *Cell Cycle*, 2006. **5**(16): p. 1735-9.
210. Melino, S., et al. p63 threonine phosphorylation signals the interaction with the WW domain of the E3 ligase Itch. *Cell Cycle*, 2014. **13**(20): p. 3207-17.
211. Rossi, M., et al. The ubiquitin-protein ligase Itch regulates p73 stability. *EMBO J*, 2005. **24**(4): p. 836-48.
212. Halaby, M.J., R. Hakem, and A. Hakem. Pirh2: an E3 ligase with central roles in the regulation of cell cycle, DNA damage response, and differentiation. *Cell Cycle*, 2013. **12**(17): p. 2733-7.
213. Leng, R.P., et al. Pirh2, a p53-induced ubiquitin-protein ligase, promotes p53 degradation. *Cell*, 2003. **112**(6): p. 779-91.
214. Wu, H., et al. Pirh2, a ubiquitin E3 ligase, inhibits p73 transcriptional activity by promoting its ubiquitination. *Mol Cancer Res*, 2011. **9**(12): p. 1780-90.
215. Jung, Y.S., Y. Qian, and X. Chen. The p73 tumor suppressor is targeted by Pirh2 RING finger E3 ubiquitin ligase for the proteasome-dependent degradation. *J Biol Chem*, 2011. **286**(41): p. 35388-95.
216. Conforti, F., et al. PIR2/Rnf144B regulates epithelial homeostasis by mediating degradation of p21WAF1 and p63. *Oncogene*, 2013. **32**(40): p. 4758-65.

217. Li, Y., Z. Zhou, and C. Chen. WW domain-containing E3 ubiquitin protein ligase 1 targets p63 transcription factor for ubiquitin-mediated proteasomal degradation and regulates apoptosis. *Cell Death Differ*, 2008. **15**(12): p. 1941-51.
218. Kumar, S., et al. cDNA cloning, expression analysis, and mapping of the mouse Nedd4 gene. *Genomics*, 1997. **40**(3): p. 435-43.
219. Paul, I. and M.K. Ghosh. The E3 ligase CHIP: insights into its structure and regulation. *Biomed Res Int*, 2014. **2014**: p. 918183.
220. Ballinger, C.A., et al. Identification of CHIP, a novel tetratricopeptide repeat-containing protein that interacts with heat shock proteins and negatively regulates chaperone functions. *Mol Cell Biol*, 1999. **19**(6): p. 4535-45.
221. Nikolay, R., et al. Dimerization of the human E3 ligase CHIP via a coiled-coil domain is essential for its activity. *J Biol Chem*, 2004. **279**(4): p. 2673-8.
222. Ohi, M.D., et al. Structural insights into the U-box, a domain associated with multi-ubiquitination. *Nat Struct Biol*, 2003. **10**(4): p. 250-5.
223. Ronnebaum, S.M., et al. The ubiquitin ligase CHIP prevents SirT6 degradation through noncanonical ubiquitination. *Mol Cell Biol*, 2013. **33**(22): p. 4461-72.
224. Xu, Z., et al. Interactions between the quality control ubiquitin ligase CHIP and ubiquitin conjugating enzymes. *BMC Struct Biol*, 2008. **8**: p. 26.
225. Dai, Q., et al. CHIP activates HSF1 and confers protection against apoptosis and cellular stress. *EMBO J*, 2003. **22**(20): p. 5446-58.
226. Stankiewicz, M., et al. CHIP participates in protein triage decisions by preferentially ubiquitinating Hsp70-bound substrates. *FEBS J*, 2010. **277**(16): p. 3353-67.

227. Sun, C., et al. Diverse roles of C-terminal Hsp70-interacting protein (CHIP) in tumorigenesis. *J Cancer Res Clin Oncol*, 2014. **140**(2): p. 189-97.
228. Jolly, C. and R.I. Morimoto. Role of the heat shock response and molecular chaperones in oncogenesis and cell death. *J Natl Cancer Inst*, 2000. **92**(19): p. 1564-72.
229. Anckar, J. and L. Sistonen. Regulation of HSF1 function in the heat stress response: implications in aging and disease. *Annu Rev Biochem*, 2011. **80**: p. 1089-115.
230. Richter, K., M. Haslbeck, and J. Buchner. The heat shock response: life on the verge of death. *Mol Cell*, 2010. **40**(2): p. 253-66.
231. Ozaki, T., N. Kubo, and A. Nakagawara. p73-Binding Partners and Their Functional Significance. *Int J Proteomics*, 2010. **2010**: p. 283863.
232. Millan, I.C., et al. The stability of wild-type and deletion mutants of human C-terminus Hsp70-interacting protein (CHIP). *Protein Pept Lett*, 2013. **20**(5): p. 524-9.
233. Li, D., et al. Functional inactivation of endogenous MDM2 and CHIP by HSP90 causes aberrant stabilization of mutant p53 in human cancer cells. *Mol Cancer Res*, 2011. **9**(5): p. 577-88.
234. Shang, Y., et al. Hsp70 and Hsp90 oppositely regulate TGF-beta signaling through CHIP/Stub1. *Biochem Biophys Res Commun*, 2014. **446**(1): p. 387-92.
235. Paul, I., et al. The ubiquitin ligase CHIP regulates c-Myc stability and transcriptional activity. *Oncogene*, 2013. **32**(10): p. 1284-95.
236. Wang, T., et al. CHIP is a novel tumor suppressor in pancreatic cancer through targeting EGFR. *Oncotarget*, 2014. **5**(7): p. 1969-86.

237. Bouker, K.B., et al. Interferon regulatory factor-1 (IRF-1) exhibits tumor suppressor activities in breast cancer associated with caspase activation and induction of apoptosis. *Carcinogenesis*, 2005. **26**(9): p. 1527-35.
238. Narayan, V., et al. Docking-dependent ubiquitination of the interferon regulatory factor-1 tumor suppressor protein by the ubiquitin ligase CHIP. *J Biol Chem*, 2011. **286**(1): p. 607-19.
239. Oh, K.H., et al. Control of AIF-mediated cell death by antagonistic functions of CHIP ubiquitin E3 ligase and USP2 deubiquitinating enzyme. *Cell Death Differ*, 2011. **18**(8): p. 1326-36.
240. Esser, C., M. Scheffner, and J. Hohfeld. The chaperone-associated ubiquitin ligase CHIP is able to target p53 for proteasomal degradation. *J Biol Chem*, 2005. **280**(29): p. 27443-8.
241. Jordan, M. and F. Wurm. Transfection of adherent and suspended cells by calcium phosphate. *Methods*, 2004. **33**(2): p. 136-43.
242. Eustice, D.C. and J.M. Wilhelm. Mechanisms of action of aminoglycoside antibiotics in eucaryotic protein synthesis. *Antimicrob Agents Chemother*, 1984. **26**(1): p. 53-60.
243. Shapiro, A.L., E. Vinuela, and J.V. Maizel, Jr. Molecular weight estimation of polypeptide chains by electrophoresis in SDS-polyacrylamide gels. *Biochem Biophys Res Commun*, 1967. **28**(5): p. 815-20.
244. D'Mello, F.J.P. *Amino Acids in Human Nutrition and Health*. Croydon, UK: CAB International; 2012.
245. Prelich, G. Gene overexpression: uses, mechanisms, and interpretation. *Genetics*, 2012. **190**(3): p. 841-54.

246. Anderson, N.G. Co-immunoprecipitation. Identification of interacting proteins. *Methods Mol Biol*, 1998. **88**: p. 35-45.
247. Goldberg, A.L. Development of proteasome inhibitors as research tools and cancer drugs. *J Cell Biol*, 2012. **199**(4): p. 583-8.
248. Wetten, F.R. and A.P. Jackson. Luciferase reporter assay. *Subcell Biochem*, 2006. **40**: p. 423-5.
249. Nelson, C.M., et al. Change in cell shape is required for matrix metalloproteinase-induced epithelial-mesenchymal transition of mammary epithelial cells. *J Cell Biochem*, 2008. **105**(1): p. 25-33.
250. Muller, P.A., et al. Mutant p53 enhances MET trafficking and signalling to drive cell scattering and invasion. *Oncogene*, 2013. **32**(10): p. 1252-65.
251. van den Eijnde, S.M., et al. Cell surface exposure of phosphatidylserine during apoptosis is phylogenetically conserved. *Apoptosis*, 1998. **3**(1): p. 9-16.
252. Jayat, C. and M.H. Ratinaud. Cell cycle analysis by flow cytometry: principles and applications. *Biol Cell*, 1993. **78**(1-2): p. 15-25.
253. Montironi, R., et al. Prostate cancer: from Gleason scoring to prognostic grade grouping. *Expert Rev Anticancer Ther*, 2016. **16**(4): p. 433-40.
254. Pierorazio, P.M., et al. Prognostic Gleason grade grouping: data based on the modified Gleason scoring system. *BJU Int*, 2013. **111**(5): p. 753-60.
255. Bourdon, J.C., et al. p53 isoforms can regulate p53 transcriptional activity. *Genes Dev*, 2005. **19**(18): p. 2122-37.
256. Kung, M., et al. Addition of G418 and other aminoglycoside antibiotics to mammalian cells results in the release of GPI-anchored proteins. *FEBS Lett*, 1997. **409**(3): p. 333-8.

257. Rieger, A.M., et al. Modified annexin V/propidium iodide apoptosis assay for accurate assessment of cell death. *J Vis Exp*, 2011. (50).
258. Chen, H.-C. Cell Migration, Developmental Methods and Protocols. *Methods in Molecular Biology*, ed. J.-L. Guan. Vol. 294. 2005, Totowa, NJ, USA: Humana Press.
259. Zhang, H., et al., A bipartite interaction between Hsp70 and CHIP regulates ubiquitination of chaperoned client proteins. *Structure*, 2015. **23**(3): p. 472-82.
260. Hatakeyama, S., et al. Interaction of U-box-type ubiquitin-protein ligases (E3s) with molecular chaperones. *Genes Cells*, 2004. **9**(6): p. 533-48.
261. Murphy, M.E. The HSP70 family and cancer. *Carcinogenesis*, 2013. **34**(6): p. 1181-8.
262. Brown, L., et al. Transcriptional targets of p53 that regulate cellular proliferation. *Crit Rev Eukaryot Gene Expr*, 2007. **17**(1): p. 73-85.
263. Napoli, M. and E.R. Flores. The family that eats together stays together: new p53 family transcriptional targets in autophagy. *Genes Dev*, 2013. **27**(9): p. 971-4.
264. Yu, J. and L. Zhang. The transcriptional targets of p53 in apoptosis control. *Biochem Biophys Res Commun*, 2005. **331**(3): p. 851-8.
265. Sayan, B.S., et al. Cleavage of the transactivation-inhibitory domain of p63 by caspases enhances apoptosis. *Proc Natl Acad Sci U S A*, 2007. **104**(26): p. 10871-6.
266. Pope, M.D., et al. Automated quantitative analysis of epithelial cell scatter. *Cell Adh Migr*, 2008. **2**(2): p. 110-6.
267. Du Toit, A. RNA interference: nuclear Dicer makes the cut. *Nat Rev Mol Cell Biol*, 2014. **15**(6): p. 366-7.
268. Valastyan, S. and R.A. Weinberg. Metastasis suppression: a role of the Dice(r). *Genome Biol*, 2010. **11**(11): p. 141.

269. Justus, C.R., et al. In vitro cell migration and invasion assays. *J Vis Exp*, 2014(88).
270. M, D. and S.A. Brooks, In vitro invasion assay using matrigel(R). *Methods Mol Med*, 2001. **58**: p. 61-70.
271. Moutasim, K.A., M.L. Nystrom, and G.J. Thomas. Cell migration and invasion assays. *Methods Mol Biol*, 2011. **731**: p. 333-43.
272. Kameda, Y., et al. Expression of the epithelial marker E-cadherin by thyroid C cells and their precursors during murine development. *J Histochem Cytochem*, 2007. **55**(10): p. 1075-88.
273. Fraga, C.H., L.D. True, and D. Kirk. Enhanced expression of the mesenchymal marker, vimentin, in hyperplastic versus normal human prostatic epithelium. *J Urol*, 1998. **159**(1): p. 270-4.
274. Ishimine, H., et al. N-Cadherin is a prospective cell surface marker of human mesenchymal stem cells that have high ability for cardiomyocyte differentiation. *Biochem Biophys Res Commun*, 2013. **438**(4): p. 753-9.
275. Barbieri, C.E., et al. Loss of p63 leads to increased cell migration and up-regulation of genes involved in invasion and metastasis. *Cancer Res*, 2006. **66**(15): p. 7589-97.
276. Hughes, P., et al. The costs of using unauthenticated, over-passaged cell lines: how much more data do we need? *Biotechniques*, 2007. **43**(5): p. 575, 577-8, 581-2.
277. Massey, A.J., et al. A novel, small molecule inhibitor of Hsc70/Hsp70 potentiates Hsp90 inhibitor induced apoptosis in HCT116 colon carcinoma cells. *Cancer Chemother Pharmacol*, 2010. **66**(3): p. 535-45.
278. Mali, P., K.M. Esvelt, and G.M. Church. Cas9 as a versatile tool for engineering biology. *Nat Methods*, 2013. **10**(10): p. 957-63.

